

Measurement of the ratio of cross sections for inclusive isolated-photon production in pp collisions at $\sqrt{s} = 13$ and 8 TeV with the ATLAS detector

ATLAS Collaboration; Newman, Paul

DOI:

[10.1007/JHEP04\(2019\)093](https://doi.org/10.1007/JHEP04(2019)093)

License:

Creative Commons: Attribution (CC BY)

Document Version

Publisher's PDF, also known as Version of record

Citation for published version (Harvard):

ATLAS Collaboration & Newman, P 2019, 'Measurement of the ratio of cross sections for inclusive isolated-photon production in pp collisions at $\sqrt{s} = 13$ and 8 TeV with the ATLAS detector', *JHEP*, vol. 2019, no. 4, 93. [https://doi.org/10.1007/JHEP04\(2019\)093](https://doi.org/10.1007/JHEP04(2019)093)

[Link to publication on Research at Birmingham portal](#)

Publisher Rights Statement:

Checked for eligibility: 08/05/2019

General rights

Unless a licence is specified above, all rights (including copyright and moral rights) in this document are retained by the authors and/or the copyright holders. The express permission of the copyright holder must be obtained for any use of this material other than for purposes permitted by law.

- Users may freely distribute the URL that is used to identify this publication.
- Users may download and/or print one copy of the publication from the University of Birmingham research portal for the purpose of private study or non-commercial research.
- User may use extracts from the document in line with the concept of 'fair dealing' under the Copyright, Designs and Patents Act 1988 (?)
- Users may not further distribute the material nor use it for the purposes of commercial gain.

Where a licence is displayed above, please note the terms and conditions of the licence govern your use of this document.

When citing, please reference the published version.

Take down policy

While the University of Birmingham exercises care and attention in making items available there are rare occasions when an item has been uploaded in error or has been deemed to be commercially or otherwise sensitive.

If you believe that this is the case for this document, please contact UBIRA@lists.bham.ac.uk providing details and we will remove access to the work immediately and investigate.

RECEIVED: January 30, 2019

REVISED: March 26, 2019

ACCEPTED: March 31, 2019

PUBLISHED: April 12, 2019

Measurement of the ratio of cross sections for inclusive isolated-photon production in pp collisions at $\sqrt{s} = 13$ and 8 TeV with the ATLAS detector



The ATLAS collaboration

E-mail: atlas.publications@cern.ch

ABSTRACT: The ratio of the cross sections for inclusive isolated-photon production in pp collisions at centre-of-mass energies of 13 and 8 TeV is measured using the ATLAS detector at the LHC. The integrated luminosities of the 13 TeV and 8 TeV datasets are 3.2 fb^{-1} and 20.2 fb^{-1} , respectively. The ratio is measured as a function of the photon transverse energy in different regions of the photon pseudorapidity. The predictions from next-to-leading-order perturbative QCD calculations are compared with the measured ratio. The experimental systematic uncertainties as well as the uncertainties affecting the predictions are evaluated taking into account the correlations between the two centre-of-mass energies, resulting in a reduction of up to a factor of 2.5 (5) in the experimental (theoretical) systematic uncertainties. The predictions based on several parameterisations of the proton parton distribution functions agree with the data within the reduced experimental and theoretical uncertainties. In addition, this ratio to that of the fiducial cross sections for Z boson production at 13 and 8 TeV using the decay channels $Z \rightarrow e^+e^-$ and $Z \rightarrow \mu^+\mu^-$ is made and compared with the theoretical predictions. In this double ratio, a further reduction of the experimental uncertainty is obtained because the uncertainties arising from the luminosity measurement cancel out. The predictions describe the measurements of the double ratio within the theoretical and experimental uncertainties.

KEYWORDS: Hadron-Hadron scattering (experiments), Photon production, QCD

ARXIV EPRINT: [1901.10075](https://arxiv.org/abs/1901.10075)

Contents

| | | |
|----------|---|-----------|
| 1 | Introduction | 1 |
| 2 | ATLAS detector | 3 |
| 3 | Analysis strategy | 4 |
| 3.1 | Analysis strategy for $R_{13/8}^\gamma$ | 4 |
| 3.2 | Analysis strategy for $D_{13/8}^{\gamma/Z}$ | 5 |
| 4 | Fixed-order QCD predictions | 6 |
| 4.1 | Theoretical predictions for $R_{13/8}^\gamma$ | 6 |
| 4.2 | Theoretical predictions for $D_{13/8}^{\gamma/Z}$ | 8 |
| 5 | Experimental uncertainties | 10 |
| 5.1 | Photon energy scale | 11 |
| 5.2 | Other sources of experimental uncertainty | 12 |
| 5.3 | Total experimental uncertainties in $R_{13/8}^\gamma$ | 14 |
| 5.4 | Total experimental uncertainties in $D_{13/8}^{\gamma/Z}$ | 16 |
| 6 | Results | 17 |
| 6.1 | Results for $R_{13/8}^\gamma$ | 17 |
| 6.2 | Results for $D_{13/8}^{\gamma/Z}$ | 22 |
| 7 | Summary and conclusions | 25 |
| | The ATLAS collaboration | 30 |

1 Introduction

The production of prompt photons in proton-proton collisions, $pp \rightarrow \gamma + X$, provides a means of testing perturbative QCD (pQCD) with a hard colourless probe. Since the dominant production mechanism in pp collisions at the LHC proceeds via the $qg \rightarrow q\gamma$ process, measurements of prompt-photon¹ production are sensitive to the gluon density in the proton [1, 2]. These measurements can also be used to tune Monte Carlo (MC) models to improve our understanding of prompt-photon production and aid those analyses for which events containing photons are an important background.

¹All photons produced in pp collisions that are not secondaries from hadron decays are considered to be “prompt”.

At leading order (LO) in pQCD, two processes contribute to prompt-photon production: the direct-photon process, in which the photon originates directly from the hard interaction, and the fragmentation-photon process, in which the photon is emitted in the fragmentation of a high transverse momentum (p_T) parton [3, 4].

Measurements of prompt-photon production at a hadron collider necessitate an isolation requirement to reduce the large contribution of photons from hadron decays and the fragmentation component in which the emitted photon is close to a jet. The production of isolated photons in pp collisions has been measured previously by the ATLAS [5–9] and CMS [10, 11] collaborations at centre-of-mass energies (\sqrt{s}) of 7, 8 and 13 TeV.

Comparisons of measurements of prompt-photon production and pQCD predictions are usually limited by the theoretical uncertainties associated with the missing higher-order terms in the perturbative expansion. The measurements of inclusive isolated-photon cross sections performed by ATLAS at 13 TeV [9] and 8 TeV [8] were compared with the predictions of pQCD at next-to-leading order (NLO) [12, 13]. At both centre-of-mass energies, the uncertainties affecting the predictions are dominated by terms beyond NLO and are larger than those of experimental nature, preventing a more precise test of the theory. An avenue to reach a more stringent test is the inclusion of next-to-next-to-leading-order (NNLO) QCD corrections in the calculations [14]. Another avenue is to make measurements of the ratio of cross sections for inclusive isolated-photon production at 13 and 8 TeV ($R_{13/8}^\gamma$) and compare them with the predictions [15, 16]. The impact of the experimental systematic uncertainties and theoretical uncertainties on the ratio of the cross sections is reduced, allowing a more precise comparison between data and theory. This is achieved by accounting for inter- \sqrt{s} correlations in the experimental systematic uncertainties affecting the measurements and in the uncertainties of the theory predictions.

A further reduction of the experimental uncertainty can be achieved by measuring a double ratio: the ratio of $R_{13/8}^\gamma$ to the ratio of the fiducial cross sections for Z boson production at 13 TeV and 8 TeV ($R_{13/8}^Z \equiv \sigma_Z^{\text{fid}}(13 \text{ TeV})/\sigma_Z^{\text{fid}}(8 \text{ TeV})$) presented in ref. [17]. The measurements of the fiducial cross sections for Z boson production use the decay channels $Z \rightarrow e^+e^-$ and $Z \rightarrow \mu^+\mu^-$. This observable, $D_{13/8}^{\gamma/Z} \equiv R_{13/8}^\gamma/R_{13/8}^Z$, can be viewed as the increase of the cross section for isolated-photon production as a function of \sqrt{s} normalised to the increase for Z boson production as a function of \sqrt{s} . Measuring $D_{13/8}^{\gamma/Z}$ is beneficial because the uncertainties from the luminosity measurement cancel out, and $D_{13/8}^{\gamma/Z}$ has only a slightly larger theory uncertainty than $R_{13/8}^\gamma$.

This paper presents measurements of the ratio of cross sections for isolated-photon production in pp collisions at $\sqrt{s} = 13$ TeV and 8 TeV with the ATLAS detector at the LHC. The phase-space region is given by the overlap of the ATLAS measurements at $\sqrt{s} = 13$ and 8 TeV, defined by the photon transverse energy² (E_T^γ) in the range $E_T^\gamma > 125$ GeV and the photon pseudorapidity (η^γ) in the region $|\eta^\gamma| < 2.37$, excluding

²ATLAS uses a right-handed coordinate system with its origin at the nominal interaction point (IP) in the centre of the detector and the z -axis along the beam pipe. The x -axis points from the IP to the centre of the LHC ring, and the y -axis points upwards. Cylindrical coordinates (r, ϕ) are used in the transverse plane, ϕ being the azimuthal angle around the z -axis. The pseudorapidity is defined in terms of the polar angle θ as $\eta = -\ln \tan(\theta/2)$.

the region $1.37 < |\eta^\gamma| < 1.56$. The photon is isolated by requiring that the transverse energy inside a cone of size $\Delta R \equiv \sqrt{(\Delta\eta)^2 + (\Delta\phi)^2} = 0.4$ in the η - ϕ plane around the photon direction, E_T^{iso} , is smaller than $E_{T,\text{cut}}^{\text{iso}} \equiv 4.2 \cdot 10^{-3} \cdot E_T^\gamma + 4.8 \text{ GeV}$ [8, 9]. Non-isolated prompt photons are not considered as signal. The measurements of the ratios are based on the ATLAS measurements at 13 TeV [9] and 8 TeV [8] and a detailed study of the correlations of the experimental systematic uncertainties between the two centre-of-mass energies is presented here. The measurement of the ratios is presented as a function of E_T^γ in different regions of η^γ , namely $|\eta^\gamma| < 0.6$, $0.6 < |\eta^\gamma| < 1.37$, $1.56 < |\eta^\gamma| < 1.81$ and $1.81 < |\eta^\gamma| < 2.37$. Next-to-leading-order pQCD predictions for the ratio are compared with the measurements. In addition, measurements of $D_{13/8}^{\gamma/Z}$ are presented using the ATLAS results for $R_{13/8}^Z$ [17]; the measurements are compared with available theory predictions.

The paper is organised as follows: the ATLAS detector is described in section 2. The analysis strategy is summarised in section 3. Fixed-order QCD predictions and their uncertainties are discussed in section 4. Section 5 is devoted to the description of the experimental uncertainties. The results are reported in section 6. A summary is given in section 7.

2 ATLAS detector

The ATLAS experiment [18] at the LHC uses a multipurpose particle detector with a forward-backward symmetric cylindrical geometry and a near 4π coverage in solid angle. It consists of an inner tracking detector, electromagnetic (EM) and hadronic calorimeters, and a muon spectrometer. The inner detector is surrounded by a thin superconducting solenoid and includes silicon detectors, which provide precision tracking in the pseudorapidity range $|\eta| < 2.5$, and a transition-radiation tracker providing additional tracking and electron identification information for $|\eta| < 2.0$. For the $\sqrt{s} = 13 \text{ TeV}$ data-taking period, the inner detector also includes a silicon-pixel insertable B-layer [19, 20], providing an additional layer of tracking information close to the interaction point. The calorimeter system covers the range $|\eta| < 4.9$. Within the region $|\eta| < 3.2$, EM calorimetry is provided by barrel and endcap high-granularity lead/liquid-argon (LAr) EM calorimeters, with an additional thin LAr presampler covering $|\eta| < 1.8$ to correct for energy loss in material upstream of the calorimeters; for $|\eta| < 2.5$ the LAr calorimeters are divided into three layers in depth. Hadronic calorimetry is provided by a steel/scintillator-tile calorimeter for $|\eta| < 1.7$ and two copper/LAr hadronic endcap calorimeters for $1.5 < |\eta| < 3.2$. The forward region is covered by additional coarser-granularity LAr calorimeters up to $|\eta| = 4.9$. The muon spectrometer consists of three large superconducting toroidal magnets, one barrel and two endcaps, each containing eight coils, precision tracking chambers covering the region $|\eta| < 2.7$, and separate trigger chambers up to $|\eta| = 2.4$. For the data taken at 8 TeV, a three-level trigger system was used. The first-level trigger was implemented in hardware and used a subset of the detector information. This was followed by two software-based trigger levels that together reduce the accepted event rate to approximately 400 Hz. For the data taken at 13 TeV, the trigger was changed [21] to a two-level system, using custom hardware

followed by a software-based level which runs offline reconstruction software, reducing the event rate to approximately 1 kHz.

3 Analysis strategy

The measurements of ratios of cross sections presented in this paper are based on the measurements presented in previous ATLAS publications [8, 9, 17], where details of the analyses are given. The strategies followed for the measurement of the ratios and for the theoretical predictions are described below.

3.1 Analysis strategy for $R_{13/8}^\gamma$

The measurements of $d\sigma/dE_T^\gamma$ at $\sqrt{s} = 8$ TeV (13 TeV) used in the measurement of $R_{13/8}^\gamma$ are based on an integrated luminosity of $20.2 \pm 0.4 \text{ fb}^{-1}$ ($3.16 \pm 0.07 \text{ fb}^{-1}$). The measurement of the ratio covers the range $E_T^\gamma > 125$ GeV and is performed separately in the four regions of η^γ defined in section 1. A summary of the analyses leading to the measurements of the differential cross sections for inclusive isolated-photon production at $\sqrt{s} = 13$ and 8 TeV is given below.

Photon candidates are reconstructed from clusters of energy deposited in the EM calorimeter. Candidates without a matching track or reconstructed conversion vertex in the inner detector are classified as unconverted photons, while those with a matching reconstructed conversion vertex or a matching track consistent with originating from a photon conversion are classified as converted photons [22]. The photon identification is based primarily on shower shapes in the calorimeter [22]. It uses information from the hadronic calorimeter, the lateral shower shape in the second layer of the EM calorimeter and the shower shapes in the finely segmented first EM calorimeter layer to ensure the compatibility of the measured shower profile with that originating from a single photon impacting the calorimeter. The photon energy measurement is made using calorimeter and, when available, tracking information. An energy calibration [23] is applied to the candidates to account for upstream energy loss and both lateral and longitudinal leakage. Events with at least one photon candidate with calibrated $E_T^\gamma > 125$ GeV and $|\eta^\gamma| < 2.37$ excluding the region $1.37 < |\eta^\gamma| < 1.56$ are selected. The isolation transverse energy E_T^{iso} is corrected for leakage of the photon energy into the isolation cone and the estimated contributions from the underlying event (UE) and additional inelastic pp interactions (pile-up). The latter two corrections are computed simultaneously on an event-by-event basis using the jet-area method [24, 25]. After these corrections, isolated photons are selected by requiring E_T^{iso} to be lower than $E_{T,\text{cut}}^{\text{iso}}$. A small background contribution still remains after imposing the photon identification and isolation requirements and is subtracted using a data-driven method based on background control regions [8, 9]. The selected samples of events are used to unfold the distribution in E_T^γ for each $|\eta^\gamma|$ region to a phase-space region close to that used for event selection.

The phase-space region at particle level uses particles with a decay length $c\tau > 10$ mm; these particles are referred to as “stable”. The particle-level isolation requirement for the photon is built by summing the transverse energy of all stable particles, except for muons

and neutrinos, in a cone of size $\Delta R = 0.4$ around the photon direction after the contribution from the UE is subtracted; the same subtraction procedure and isolation requirement used on data are applied at the particle level.

An important part of this analysis is the evaluation of the experimental systematic uncertainties in the ratio of the cross sections at 13 and 8 TeV taking into account correlations. This study is described in section 5. Given the dominance of the systematic uncertainty arising from the photon energy scale when measuring the cross sections, it is necessary to carefully study this source of uncertainty. This source of systematic uncertainty is decomposed into independent components [23] and the treatment of the correlations of these components between the measurements at 13 and 8 TeV results in a reduction of the systematic uncertainty of the ratio.

The measurements of the ratio of cross sections are compared with NLO pQCD predictions for which a proper evaluation of the theoretical uncertainties is also of importance. The theoretical uncertainties in the predictions for the cross sections are $\mathcal{O}(10\text{--}15\%)$ for both centre-of-mass energies and are dominated by contributions from terms beyond NLO. These uncertainties are much larger than those of experimental nature and limit how precisely the predictions can be tested. The study of the theoretical uncertainties in the ratio is described in section 4. As is the case for the experimental systematic uncertainties, it is imperative that for each source of theoretical uncertainty the degree of correlation between the two centre-of-mass energies is taken into account. As a result, the theoretical uncertainty is reduced in the ratio, thus allowing a more stringent test of the predictions.

3.2 Analysis strategy for $D_{13/8}^{\gamma/Z}$

The measurement of the double ratio $D_{13/8}^{\gamma/Z}$ is based on the measurement of $R_{13/8}^{\gamma}$ described above as well as on the measurement of $R_{13/8}^Z$. It should be noted that $R_{13/8}^{\gamma}$ is measured as a function of E_T^{γ} in different ranges of η^{γ} , while $R_{13/8}^Z$ is a single number. The measurement of $R_{13/8}^Z$ used here is the one reported in ref. [17]. The fiducial cross section at a given \sqrt{s} , $\sigma_Z^{\text{fid}}(\sqrt{s})$, is defined as the production cross section of a Z boson times the branching ratio of the decay into a lepton pair of flavour $\ell^+\ell^- = e^+e^-$ or $\mu^+\mu^-$ within the following phase space: the lepton transverse momentum $p_T^{\ell} > 25$ GeV, the lepton pseudorapidity $|\eta_{\ell}| < 2.5$ and the dilepton invariant mass $66 < m_{\ell\ell} < 116$ GeV. The measurement at $\sqrt{s} = 13$ TeV was performed in the aforementioned phase space while the measurement at $\sqrt{s} = 8$ TeV was extrapolated to the same phase space as described in ref. [17]. Measurements of the fiducial cross sections were made using the decay channels $Z \rightarrow e^+e^-$ and $Z \rightarrow \mu^+\mu^-$, and combined for the final result. The measured $R_{13/8}^Z$ is 1.537 ± 0.001 (stat.) ± 0.010 (syst.) ± 0.044 (lumi.) [17], where “stat.” denotes the statistical uncertainty, “syst.” denotes the systematic uncertainty and “lumi.” denotes the uncertainty due to the ratio of the integrated luminosities. The evaluation of the systematic uncertainty in the ratio takes into account correlations of systematic uncertainties across channels and \sqrt{s} as described in ref. [17].

The predictions for $D_{13/8}^{\gamma/Z}$ are obtained from NLO pQCD calculations for $R_{13/8}^{\gamma}$ [12, 13] and NNLO pQCD calculations for $R_{13/8}^Z$ [26, 27]. The evaluation of the uncertainties affecting

the predictions for $D_{13/8}^{\gamma/Z}$ requires considerations that account for the correlations arising from the parton distribution functions (PDFs) and the strong coupling constant, $\alpha_s(m_Z)$.

4 Fixed-order QCD predictions

The theoretical predictions for the ratios of cross sections are obtained using fixed-order QCD calculations. Details of the generators and of the estimations of the theoretical uncertainties are given below, especially emphasising the correlations between the two centre-of-mass energies.

4.1 Theoretical predictions for $R_{13/8}^\gamma$

The theoretical predictions for $R_{13/8}^\gamma$ presented here are based on NLO QCD calculations computed using the program JETPHOX 1.3.1.2 [12, 13]. This program includes a full NLO QCD treatment of both the direct- and fragmentation-photon contributions to the cross section for the $pp \rightarrow \gamma + X$ reaction. The number of quark flavours is set to five. The renormalisation (μ_R), factorisation (μ_F) and fragmentation (μ_f) scales are chosen to be $\mu_R = \mu_F = \mu_f = E_T^\gamma$. The calculations are performed using various parameterisations of the proton PDFs and the BFG set II of parton-to-photon fragmentation functions at NLO [28]. The nominal calculation is based on the MMHT2014 PDF set [29]. Predictions are also obtained with other PDFs, namely CT14 [30], HERAPDF2.0 [31], NNPDF3.0 [32] and ABMP16 [33]. For MMHT2014, CT14, HERAPDF2.0 and NNPDF3.0 parameterisations of the PDFs, the sets determined at NLO are used. For ABMP16, the set at NNLO is used. The strong coupling constant $\alpha_s(m_Z)$ is set to the value assumed in the fit to determine the PDFs; as an example, in the case of MMHT2014 PDFs, $\alpha_s(m_Z)$ is set to the value 0.120.

The calculations are performed using a parton-level isolation criterion for the photon, which requires a total transverse energy of the partons inside a cone of radius $R = 0.4$ around the photon direction below $E_{T,\text{cut}}^{\text{iso}}$. The predictions from JETPHOX are at parton level,³ while the measurements are at particle level. Corrections for the non-perturbative (NP) effects of hadronisation and the UE are estimated using samples from PYTHIA 8.186 [34] as described below. First, a correction factor ($C_{\sqrt{s}}^{\text{NP}}$) is derived for the isolated-photon cross section at each centre-of-mass energy as the ratio of the cross section at particle level for a PYTHIA sample with UE effects to the PYTHIA cross section at parton level without UE effects. Second, the ratio of the correction factor for $\sqrt{s} = 13$ TeV to that for $\sqrt{s} = 8$ TeV, $C_R^{\text{NP}} = C_{13}^{\text{NP}}/C_8^{\text{NP}}$, is evaluated. The ratio of correction factors is obtained using the ATLAS set of tuned parameters A14 [35] with the LO NNPDF2.3 PDF set [36]. The ratio of correction factors for non-perturbative effects applied to the ratio predictions from JETPHOX is $C_R^{\text{NP}} = 0.9964 \pm 0.0020$.

The following sources of uncertainty in the theoretical predictions are considered:

- The uncertainty in the NLO QCD predictions due to terms beyond NLO is estimated by repeating the calculations using values of μ_R , μ_F and μ_f scaled by the factors 0.5 and 2. The three scales are either varied simultaneously or individually; in addition,

³The parton level in JETPHOX consists of the generated photon and the few partons simulated with the matrix elements, while in PYTHIA it includes the partons after the parton shower.

configurations in which one scale is fixed and the other two are varied simultaneously are also considered. In all cases, the condition $0.5 \leq \mu_A/\mu_B \leq 2$ is imposed, where $A, B = R, F, f$. The final uncertainty is taken as the largest deviation from the nominal value among the 14 possible variations.

- The uncertainty in the NLO QCD predictions related to the proton PDFs is estimated by repeating the calculations using the 50 additional sets from the MMHT2014 error analysis.
- The uncertainty in the NLO QCD predictions related to the value of $\alpha_s(m_Z)$ is estimated by repeating the calculations using two additional sets of proton PDFs from the MMHT2014 analysis for which different values of $\alpha_s(m_Z)$ were assumed in the fits, namely $\alpha_s(m_Z) = 0.118$ and 0.122 [37].
- The impact of the beam energy uncertainty is estimated by repeating the calculations with \sqrt{s} varied by its uncertainty of 0.1% [38].
- The uncertainty in the corrections for non-perturbative effects is estimated by comparing the results of using variations of the A14 tune in which the parameter settings related to the modelling of the UE are changed [35].

For the individual differential cross sections and for both centre-of-mass energies, the dominant theoretical uncertainty arises from the estimate of contributions from terms beyond NLO [8, 9].

The predictions for $R_{13/8}^\gamma$ are obtained by calculating the ratio of the individual differential cross sections at each centre-of-mass energy. To estimate the theoretical uncertainty in $R_{13/8}^\gamma$, the correlation between the two centre-of-mass energies for each source listed above needs to be considered. The uncertainties due to the PDFs, $\alpha_s(m_Z)$, beam energy and non-perturbative effects are fully correlated between the two centre-of-mass energies. The relative uncertainties in $R_{13/8}^\gamma$ due to the uncertainties in $\alpha_s(m_Z)$, the PDFs and the beam energy exhibit a significant degree of cancellation with respect to the individual predictions. However, for the scale uncertainties, the correlation is a priori unknown. In the standard approach, varying the scales coherently or incoherently at both centre-of-mass energies leads to very different theoretical uncertainties:

- In the coherent case, there are large cancellations in the uncertainties in the predictions for $R_{13/8}^\gamma$, particularly in the variation of μ_R , which is $\mathcal{O}(10\%)$ for the individual predictions and below 1% for $R_{13/8}^\gamma$. The envelope of the scale variations for $R_{13/8}^\gamma$ shrinks in comparison with the envelopes for the individual predictions: from $\mathcal{O}(10\%)$ for the individual predictions to below 2% for $R_{13/8}^\gamma$ across most of the range in E_T^γ .
- In the incoherent case, the envelope of the scale variations for $R_{13/8}^\gamma$ is $\mathcal{O}(14\%)$ in all regions of phase space.

A second approach is also investigated, which is free from ambiguity in the correlation. It consists of considering the difference between the LO and NLO predictions for $R_{13/8}^\gamma$. The LO predictions are obtained with JETPHOX using the same parameter settings and PDF set

as the baseline NLO predictions. The LO and NLO predictions for $R_{13/8}^\gamma$ are compared and the differences are up to 3.5%, which are similar to the estimates based on the standard approach with coherent variations at the two centre-of-mass energies. Thus, the results of this second approach support the use of the standard approach with a coherent variation of the scales; an incoherent variation of the scales clearly leads to an overestimation of the theoretical uncertainty.

Figure 1 shows an overview of the theoretical uncertainties in $R_{13/8}^\gamma$. The total relative uncertainty is below 2% (4%) at low (high) E_T^γ in all regions of $|\eta^\gamma|$. The uncertainty due to the variation of the scales is dominant everywhere. At high E_T^γ for $|\eta^\gamma| < 0.6$ and $0.6 < |\eta^\gamma| < 1.37$, the uncertainty due to the PDFs can be as large as the contribution from the scale variations.

The NLO pQCD predictions of JETPHOX for $R_{13/8}^\gamma$ based on the MMHT2014 parameterisations of the proton PDFs are about 2 at $E_T^\gamma = 125$ GeV and increase as E_T^γ increases, to about 10 for $E_T^\gamma = 1300$ (1000) GeV for $|\eta^\gamma| < 0.6$ ($0.6 < |\eta^\gamma| < 1.37$). For $1.56 < |\eta^\gamma| < 1.81$ ($1.81 < |\eta^\gamma| < 2.37$), the predicted $R_{13/8}^\gamma$ increases from about 2 at $E_T^\gamma = 125$ GeV to around 10 (25) at $E_T^\gamma = 600$ GeV. The increase is greater for the forward regions than for the central regions. Predictions based on different parameterisations of the proton PDFs are compared. Those based on MMHT2014, NNPDF3.0 and CT14 are found to be similar in all η^γ and E_T^γ regions. The predictions of $R_{13/8}^\gamma$ based on HERAPDF2.0 and ABMP16 show some differences from the predictions based on the other PDFs in some regions of phase space, especially at high E_T^γ (see section 6).

4.2 Theoretical predictions for $D_{13/8}^{\gamma/Z}$

The theoretical predictions for $D_{13/8}^{\gamma/Z}$ presented here are based on NNLO QCD calculations for the predictions of $R_{13/8}^Z$ computed using the program DYTURBO, which is an optimised version of the DYNNLO program [26, 27], and NLO QCD calculations for the predictions of $R_{13/8}^\gamma$ using JETPHOX with the procedure described in section 4.1.

The calculations using DYTURBO are based on sets of PDFs extracted using NNLO QCD fits, namely MMHT2014nnlo, CT14nnlo, HERAPDF2.0nnlo and NNPDF3.0nnlo. The strong coupling constant $\alpha_s(m_Z)$ is set to the value assumed in the fit to determine the PDFs. In the case of MMHT2014nnlo PDFs, $\alpha_s(m_Z)$ is set to the value 0.118.

For consistency, and to properly take into account the correlations in the PDF uncertainties, the calculations of JETPHOX for $R_{13/8}^\gamma$ are repeated using the NNLO PDF sets mentioned above. It is consistent to use NLO matrix elements convolved with PDF sets determined at NNLO. The resulting predictions include partially NNLO corrections and, therefore, are understood to still have NLO accuracy. For these additional calculations, the same parameter settings for the number of flavours, scales and fragmentation functions mentioned in section 4.1 are used. The change in the predictions for $R_{13/8}^\gamma$ based on MMHT2014nnlo relative to those using MMHT2014nlo is $\sim 0.5\%$ at low E_T^γ . At high E_T^γ the change depends on the $|\eta^\gamma|$ region: for $|\eta^\gamma| < 0.6$ the change is below 2% for $E_T^\gamma < 750$ GeV and increases to 6% in the highest- E_T^γ measured point; for $0.6 < |\eta^\gamma| < 1.37$ ($1.56 < |\eta^\gamma| < 1.81$) the change is below 2% (1.3%) for the entire measured range; for

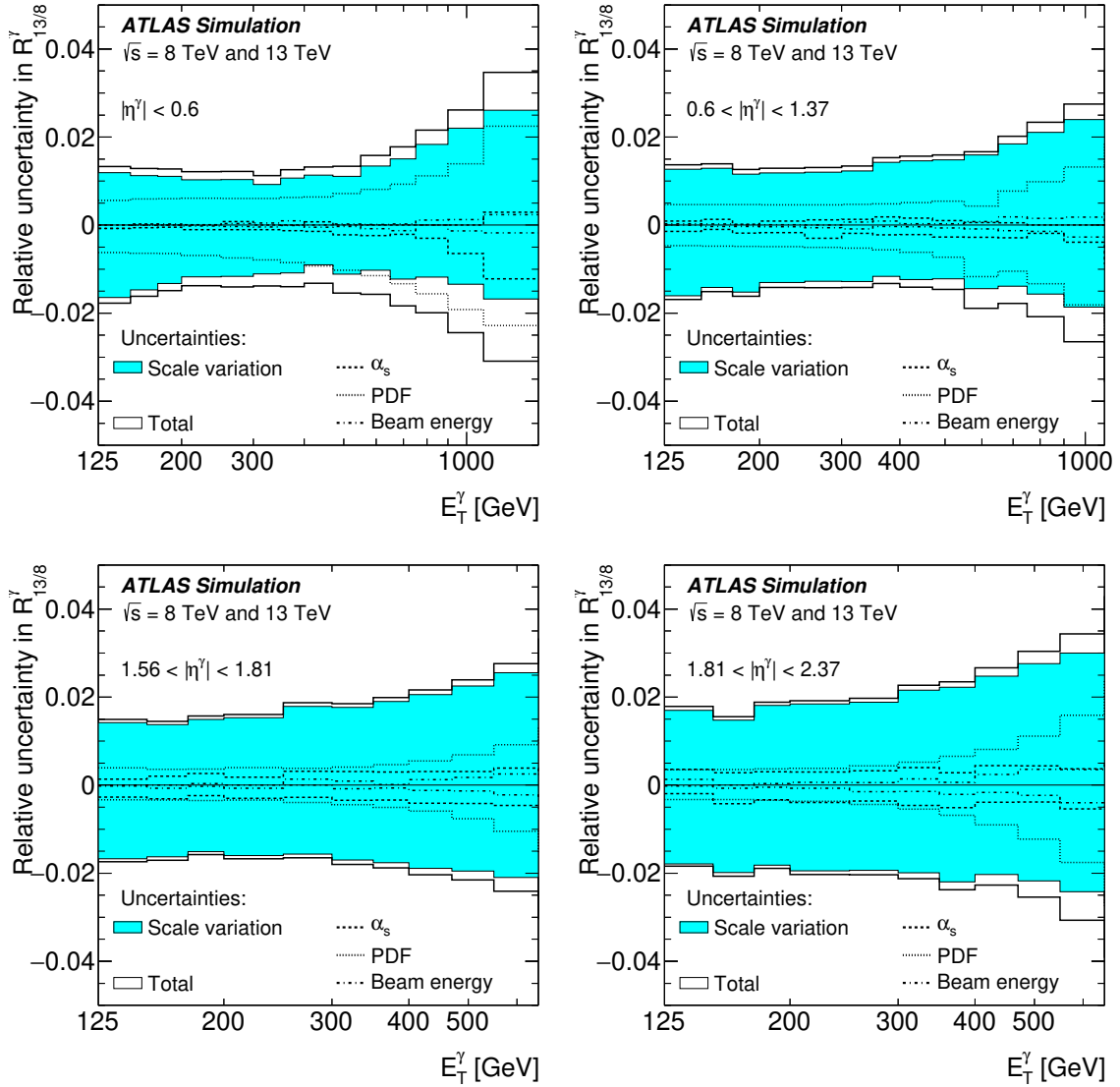


Figure 1. Relative theoretical uncertainty in $R_{13/8}^\gamma$ as a function of E_T^γ for different η^γ regions arising from the scale variations (shaded area), the value of α_s (dashed lines), the PDF (dotted lines) and the beam energy (dot-dashed lines). The total theoretical uncertainty is shown as the solid line.

for $1.81 < |\eta^\gamma| < 2.37$ the change is below 2% for $E_T^\gamma < 550$ GeV and increases to 2.7% in the highest- E_T^γ measured point.

The sources of uncertainty in the theoretical predictions based on MMHT2014nnlo are the same as those described in section 4.1. The uncertainty related to the beam energy is neglected, due to the small size of its effect on $R_{13/8}^\gamma$. The uncertainties in the prediction of $R_{13/8}^Z$ due to the scale variations, the PDFs and $\alpha_s(m_Z)$ are $^{+0.02\%}_{-0.3\%}$, $^{+0.9\%}_{-0.8\%}$ and $^{-0.03\%}_{-0.3\%}$, respectively. For the predictions of $D_{13/8}^{\gamma/Z}$, the uncertainties have been estimated as follows:

- The scale variations are considered uncorrelated between Z boson production and isolated-photon production since they are different processes.

- The PDF uncertainties are considered fully correlated between Z boson production and isolated-photon production.
- The $\alpha_s(m_Z)$ uncertainties are considered fully correlated between Z boson production and isolated-photon production. The uncertainty in the predictions due to that in $\alpha_s(m_Z)$ is estimated by using PDF sets in which $\alpha_s(m_Z)$ was fixed at 0.116 or 0.120.

In what follows, the resulting uncertainties in the predictions of $D_{13/8}^{\gamma/Z}$ are described. In the region $|\eta^\gamma| < 0.6$ ($0.6 < |\eta^\gamma| < 1.37$), the total relative uncertainty is below 2% for $125 \leq E_T^\gamma \leq 650$ (650) GeV and it rises to $\approx 4.5\%$ (3.3%) for $E_T^\gamma = 1300$ (1000) GeV. In both η^γ regions, the total uncertainty is mostly dominated by the variation of the scales. For $|\eta^\gamma| < 0.6$ and $E_T^\gamma \gtrsim 300$ GeV, the uncertainties in the PDFs are dominant, and for $0.6 < |\eta^\gamma| < 1.37$ and $E_T^\gamma \gtrsim 750$ GeV, the contributions from the scale variations and the PDFs are equally large. In the region $1.56 < |\eta^\gamma| < 1.81$ ($1.81 < |\eta^\gamma| < 2.37$), the total relative uncertainty is below 2% (3%) for $125 \leq E_T^\gamma \leq 350$ (470) GeV and it rises to $\approx 3\%$ (3.6%) for $E_T^\gamma = 600$ GeV. For $1.56 < |\eta^\gamma| < 1.81$, the uncertainty due to the variation of the scales is dominant, but for $1.81 < |\eta^\gamma| < 2.37$ and $E_T^\gamma \gtrsim 550$ GeV, the contributions from the scale variations and the PDFs are equally important.

The theoretical predictions based on the MMHT2014nnlo parameterisations of the proton PDFs for $D_{13/8}^{\gamma/Z}$ are about 1.4 at $E_T^\gamma = 125$ GeV and increase as E_T^γ increases, to 6–17 at the high end of the spectrum, depending on the η^γ region. The increase is larger for the forward regions than for the central regions. Predictions based on different parameterisations of the proton PDFs are compared; those based on MMHT2014nnlo, NNPDF3.0nnlo and CT14nnlo are found to be similar in all η^γ and E_T^γ regions. The predictions of $D_{13/8}^{\gamma/Z}$ based on HERAPDF2.0nnlo show some differences from the predictions based on the other PDFs in some regions of phase space, especially at high E_T^γ (see section 6).

5 Experimental uncertainties

The sources of systematic uncertainties that affect the measurements of the photon differential cross sections at $\sqrt{s} = 8$ and 13 TeV are detailed in refs. [8] and [9], respectively. A proper estimation of the systematic uncertainties in this measurement of cross-section ratios requires taking into account inter- \sqrt{s} correlations for each source of systematic uncertainty. Assuming no correlation provides a conservative estimate and full correlation is used only when justified. The estimation of the systematic uncertainties in the ratio has to take into account the changes in the data-taking conditions as well as changes in the detector conditions. The measurements at $\sqrt{s} = 8$ (13) TeV are based on data taken when the LHC operated with a bunch spacing of 50 (25) ns. During the data-taking period at $\sqrt{s} = 8$ (13) TeV there were on average 20.7 (13.5) proton-proton interactions per bunch crossing. Furthermore, the addition of the silicon-pixel insertable B-layer leads to extra material upstream of the calorimeters for data-taking at $\sqrt{s} = 13$ TeV. The procedures used to account for the impact of each source of systematic uncertainty on the ratio $R_{13/8}^\gamma$ are described below.

5.1 Photon energy scale

The systematic uncertainties associated with the photon energy scale and resolution represent the dominant experimental uncertainties in the measurements of the differential cross sections for inclusive isolated-photon production at both centre-of-mass energies. The uncertainty arising from the photon energy scale (γ ES) in $R_{13/8}^\gamma$ is estimated by decomposing it into uncorrelated sources for both the 8 TeV and 13 TeV measurements. A total of 22 individual components [23] influencing the energy scale and resolution of the photon are considered. Twenty of these components are common to both centre-of-mass energies. For some of the components the uncertainty is separated into a part which is correlated between the two centre-of-mass energies and another part which is specific to 13 TeV data and which is treated as uncorrelated (see below). These components include the uncertainties in: the overall energy scale adjustment using $Z \rightarrow e^+e^-$ events; the non-linearity of the energy measurement at the cell level; the relative calibration of the different calorimeter layers; the amount of material in front of the calorimeter; the modelling of the reconstruction of photon conversions; the modelling of the lateral shower shape; the modelling of the sampling term;⁴ and the measurement of the constant term in Z boson decays. The uncertainties depend on E_T^γ as well as on $|\eta^\gamma|$ and are larger in the region $1.56 < |\eta^\gamma| < 1.81$ due to the presence of more material than in other $|\eta^\gamma|$ regions. The remaining two components are specific to the 13 TeV measurement and take into account the differences in the configuration of the ATLAS detector between 2012 and 2015, namely changes in the LAr temperature, in the stability of the layer intercalibration and in the material in front of the calorimeters between Run 1 and Run 2 [39].

The procedure used to estimate the systematic uncertainty in $R_{13/8}^\gamma$ is as follows: all the uncertainty components described above are taken as fully correlated except for the uncertainty in the overall energy scale adjustment using $Z \rightarrow e^+e^-$ events, which for 2015 includes the effects of the changes in the configuration of the ATLAS detector mentioned above, and the uncertainties specific to the 13 TeV measurement. Calibration differences due to a change of optimal filtering coefficients and LAr timing samples between Run 1 and Run 2 are considered as a source of uncertainty in $R_{13/8}^\gamma$. The uncertainties in the photon energy scale due to pile-up are small enough compared to other uncertainties that the specific treatment of the correlation does not impact the results. The uncertainties due the photon energy resolution are treated as uncorrelated between $\sqrt{s} = 13$ TeV and 8 TeV since they include the effects of pile-up, which was different in the 2012 and 2015 data-taking periods.

The relative uncertainty due to the correlated components of the photon energy scale in $R_{13/8}^\gamma$ as a function of E_T^γ is shown in figure 2 for each region in η^γ . For illustration purposes, the result of estimating that part of the systematic uncertainty assuming no correlation is also shown in this figure: the results obtained using the complete correlation model exhibit a large reduction in comparison with those in which the correlations are ignored. This demonstrates that a proper treatment of the inter- \sqrt{s} correlations in the

⁴The relative energy resolution is parameterised as $\sigma(E)/E = a/\sqrt{E} \oplus c$, where a is the sampling term and c is the constant term.

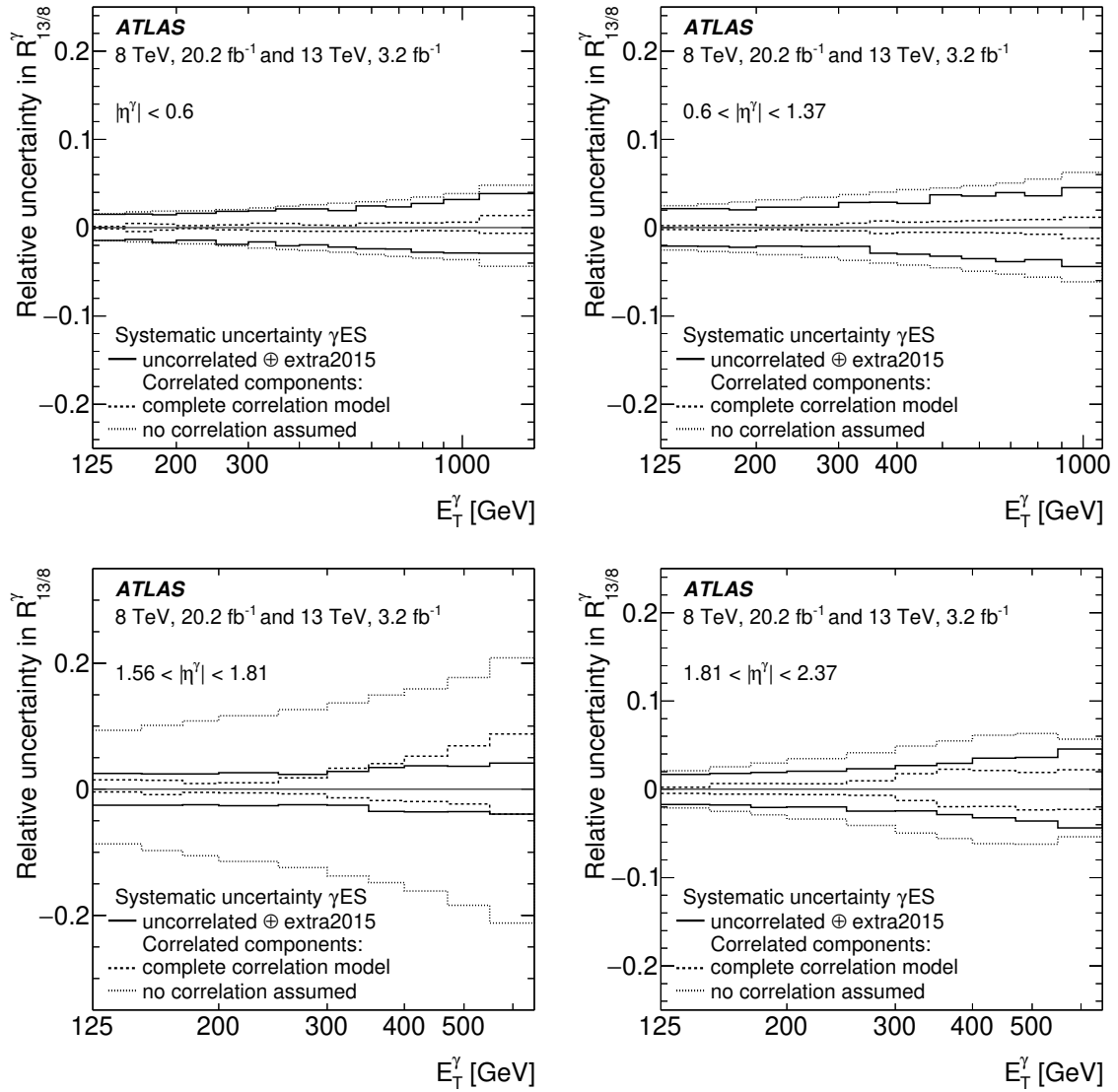


Figure 2. Relative systematic uncertainty in $R_{13/8}^\gamma$ as a function of E_T^γ for different η^γ regions due to the γ ES correlated components (dashed lines). For comparison, the results of considering the components as uncorrelated are also shown (dotted lines) to illustrate the reduction in the size of the systematic uncertainty when the proper treatment is applied. The relative uncertainty due to the uncorrelated components of the photon energy scale and the components specific to 2015 is also shown (solid lines).

systematic uncertainties associated with the photon energy scale is important. In addition, the relative uncertainty due to the uncorrelated components of the photon energy scale and the components specific to 2015 is also shown in figure 2.

5.2 Other sources of experimental uncertainty

The other sources of experimental uncertainty affecting the measurements are treated as listed below. For several of these sources, the uncertainties in the measurements at

$\sqrt{s} = 13$ TeV and 8 TeV are treated conservatively as uncorrelated since their impact is small.

- *Statistical uncertainties.* The statistical uncertainties in both the data and the Monte Carlo simulations at $\sqrt{s} = 13$ and 8 TeV are treated as uncorrelated.
- *Luminosity uncertainty.* The luminosity uncertainties associated to the measurements of the photon cross sections at $\sqrt{s} = 8$ TeV and 13 TeV are dominated by effects that are uncorrelated between different centre-of-mass energies and data-taking periods. The resulting relative uncertainty in $R_{13/8}^\gamma$ amounts to $\pm 2.8\%$.
- *Trigger uncertainty.* The uncertainties in the trigger efficiency are treated as uncorrelated for data at different \sqrt{s} . Different trigger requirements were used during 2012 and 2015. In addition, during 2012 a three-level trigger system was used to select events while in 2015 a two-level system was employed.
- *Photon-identification uncertainty.* In both measurements, the photon identification is based primarily on shower shapes in the EM calorimeter. These uncertainties are treated as uncorrelated since different methods are used at $\sqrt{s} = 13$ TeV [40] and 8 TeV [22] to estimate the uncertainties; in addition, the photon identification criteria are re-optimised for data taken at 13 TeV.
- *Modelling of the photon isolation in Monte Carlo.* In both measurements, the photon candidate is required to be isolated. The in-time (out-of-time) pile-up, which is due to additional pp collisions in the same (earlier or later than) bunch crossing as the event of interest, was different in 2012 and 2015 due to the different LHC conditions, namely the instantaneous luminosity and the bunch spacing. For simulated events, data-driven corrections to E_T^{iso} are applied such that the peak position in the E_T^{iso} distribution coincides in data and simulation. These uncertainties are treated as uncorrelated since different methods are used at $\sqrt{s} = 13$ and 8 TeV for the corrections and uncertainties.
- *Choice of background control regions.* The background subtraction is performed using a data-driven two-dimensional sideband technique based on background control regions. A plane is formed by the variable E_T^{iso} and a binary variable that encapsulates the photon identification (“tight” vs. “non-tight”). A photon candidate is classified as “non-tight” if it fails at least one of four requirements on the shower-shape variables computed from the energy deposits in the first layer of the EM calorimeter, but satisfies the tight requirement on the total lateral shower width in the first layer and all the other tight identification criteria in other layers [22]. The plane is divided into four regions: region A for tight isolated photons, region B for tight non-isolated photons, region C for non-tight isolated photons and region D for non-tight non-isolated photons. The background control regions B, C and D are specified by lower and upper limits on E_T^{iso} as well as by the definition of “non-tight” photon candidates. Variations of the limits and alternative definitions of the “non-tight” condition are used to estimate

the uncertainties due to the choice of background control regions. These uncertainties are treated as uncorrelated since, as mentioned above, the photon-identification requirements are re-optimised for data-taking at 13 TeV.

- *Photon identification and isolation correlation in the background.* In the background subtraction method described above, the photon isolation and identification variables are assumed to be uncorrelated for background events. Uncertainties due to this assumption are estimated by using validation regions, which are dominated by background. These uncertainties are treated as uncorrelated since, as mentioned above, the photon-identification requirements are re-optimised for data-taking at 13 TeV.
- *Signal modelling.* MC simulations of signal processes are used to estimate the signal leakage fractions in the background control regions and to compute the unfolding corrections. For both measurements, at $\sqrt{s} = 13$ and 8 TeV, the PYTHIA [34] generator is used for the nominal results and the SHERPA [41] generator for studies of systematic uncertainties related to the model dependence. The uncertainty due to the mixture of direct and fragmentation processes in the simulations is estimated using the MC simulations of PYTHIA. These uncertainties are treated as uncorrelated since different methods and versions of the generators are used at $\sqrt{s} = 13$ TeV and 8 TeV to estimate the uncertainties. For $\sqrt{s} = 13$ (8) TeV, PYTHIA 8.186 with the A14 tune (PYTHIA 8.165 with the AU2 tune) and SHERPA 2.1.1 (SHERPA 1.4.0) with the CT10 tune are used. For the 8 TeV analysis the results of using the default admixture of direct and fragmentation contributions in PYTHIA are compared with those using an optimal admixture obtained by fitting the two components to the data; for the 13 TeV analysis the results of enhancing the fragmentation contribution by a factor of two or removing it completely are compared with those using the default admixture.
- *QCD-cascade and hadronisation model dependence.* These uncertainties are treated as uncorrelated since different versions and tunes of the Monte Carlo generators PYTHIA and SHERPA are used at $\sqrt{s} = 13$ and 8 TeV.
- *Pile-up uncertainties.* The in-time and out-of-time pile-up in the 2012 and 2015 data-taking periods were different. Conservatively and given the fact that the impact is rather small, these uncertainties are treated as uncorrelated.

5.3 Total experimental uncertainties in $R_{13/8}^\gamma$

Using the prescription for the treatment of the correlations between the measurements described in the previous sections, the systematic uncertainties in $R_{13/8}^\gamma$ are evaluated. Figure 3 shows the relative uncertainties in $R_{13/8}^\gamma$ due to (i) the photon energy scale, which includes the correlated and uncorrelated contributions as well as the additional ones associated with 2015 data, (ii) the remaining sources of systematic uncertainty excluding that in the luminosity measurements and (iii) the sum in quadrature of the non- γ ES uncertainties and the uncertainty due to the luminosity determination. The uncertainty due to the photon energy scale increases as E_T^γ increases and is larger for the region

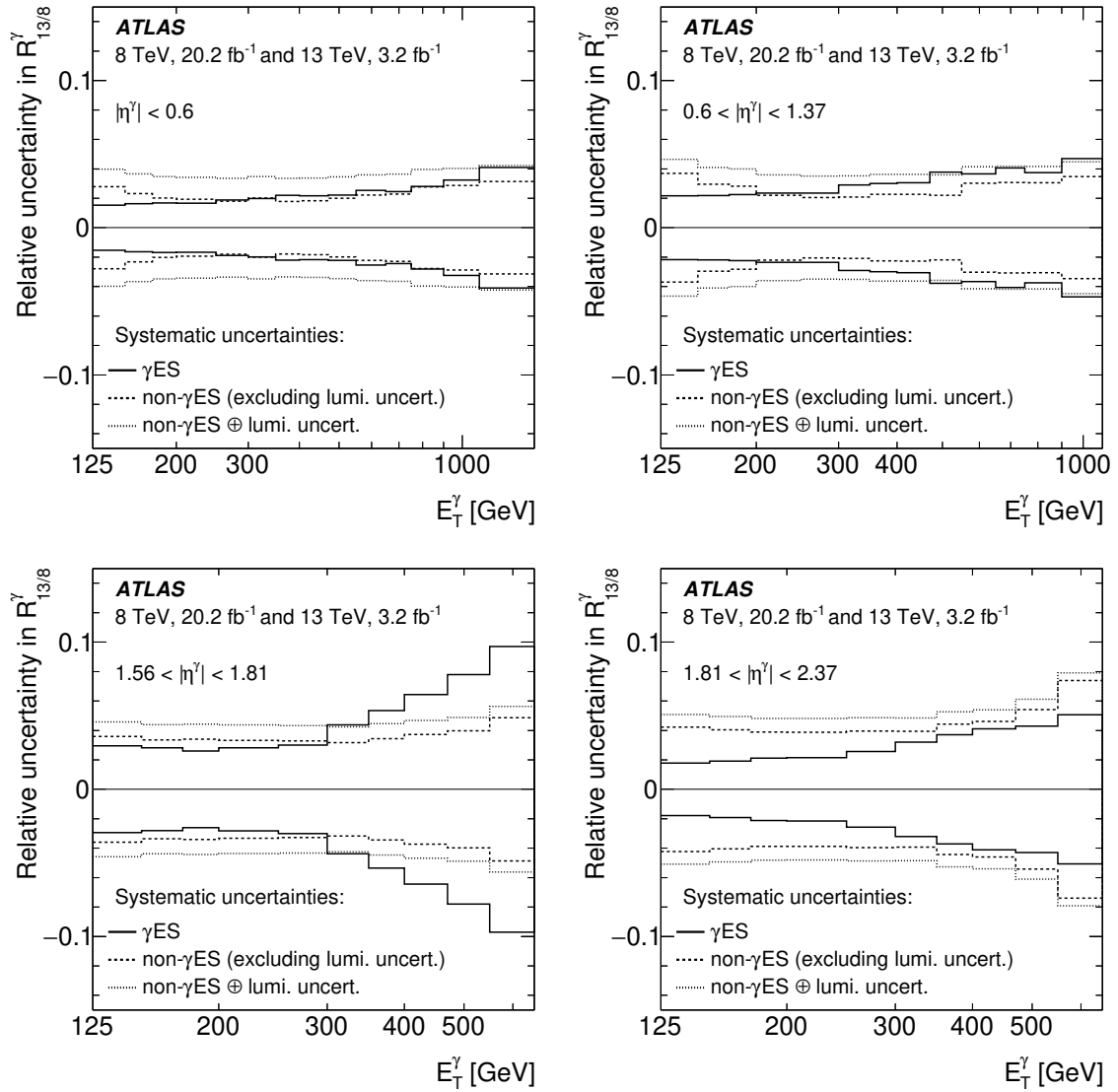


Figure 3. Relative systematic uncertainty in $R_{13/8}^\gamma$ as a function of E_T^γ for different η^γ regions due to different sources: γ ES uncertainties (solid lines), non- γ ES uncertainties excluding the luminosity uncertainty (dashed lines) and non- γ ES and luminosity uncertainties added in quadrature (dotted lines).

$1.56 < |\eta^\gamma| < 1.81$ due to more material in front of the calorimeters than in the other regions. From figure 3 it is concluded that the relative uncertainty in $R_{13/8}^\gamma$ due to the photon energy scale is no longer the dominant uncertainty, except for $E_T^\gamma > 300$ GeV in the regions $0.6 < |\eta^\gamma| < 1.37$ and $1.56 < |\eta^\gamma| < 1.81$.

The total relative experimental systematic uncertainty in $R_{13/8}^\gamma$ is shown in figure 4, as is its sum in quadrature with the relative statistical uncertainty. In all pseudo-rapidity regions, the systematic uncertainty is dominant compared to the statistical uncertainty up to $E_T^\gamma \sim 300$ GeV, while the measurement becomes statistically limited for $E_T^\gamma \gtrsim 600$ GeV.

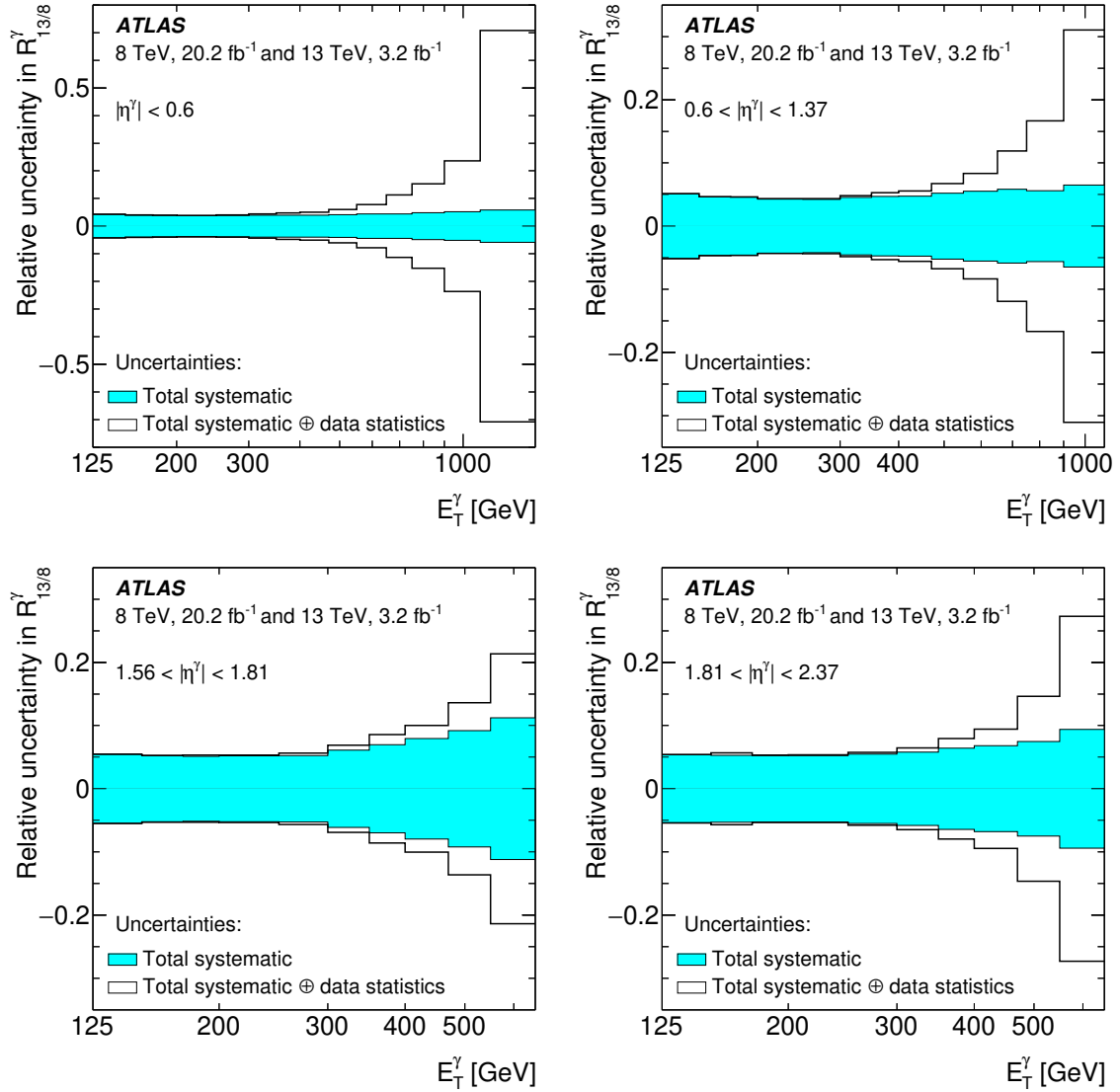


Figure 4. Total relative systematic uncertainty in $R_{13/8}^\gamma$ as a function of E_T^γ for different η^γ regions (shaded band) and the sum in quadrature of the total relative systematic and statistical uncertainties (solid line).

There are significant correlations in the systematic uncertainties across bins in E_T^γ ; the uncertainty in the luminosity measurement is one of the major contributions and is fully correlated for all bins in E_T^γ and all η^γ regions.

5.4 Total experimental uncertainties in $D_{13/8}^{\gamma/Z}$

The total relative experimental uncertainty in $D_{13/8}^{\gamma/Z}$ is obtained as follows:

- The uncertainty in $R_{13/8}^\gamma$ as presented in section 5.2, not including the contribution from the luminosity, is used. The uncertainty in the luminosity measurement cancels out in $D_{13/8}^{\gamma/Z}$ since the measurements of $R_{13/8}^\gamma$ and $R_{13/8}^Z$ are performed using data taken during the same periods of 2012 and 2015.

- The statistical (0.1%) and systematic (0.7%) uncertainties in $R_{13/8}^Z$ are added in quadrature to the total uncertainty in $R_{13/8}^\gamma$ (see section 5.3). The systematic uncertainty in $R_{13/8}^Z$ is dominated by the uncertainty in the lepton reconstruction and efficiency; the correlation between the small contribution due to the electron energy scale and the photon energy scale in $D_{13/8}^{\gamma/Z}$ can be safely neglected.

The relative total systematic uncertainty in the measured $D_{13/8}^{\gamma/Z}$ as a function of E_T^γ is shown for each η^γ region in figure 5. For comparison, the relative total systematic uncertainty in $R_{13/8}^\gamma$ is also shown. Since the total systematic uncertainty in $R_{13/8}^Z$ is at least a factor of three smaller than the total systematic uncertainty in $R_{13/8}^\gamma$, the effect of adding in quadrature such a contribution has a small impact. On the other hand, the luminosity uncertainty, which amounts to 2.8% for $R_{13/8}^\gamma$, cancels out in $D_{13/8}^{\gamma/Z}$ and this has a significant impact except at high E_T^γ , where the statistical uncertainty dominates.

6 Results

The measurements of the ratios of cross sections are presented and the main features exhibited by the data are described. The theoretical predictions are compared with the experimental results for both $R_{13/8}^\gamma$ and $D_{13/8}^{\gamma/Z}$.

6.1 Results for $R_{13/8}^\gamma$

The measured $R_{13/8}^\gamma$ as a function of E_T^γ in different regions of $|\eta^\gamma|$ is shown in figures 6 and 7 and table 1. The measured $R_{13/8}^\gamma$ increases with E_T^γ from approximately 2 at $E_T^\gamma = 125$ GeV to approximately 8–29 at the high end of the spectrum. In the forward regions the increase of $R_{13/8}^\gamma$ with E_T^γ is larger than in the central regions. At a fixed value of E_T^γ , the measured ratio increases as $|\eta^\gamma|$ increases.

The NLO QCD predictions based on the MMHT2014 PDFs are compared with the measured $R_{13/8}^\gamma$ in figures 6 and 7. Even though there is a tendency for the predictions to underestimate the data, the measurements and the theory are consistent within the uncertainties; in particular, the increase as E_T^γ increases and the dependence on η^γ are reproduced by the predictions. To study in more detail the description of the measured $R_{13/8}^\gamma$ by the NLO QCD predictions, the ratio of the predictions to the data is shown in figures 6 and 7. In these figures, the predictions based on different PDFs, namely MMHT2014, CT14, NNPDF3.0, HERAPDF2.0 and ABMP16 are included to ascertain the sensitivity of $R_{13/8}^\gamma$ to the proton PDFs. The predictions generally agree with the measured $R_{13/8}^\gamma$ within the experimental and theoretical uncertainties for all PDFs considered within the measured range.

The comparison of the NLO QCD predictions for $d\sigma/dE_T^\gamma$ and the measured differential cross sections in the ATLAS analyses at 8 and 13 TeV is limited by the theoretical uncertainties, which are larger than those of experimental nature and dominated by the uncertainties due to the terms beyond NLO. The theoretical uncertainties in $d\sigma/dE_T^\gamma$ are 10–15%; in contrast, the theoretical uncertainties for $R_{13/8}^\gamma$ are below 2% for most of the phase space considered and smaller than the experimental uncertainties. The experimental

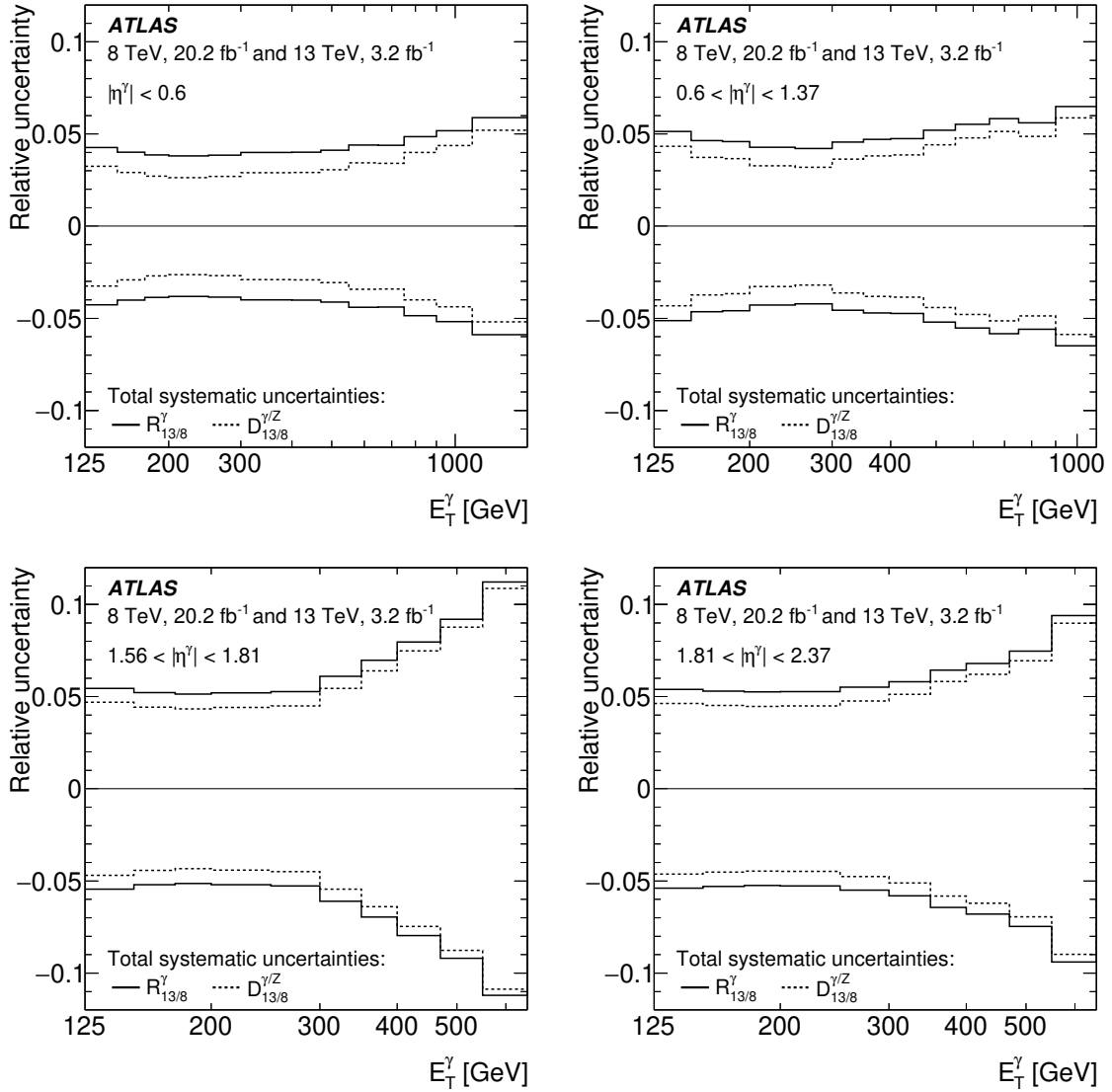


Figure 5. Relative total systematic uncertainty in $R_{13/8}^\gamma$ (solid lines) and in $D_{13/8}^{\gamma/Z}$ (dashed lines) as functions of E_T^γ for different η^γ regions.

uncertainties in $R_{13/8}^\gamma$ also benefit from a significant reduction since the systematic uncertainties partially cancel out, in particular those related to the photon energy scale, which is dominant in the measurement of $d\sigma/dE_T^\gamma$. The total systematic uncertainty in $R_{13/8}^\gamma$ is below 5% for most of the phase space considered. Thus, the significant reduction of the experimental and theoretical uncertainties in $R_{13/8}^\gamma$ allows a more stringent test of NLO QCD. The overall level of agreement between data and the NLO QCD predictions based on several parameterisations of the proton PDFs within these reduced uncertainties validates the description of the evolution of isolated-photon production in pp collisions with the centre-of-mass energy.

| E_T^γ [GeV] | $R_{13/8}^\gamma \pm \text{statistical uncertainty} \pm \text{systematic uncertainty}$ | | | |
|--------------------|--|------------------------------|-------------------------------|-------------------------------|
| | $ \eta^\gamma < 0.6$ | $0.6 < \eta^\gamma < 1.37$ | $1.56 < \eta^\gamma < 1.81$ | $1.81 < \eta^\gamma < 2.37$ |
| 125–150 | $2.08 \pm 0.01 \pm 0.09$ | $2.11 \pm 0.01 \pm 0.11$ | $2.16 \pm 0.01 \pm 0.12$ | $2.25 \pm 0.01 \pm 0.12$ |
| 150–175 | $2.12 \pm 0.01 \pm 0.08$ | $2.15 \pm 0.01 \pm 0.10$ | $2.22 \pm 0.02 \pm 0.12$ | $2.46 \pm 0.05 \pm 0.13$ |
| 175–200 | $2.23 \pm 0.02 \pm 0.09$ | $2.21 \pm 0.02 \pm 0.10$ | $2.35 \pm 0.03 \pm 0.12$ | $2.66 \pm 0.03 \pm 0.14$ |
| 200–250 | $2.28 \pm 0.02 \pm 0.09$ | $2.28 \pm 0.02 \pm 0.10$ | $2.63 \pm 0.03 \pm 0.14$ | $3.10 \pm 0.03 \pm 0.16$ |
| 250–300 | $2.42 \pm 0.03 \pm 0.09$ | $2.43 \pm 0.03 \pm 0.10$ | $3.06 \pm 0.06 \pm 0.16$ | $3.89 \pm 0.06 \pm 0.21$ |
| 300–350 | $2.53 \pm 0.04 \pm 0.10$ | $2.72 \pm 0.04 \pm 0.12$ | $3.67 \pm 0.12 \pm 0.22$ | $5.18 \pm 0.15 \pm 0.30$ |
| 350–400 | $2.64 \pm 0.07 \pm 0.11$ | $2.78 \pm 0.07 \pm 0.13$ | $3.95 \pm 0.20 \pm 0.27$ | $6.66 \pm 0.31 \pm 0.43$ |
| 400–470 | $2.83 \pm 0.09 \pm 0.11$ | $3.11 \pm 0.09 \pm 0.15$ | $5.73 \pm 0.35 \pm 0.46$ | $8.43 \pm 0.55 \pm 0.57$ |
| 470–550 | $3.11 \pm 0.14 \pm 0.13$ | $3.46 \pm 0.15 \pm 0.18$ | $8.68 \pm 0.87 \pm 0.80$ | $16.1 \pm 2.0 \pm 1.2$ |
| 550–650 | $3.28 \pm 0.21 \pm 0.14$ | $4.35 \pm 0.27 \pm 0.24$ | $12.5 \pm 2.3 \pm 1.4$ | $29.3 \pm 7.5 \pm 2.8$ |
| 650–750 | $4.00 \pm 0.42 \pm 0.18$ | $5.03 \pm 0.52 \pm 0.29$ | | |
| 750–900 | $5.20 \pm 0.75 \pm 0.25$ | $8.4 \pm 1.3 \pm 0.5$ | | |
| 900–1100 | $9.9 \pm 2.3 \pm 0.5$ | $7.9 \pm 2.4 \pm 0.5$ | | |
| 1100–1500 | $13.9 \pm 9.8 \pm 0.8$ | | | |

Table 1. The measured $R_{13/8}^\gamma$ as a function of E_T^γ together with the statistical uncertainty and total systematic uncertainty in different regions of $|\eta^\gamma|$.

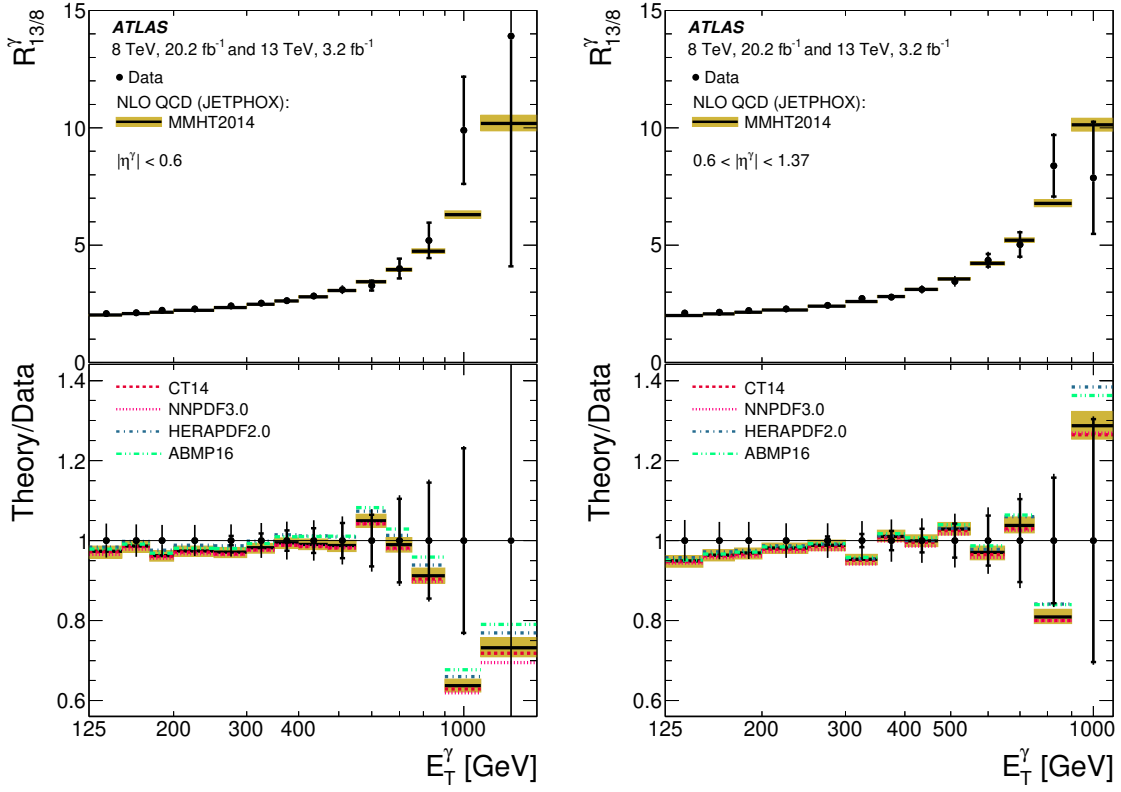


Figure 6. The measured $R_{13/8}^\gamma$ (dots) as a function of E_T^γ in different regions of $|\eta^\gamma|$. The NLO QCD predictions based on the MMHT2014 PDFs (black lines) are also shown. The inner (outer) error bars represent the statistical (total) uncertainties. The shaded band represents the theoretical uncertainty in the predictions. For most of the points, the error bars are smaller than the marker size and, thus, not visible. The lower part of the figures shows the ratio of the NLO QCD predictions based on the MMHT2014 PDFs to the measured $R_{13/8}^\gamma$ (black lines). The ratios of the NLO QCD predictions based on different PDF sets to the measured $R_{13/8}^\gamma$ are also included.

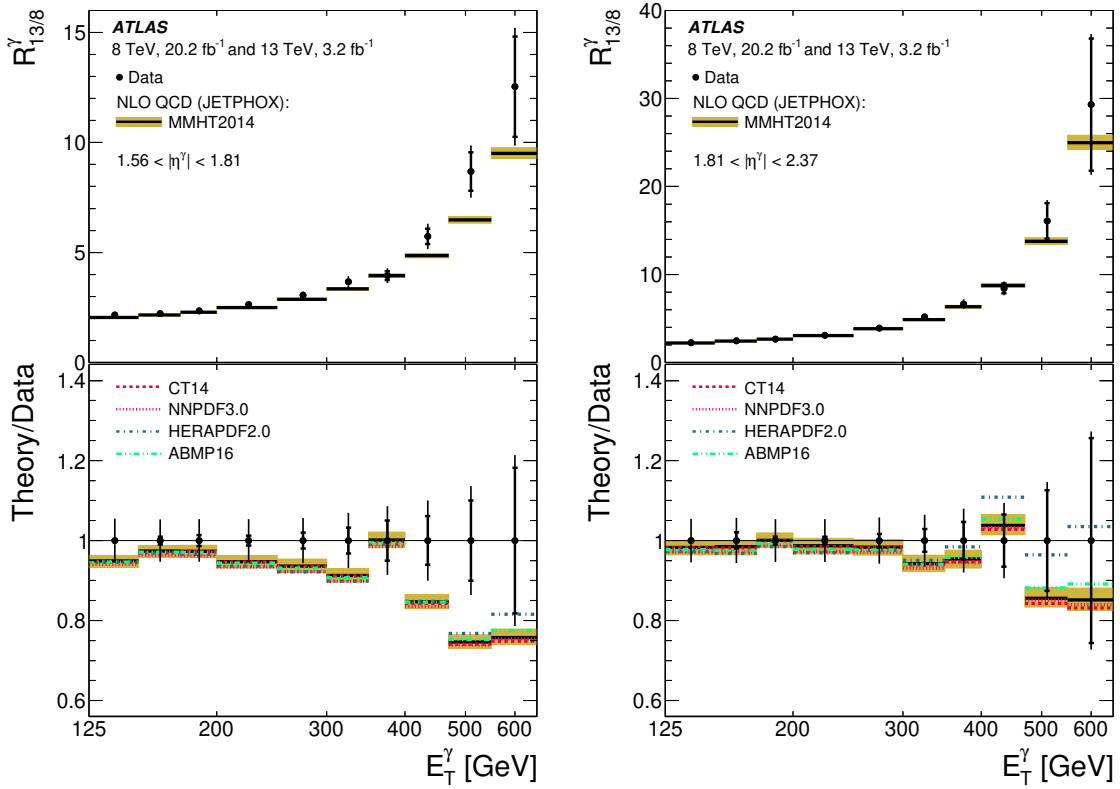


Figure 7. The measured $R_{13/8}^\gamma$ (dots) as a function of E_T^γ in different regions of $|\eta^\gamma|$. The NLO QCD predictions based on the MMHT2014 PDFs (black lines) are also shown. The inner (outer) error bars represent the statistical (total) uncertainties. The shaded band represents the theoretical uncertainty in the predictions. For most of the points, the error bars are smaller than the marker size and, thus, not visible. The lower part of the figures shows the ratio of the NLO QCD predictions based on the MMHT2014 PDFs to the measured $R_{13/8}^\gamma$ (black lines). The ratios of the NLO QCD predictions based on different PDF sets to the measured $R_{13/8}^\gamma$ are also included.

| E_{T}^{γ} [GeV] | $D_{13/8}^{\gamma/Z} \pm \text{statistical uncertainty} \pm \text{systematic uncertainty}$ | | | |
|-------------------------------|--|--------------------------------|---------------------------------|---------------------------------|
| | $ \eta^{\gamma} < 0.6$ | $0.6 < \eta^{\gamma} < 1.37$ | $1.56 < \eta^{\gamma} < 1.81$ | $1.81 < \eta^{\gamma} < 2.37$ |
| 125–150 | $1.35 \pm 0.01 \pm 0.04$ | $1.37 \pm 0.00 \pm 0.06$ | $1.40 \pm 0.01 \pm 0.07$ | $1.46 \pm 0.01 \pm 0.07$ |
| 150–175 | $1.38 \pm 0.01 \pm 0.04$ | $1.40 \pm 0.01 \pm 0.05$ | $1.44 \pm 0.01 \pm 0.06$ | $1.60 \pm 0.03 \pm 0.07$ |
| 175–200 | $1.45 \pm 0.01 \pm 0.04$ | $1.44 \pm 0.01 \pm 0.05$ | $1.53 \pm 0.02 \pm 0.07$ | $1.73 \pm 0.02 \pm 0.08$ |
| 200–250 | $1.49 \pm 0.01 \pm 0.04$ | $1.49 \pm 0.01 \pm 0.05$ | $1.71 \pm 0.02 \pm 0.08$ | $2.02 \pm 0.02 \pm 0.09$ |
| 250–300 | $1.57 \pm 0.02 \pm 0.04$ | $1.58 \pm 0.02 \pm 0.05$ | $1.99 \pm 0.04 \pm 0.09$ | $2.53 \pm 0.04 \pm 0.12$ |
| 300–350 | $1.65 \pm 0.03 \pm 0.05$ | $1.77 \pm 0.03 \pm 0.06$ | $2.39 \pm 0.08 \pm 0.13$ | $3.37 \pm 0.10 \pm 0.17$ |
| 350–400 | $1.72 \pm 0.04 \pm 0.05$ | $1.81 \pm 0.04 \pm 0.07$ | $2.57 \pm 0.13 \pm 0.16$ | $4.33 \pm 0.20 \pm 0.25$ |
| 400–470 | $1.84 \pm 0.06 \pm 0.05$ | $2.02 \pm 0.06 \pm 0.08$ | $3.73 \pm 0.23 \pm 0.28$ | $5.48 \pm 0.36 \pm 0.34$ |
| 470–550 | $2.02 \pm 0.09 \pm 0.06$ | $2.25 \pm 0.10 \pm 0.10$ | $5.65 \pm 0.57 \pm 0.50$ | $10.5 \pm 1.3 \pm 0.7$ |
| 550–650 | $2.13 \pm 0.14 \pm 0.07$ | $2.83 \pm 0.18 \pm 0.14$ | $8.2 \pm 1.5 \pm 0.9$ | $19.1 \pm 4.9 \pm 1.7$ |
| 650–750 | $2.60 \pm 0.27 \pm 0.09$ | $3.27 \pm 0.34 \pm 0.17$ | | |
| 750–900 | $3.39 \pm 0.49 \pm 0.14$ | $5.46 \pm 0.86 \pm 0.27$ | | |
| 900–1100 | $6.4 \pm 1.5 \pm 0.3$ | $5.1 \pm 1.6 \pm 0.3$ | | |
| 1100–1500 | $9.1 \pm 6.4 \pm 0.5$ | | | |

Table 2. The measured $D_{13/8}^{\gamma/Z}$ as a function of E_T^γ together with the statistical and total systematic uncertainty in different regions of $|\eta^\gamma|$.

6.2 Results for $D_{13/8}^{\gamma/Z}$

The measurements of $D_{13/8}^{\gamma/Z}$ as a function of E_T^γ in different regions of $|\eta^\gamma|$ are shown in figures 8 and 9 and table 2. The measured $D_{13/8}^{\gamma/Z}$ increases with E_T^γ from approximately 1.4 at $E_T^\gamma = 125$ GeV to approximately 5–19 at the high end of the spectrum. At a fixed value of E_T^γ , the measured ratio increases as $|\eta^\gamma|$ increases.

The theoretical predictions based on the MMHT2014nnlo PDFs are compared with the measured $D_{13/8}^{\gamma/Z}$ in figures 8 and 9. The predictions are in agreement with the measured $D_{13/8}^{\gamma/Z}$; in particular, the increase as E_T^γ increases and the dependence on η^γ are reproduced by the predictions. As an example, the measured value of $D_{13/8}^{\gamma/Z}$ at the lowest- E_T^γ point for $|\eta^\gamma| < 0.6$ is 1.35 ± 0.04 while the prediction using MMHT2014 is 1.31 ± 0.02 . The tendency of the predictions to underestimate the data observed in $R_{13/8}^\gamma$ is also present in $D_{13/8}^{\gamma/Z}$; nevertheless, they are still consistent with each other within the uncertainties. To study in more detail the description of the measured $D_{13/8}^{\gamma/Z}$ by the theoretical predictions, the ratio of the predictions to the data is shown in figures 8 and 9. In these figures, the predictions based on different PDFs, namely MMHT2014nnlo, CT14nnlo, NNPDF3.0nnlo and HERAPDF2.0nnlo are included to estimate the sensitivity of $D_{13/8}^{\gamma/Z}$ to the proton PDFs. The predictions generally agree with the measured $D_{13/8}^{\gamma/Z}$ within the experimental and theoretical uncertainties for all PDFs considered within the measured range.

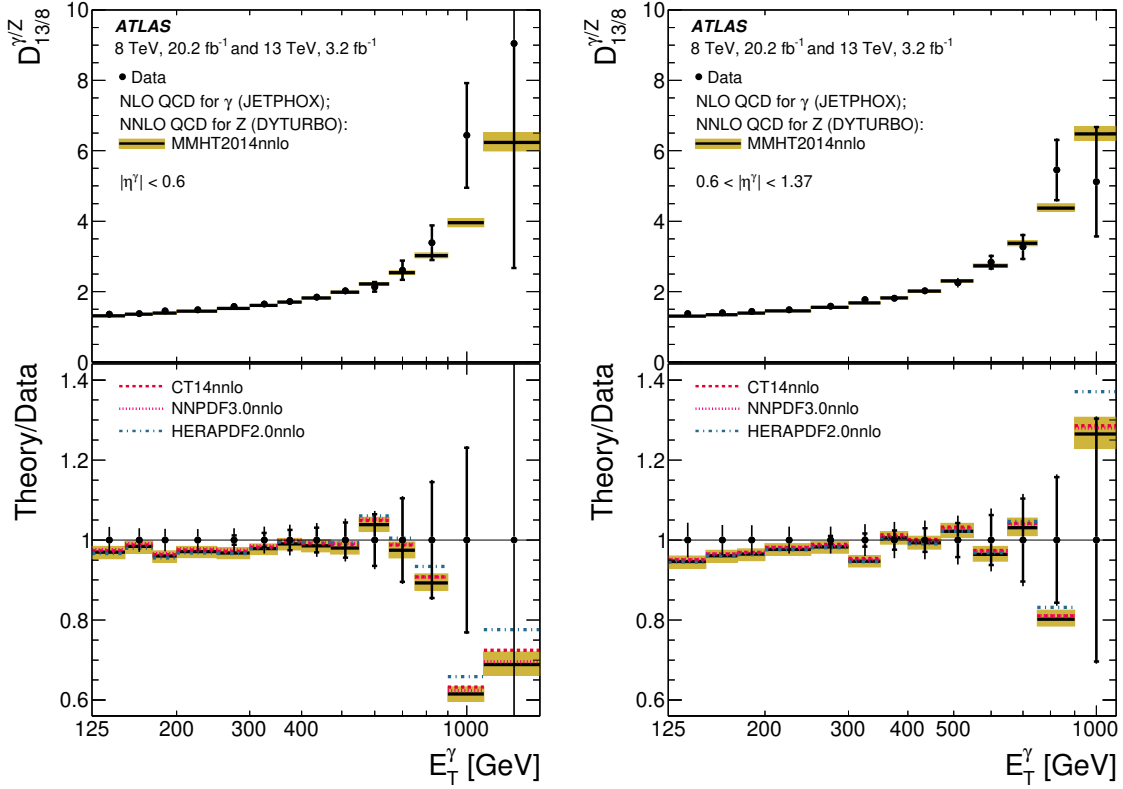


Figure 8. The measured $D_{13/8}^{\gamma/Z}$ (dots) as a function of E_T^γ in different regions of $|\eta^\gamma|$. The pQCD predictions based on the MMHT2014nnlo PDFs (black lines) are also shown. The inner (outer) error bars represent the statistical (total) uncertainties. The shaded band represents the theoretical uncertainty in the predictions. For most of the points, the error bars are smaller than the marker size and, thus, not visible. The lower part of the figures shows the ratio of the pQCD predictions based on the MMHT2014nnlo PDFs to the measured $D_{13/8}^{\gamma/Z}$ (black lines). The ratios of the pQCD predictions based on different PDF sets to the measured $D_{13/8}^{\gamma/Z}$ are also included.

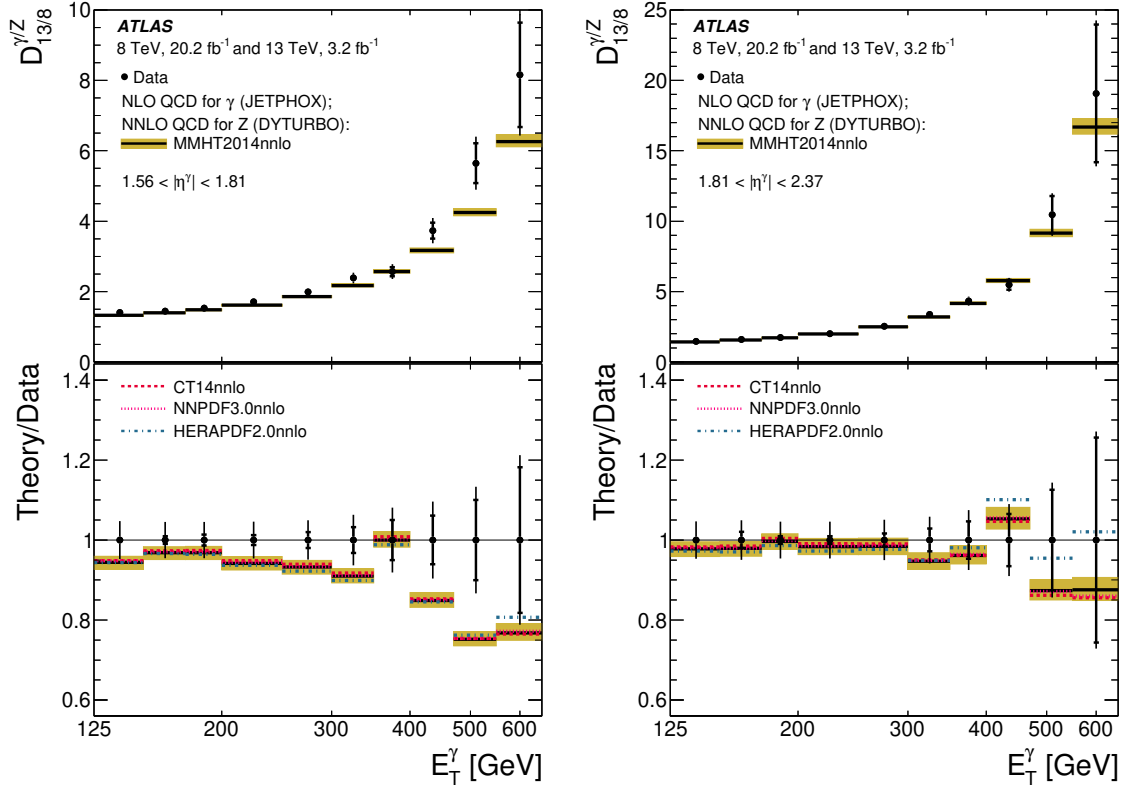


Figure 9. The measured $D_{13/8}^{\gamma/Z}$ (dots) as a function of E_T^γ in different regions of $|\eta^\gamma|$. The pQCD predictions based on the MMHT2014nnlo PDFs (black lines) are also shown. The inner (outer) error bars represent the statistical (total) uncertainties. The shaded band represents the theoretical uncertainty in the predictions. For most of the points, the error bars are smaller than the marker size and, thus, not visible. The lower part of the figures shows the ratio of the pQCD predictions based on the MMHT2014nnlo PDFs to the measured $D_{13/8}^{\gamma/Z}$ (black lines). The ratios of the pQCD predictions based on different PDF sets to the measured $D_{13/8}^{\gamma/Z}$ are also included.

7 Summary and conclusions

The ratio of cross sections for inclusive isolated-photon production in pp collisions at $\sqrt{s} = 13$ and 8 TeV ($R_{13/8}^\gamma$) is measured using the ATLAS detector at the LHC. The integrated luminosities of the 13 TeV and 8 TeV datasets are 3.2 fb^{-1} and 20.2 fb^{-1} , respectively. The ratio of differential cross sections as a function of E_T^γ is measured in different regions of $|\eta^\gamma|$ for photons with $125 < E_T^\gamma < 1500 \text{ GeV}$ and $|\eta^\gamma| < 2.37$, excluding the region $1.37 < |\eta^\gamma| < 1.56$. In the estimation of the experimental systematic uncertainties for $R_{13/8}^\gamma$, the correlations between the measurements at the two centre-of-mass energies are taken into account. The systematic uncertainty arising from the photon energy scale, which is dominant for the individual cross sections, is reduced significantly in $R_{13/8}^\gamma$ and no longer the dominant uncertainty. The total systematic uncertainty for $R_{13/8}^\gamma$ is below 5% in most of the phase space of the measurement. The measurements can be useful for tuning models of prompt-photon production in pp collisions.

The predictions from NLO QCD calculations are compared with the measured $R_{13/8}^\gamma$. The theoretical uncertainties affecting these predictions are also evaluated taking into account the correlations between the two centre-of-mass energies, resulting in a significant reduction in the uncertainty of the predicted $R_{13/8}^\gamma$. The theoretical uncertainties in $R_{13/8}^\gamma$ are below 2% for most of the phase space of the measurement, in contrast with those in the individual cross-section predictions, which have approximately 10–15% uncertainties. Thus, the comparison of the predictions with the measured $R_{13/8}^\gamma$ represents a stringent test of the pQCD calculations. Within these reduced experimental and theoretical uncertainties, the NLO QCD predictions based on several parameterisations of the proton PDFs agree with the data. Even though there is a tendency of the predictions to underestimate the data, the measurements and the theory are consistent within the uncertainties. The level of agreement achieved validates the description of the evolution of isolated-photon production in pp collisions from $\sqrt{s} = 8$ to 13 TeV.

A double ratio of cross sections is also measured: the ratio of $R_{13/8}^\gamma$ to the ratio of the fiducial cross sections for Z boson production at 13 and 8 TeV ($R_{13/8}^Z$). In $D_{13/8}^{\gamma/Z} \equiv R_{13/8}^\gamma/R_{13/8}^Z$, the uncertainty due to the luminosity cancels out at the expense of a small increase in the systematic uncertainty from all other sources, leading to a more precise measurement of the evolution of the inclusive-photon cross section with the centre-of-mass energy normalised to the evolution of the Z boson cross section. The theoretical prediction, based on NNLO (NLO) QCD calculations for Z boson (inclusive-photon) production, describes the measurements within the theoretical uncertainties and the reduced experimental uncertainties.

Acknowledgments

We thank CERN for the very successful operation of the LHC, as well as the support staff from our institutions without whom ATLAS could not be operated efficiently.

We acknowledge the support of ANPCyT, Argentina; YerPhI, Armenia; ARC, Australia; BMFWF and FWF, Austria; ANAS, Azerbaijan; SSTC, Belarus; CNPq and FAPESP,

Brazil; NSERC, NRC and CFI, Canada; CERN; CONICYT, Chile; CAS, MOST and NSFC, China; COLCIENCIAS, Colombia; MSMT CR, MPO CR and VSC CR, Czech Republic; DNRF and DNSRC, Denmark; IN2P3-CNRS, CEA-DRF/IRFU, France; SRNSFG, Georgia; BMBF, HGF, and MPG, Germany; GSRT, Greece; RGC, Hong Kong SAR, China; ISF and Benoziyo Center, Israel; INFN, Italy; MEXT and JSPS, Japan; CNRST, Morocco; NWO, Netherlands; RCN, Norway; MNiSW and NCN, Poland; FCT, Portugal; MNE/IFA, Romania; MES of Russia and NRC KI, Russian Federation; JINR; MESTD, Serbia; MSSR, Slovakia; ARRS and MIZŠ, Slovenia; DST/NRF, South Africa; MINECO, Spain; SRC and Wallenberg Foundation, Sweden; SERI, SNSF and Cantons of Bern and Geneva, Switzerland; MOST, Taiwan; TAEK, Turkey; STFC, United Kingdom; DOE and NSF, United States of America. In addition, individual groups and members have received support from BCKDF, CANARIE, CRC and Compute Canada, Canada; COST, ERC, ERDF, Horizon 2020, and Marie Skłodowska-Curie Actions, European Union; Investissements d’Avenir Labex and Idex, ANR, France; DFG and AvH Foundation, Germany; Herakleitos, Thales and Aristeia programmes co-financed by EU-ESF and the Greek NSRF, Greece; BSF-NSF and GIF, Israel; CERCA Programme Generalitat de Catalunya, Spain; The Royal Society and Leverhulme Trust, United Kingdom.

The crucial computing support from all WLCG partners is acknowledged gratefully, in particular from CERN, the ATLAS Tier-1 facilities at TRIUMF (Canada), NDGF (Denmark, Norway, Sweden), CC-IN2P3 (France), KIT/GridKA (Germany), INFN-CNAF (Italy), NL-T1 (Netherlands), PIC (Spain), ASGC (Taiwan), RAL (U.K.) and BNL (U.S.A.), the Tier-2 facilities worldwide and large non-WLCG resource providers. Major contributors of computing resources are listed in ref. [42].

Open Access. This article is distributed under the terms of the Creative Commons Attribution License ([CC-BY 4.0](https://creativecommons.org/licenses/by/4.0/)), which permits any use, distribution and reproduction in any medium, provided the original author(s) and source are credited.

References

- [1] D. d’Enterria and J. Rojo, *Quantitative constraints on the gluon distribution function in the proton from collider isolated-photon data*, *Nucl. Phys. B* **860** (2012) 311 [[arXiv:1202.1762](https://arxiv.org/abs/1202.1762)] [[INSPIRE](#)].
- [2] L. Carminati et al., *Sensitivity of the LHC isolated- γ +jet data to the parton distribution functions of the proton*, *Europhys. Lett.* **101** (2013) 61002 [[arXiv:1212.5511](https://arxiv.org/abs/1212.5511)] [[INSPIRE](#)].
- [3] T. Pietrycki and A. Szczurek, *Photon-jet correlations in pp and p \bar{p} collisions*, *Phys. Rev. D* **76** (2007) 034003 [[arXiv:0704.2158](https://arxiv.org/abs/0704.2158)] [[INSPIRE](#)].
- [4] Z. Belghobsi, M. Fontannaz, J.P. Guillet, G. Heinrich, E. Pilon and M. Werlen, *Photon-jet correlations and constraints on fragmentation functions*, *Phys. Rev. D* **79** (2009) 114024 [[arXiv:0903.4834](https://arxiv.org/abs/0903.4834)] [[INSPIRE](#)].
- [5] ATLAS collaboration, *Measurement of the inclusive isolated prompt photon cross section in pp collisions at $\sqrt{s} = 7$ TeV with the ATLAS detector*, *Phys. Rev. D* **83** (2011) 052005 [[arXiv:1012.4389](https://arxiv.org/abs/1012.4389)] [[INSPIRE](#)].

- [6] ATLAS collaboration, *Measurement of the inclusive isolated prompt photon cross-section in pp collisions at $\sqrt{s} = 7$ TeV using 35 pb^{-1} of ATLAS data*, *Phys. Lett. B* **706** (2011) 150 [[arXiv:1108.0253](#)] [[INSPIRE](#)].
- [7] ATLAS collaboration, *Measurement of the inclusive isolated prompt photons cross section in pp collisions at $\sqrt{s} = 7$ TeV with the ATLAS detector using 4.6 fb^{-1}* , *Phys. Rev. D* **89** (2014) 052004 [[arXiv:1311.1440](#)] [[INSPIRE](#)].
- [8] ATLAS collaboration, *Measurement of the inclusive isolated prompt photon cross section in pp collisions at $\sqrt{s} = 8$ TeV with the ATLAS detector*, *JHEP* **08** (2016) 005 [[arXiv:1605.03495](#)] [[INSPIRE](#)].
- [9] ATLAS collaboration, *Measurement of the cross section for inclusive isolated-photon production in pp collisions at $\sqrt{s} = 13$ TeV using the ATLAS detector*, *Phys. Lett. B* **770** (2017) 473 [[arXiv:1701.06882](#)] [[INSPIRE](#)].
- [10] CMS collaboration, *Measurement of the Isolated Prompt Photon Production Cross Section in pp Collisions at $\sqrt{s} = 7$ TeV*, *Phys. Rev. Lett.* **106** (2011) 082001 [[arXiv:1012.0799](#)] [[INSPIRE](#)].
- [11] CMS collaboration, *Measurement of the differential cross section for isolated prompt photon production in pp collisions at 7 TeV*, *Phys. Rev. D* **84** (2011) 052011 [[arXiv:1108.2044](#)] [[INSPIRE](#)].
- [12] S. Catani, M. Fontannaz, J.P. Guillet and E. Pilon, *Cross section of isolated prompt photons in hadron-hadron collisions*, *JHEP* **05** (2002) 028 [[hep-ph/0204023](#)] [[INSPIRE](#)].
- [13] P. Aurenche, M. Fontannaz, J.-P. Guillet, E. Pilon and M. Werlen, *A new critical study of photon production in hadronic collisions*, *Phys. Rev. D* **73** (2006) 094007 [[hep-ph/0602133](#)] [[INSPIRE](#)].
- [14] J.M. Campbell, R.K. Ellis and C. Williams, *Direct Photon Production at Next-to-Next-to-Leading Order*, *Phys. Rev. Lett.* **118** (2017) 222001 [[arXiv:1612.04333](#)] [[INSPIRE](#)].
- [15] M.L. Mangano and J. Rojo, *Cross section ratios between different CM energies at the LHC: opportunities for precision measurements and BSM sensitivity*, *JHEP* **08** (2012) 010 [[arXiv:1206.3557](#)] [[INSPIRE](#)].
- [16] J.M. Campbell, J. Rojo, E. Slade and C. Williams, *Direct photon production and PDF fits reloaded*, *Eur. Phys. J. C* **78** (2018) 470 [[arXiv:1802.03021](#)] [[INSPIRE](#)].
- [17] ATLAS collaboration, *Measurements of top-quark pair to Z-boson cross-section ratios at $\sqrt{s} = 13, 8, 7$ TeV with the ATLAS detector*, *JHEP* **02** (2017) 117 [[arXiv:1612.03636](#)] [[INSPIRE](#)].
- [18] ATLAS collaboration, *The ATLAS Experiment at the CERN Large Hadron Collider*, **2008 JINST** **3** S08003 [[INSPIRE](#)].
- [19] ATLAS IBL collaboration, *Production and Integration of the ATLAS Insertable B-Layer*, **2018 JINST** **13** T05008 [[arXiv:1803.00844](#)] [[INSPIRE](#)].
- [20] ATLAS collaboration, *ATLAS Insertable B-Layer Technical Design Report*, [CERN-LHCC-2010-013](#), ATLAS-TDR-19, (2010), Addendum *ibid.* ATLAS-TDR-19-ADD-1, (2012).
- [21] ATLAS collaboration, *Performance of the ATLAS trigger system in 2015*, *Eur. Phys. J. C* **77** (2017) 317 [[arXiv:1611.09661](#)] [[INSPIRE](#)].

- [22] ATLAS collaboration, *Measurement of the photon identification efficiencies with the ATLAS detector using LHC Run-1 data*, *Eur. Phys. J. C* **76** (2016) 666 [[arXiv:1606.01813](#)] [[INSPIRE](#)].
- [23] ATLAS collaboration, *Electron and photon energy calibration with the ATLAS detector using LHC Run 1 data*, *Eur. Phys. J. C* **74** (2014) 3071 [[arXiv:1407.5063](#)] [[INSPIRE](#)].
- [24] M. Cacciari, G.P. Salam and G. Soyez, *The catchment area of jets*, *JHEP* **04** (2008) 005 [[arXiv:0802.1188](#)] [[INSPIRE](#)].
- [25] M. Cacciari, G.P. Salam and S. Sapeta, *On the characterisation of the underlying event*, *JHEP* **04** (2010) 065 [[arXiv:0912.4926](#)] [[INSPIRE](#)].
- [26] S. Catani and M. Grazzini, *Next-to-Next-to-Leading-Order Subtraction Formalism in Hadron Collisions and its Application to Higgs-Boson Production at the Large Hadron Collider*, *Phys. Rev. Lett.* **98** (2007) 222002 [[hep-ph/0703012](#)] [[INSPIRE](#)].
- [27] S. Catani, L. Cieri, G. Ferrera, D. de Florian and M. Grazzini, *Vector Boson Production at Hadron Colliders: A Fully Exclusive QCD Calculation at Next-to-Next-to-Leading Order*, *Phys. Rev. Lett.* **103** (2009) 082001 [[arXiv:0903.2120](#)] [[INSPIRE](#)].
- [28] L. Bourhis, M. Fontannaz and J.P. Guillet, *Quark and gluon fragmentation functions into photons*, *Eur. Phys. J. C* **2** (1998) 529 [[hep-ph/9704447](#)] [[INSPIRE](#)].
- [29] L.A. Harland-Lang, A.D. Martin, P. Motylinski and R.S. Thorne, *Parton distributions in the LHC era: MMHT 2014 PDFs*, *Eur. Phys. J. C* **75** (2015) 204 [[arXiv:1412.3989](#)] [[INSPIRE](#)].
- [30] S. Dulat et al., *New parton distribution functions from a global analysis of quantum chromodynamics*, *Phys. Rev. D* **93** (2016) 033006 [[arXiv:1506.07443](#)] [[INSPIRE](#)].
- [31] H1 and ZEUS collaborations, *Combination of measurements of inclusive deep inelastic $e^\pm p$ scattering cross sections and QCD analysis of HERA data*, *Eur. Phys. J. C* **75** (2015) 580 [[arXiv:1506.06042](#)] [[INSPIRE](#)].
- [32] NNPDF collaboration, *Parton distributions for the LHC Run II*, *JHEP* **04** (2015) 040 [[arXiv:1410.8849](#)] [[INSPIRE](#)].
- [33] S. Alekhin, J. Blümlein, S. Moch and R. Placakyte, *Parton distribution functions, α_s , and heavy-quark masses for LHC Run II*, *Phys. Rev. D* **96** (2017) 014011 [[arXiv:1701.05838](#)] [[INSPIRE](#)].
- [34] T. Sjöstrand, S. Mrenna and P.Z. Skands, *A Brief Introduction to PYTHIA 8.1*, *Comput. Phys. Commun.* **178** (2008) 852 [[arXiv:0710.3820](#)] [[INSPIRE](#)].
- [35] ATLAS collaboration, *ATLAS Run 1 PYTHIA8 tunes*, *ATL-PHYS-PUB-2014-021* (2014).
- [36] R.D. Ball et al., *Parton distributions with LHC data*, *Nucl. Phys. B* **867** (2013) 244 [[arXiv:1207.1303](#)] [[INSPIRE](#)].
- [37] L.A. Harland-Lang, A.D. Martin, P. Motylinski and R.S. Thorne, *Uncertainties on α_s in the MMHT2014 global PDF analysis and implications for SM predictions*, *Eur. Phys. J. C* **75** (2015) 435 [[arXiv:1506.05682](#)] [[INSPIRE](#)].
- [38] E. Todesco and J. Wenninger, *Large Hadron Collider momentum calibration and accuracy*, *Phys. Rev. Accel. Beams* **20** (2017) 081003 [[INSPIRE](#)].
- [39] ATLAS collaboration, *Electron and photon energy calibration with the ATLAS detector using data collected in 2015 at $\sqrt{s} = 13$ TeV*, *ATL-PHYS-PUB-2016-015* (2016).

- [40] ATLAS collaboration, *Photon identification in 2015 ATLAS data*, [ATL-PHYS-PUB-2016-014](#) (2016).
- [41] T. Gleisberg et al., *Event generation with SHERPA 1.1*, *JHEP* **02** (2009) 007 [[arXiv:0811.4622](#)] [[INSPIRE](#)].
- [42] ATLAS collaboration, *ATLAS Computing Acknowledgements 2016–2017*, [ATL-GEN-PUB-2016-002](#) (2016).

The ATLAS collaboration

M. Aaboud^{35d}, G. Aad¹⁰¹, B. Abbott¹²⁸, D.C. Abbott¹⁰², O. Abidinov^{13,*}, D.K. Abhayasinghe⁹³, S.H. Abidi¹⁶⁷, O.S. AbouZeid⁴⁰, N.L. Abraham¹⁵⁶, H. Abramowicz¹⁶¹, H. Abreu¹⁶⁰, Y. Abulaiti⁶, B.S. Acharya^{66a,66b,o}, S. Adachi¹⁶³, L. Adam⁹⁹, L. Adamczyk^{83a}, L. Adamek¹⁶⁷, J. Adelman¹²¹, M. Adersberger¹¹⁴, A. Adiguzel^{12c,ai}, T. Adye¹⁴⁴, A.A. Affolder¹⁴⁶, Y. Afik¹⁶⁰, C. Agapopoulou¹³², M.N. Agaras³⁸, A. Aggarwal¹¹⁹, C. Agheorghiesei^{27c}, J.A. Aguilar-Saavedra^{140f,140a,ah}, F. Ahmadov⁷⁹, G. Aielli^{73a,73b}, S. Akatsuka⁸⁵, T.P.A. Åkesson⁹⁶, E. Akilli⁵⁴, A.V. Akimov¹¹⁰, K. Al Khoury¹³², G.L. Alberghi^{23b,23a}, J. Albert¹⁷⁶, M.J. Alconada Verzini⁸⁸, S. Alderweireldt¹¹⁹, M. Aleksa³⁶, I.N. Aleksandrov⁷⁹, C. Alexa^{27b}, D. Alexandre¹⁹, T. Alexopoulos¹⁰, M. Alhroob¹²⁸, B. Ali¹⁴², G. Alimonti^{68a}, J. Alison³⁷, S.P. Alkire¹⁴⁸, C. Allaire¹³², B.M.M. Allbrooke¹⁵⁶, B.W. Allen¹³¹, P.P. Allport²¹, A. Aloisio^{69a,69b}, A. Alonso⁴⁰, F. Alonso⁸⁸, C. Alpigiani¹⁴⁸, A.A. Alshehri⁵⁷, M.I. Alstaty¹⁰¹, M. Alvarez Estevez⁹⁸, B. Alvarez Gonzalez³⁶, D. Álvarez Piqueras¹⁷⁴, M.G. Alviggi^{69a,69b}, Y. Amaral Coutinho^{80b}, A. Ambler¹⁰³, L. Ambroz¹³⁵, C. Amelung²⁶, D. Amidei¹⁰⁵, S.P. Amor Dos Santos^{140a,140c}, S. Amoroso⁴⁶, C.S. Amrouche⁵⁴, F. An⁷⁸, C. Anastopoulos¹⁴⁹, N. Andari¹⁴⁵, T. Andeen¹¹, C.F. Anders^{61b}, J.K. Anders²⁰, A. Andreazza^{68a,68b}, V. Andrei^{61a}, C.R. Anelli¹⁷⁶, S. Angelidakis³⁸, I. Angelozzi¹²⁰, A. Angerami³⁹, A.V. Anisenkov^{122b,122a}, A. Annovi^{71a}, C. Antel^{61a}, M.T. Anthony¹⁴⁹, M. Antonelli⁵¹, D.J.A. Antrim¹⁷¹, F. Anulli^{72a}, M. Aoki⁸¹, J.A. Aparisi Pozo¹⁷⁴, L. Aperio Bella³⁶, G. Arabidze¹⁰⁶, J.P. Araque^{140a}, V. Araujo Ferraz^{80b}, R. Araujo Pereira^{80b}, A.T.H. Arce⁴⁹, F.A. Arduh⁸⁸, J-F. Arguin¹⁰⁹, S. Argyropoulos⁷⁷, J.-H. Arling⁴⁶, A.J. Armbruster³⁶, L.J. Armitage⁹², A. Armstrong¹⁷¹, O. Arnaez¹⁶⁷, H. Arnold¹²⁰, A. Artamonov^{111,*}, G. Artoni¹³⁵, S. Artz⁹⁹, S. Asai¹⁶³, N. Asbah⁵⁹, E.M. Asimakopoulou¹⁷², L. Asquith¹⁵⁶, K. Assamagan²⁹, R. Astalos^{28a}, R.J. Atkin^{33a}, M. Atkinson¹⁷³, N.B. Atlay¹⁵¹, K. Augsten¹⁴², G. Avolio³⁶, R. Avramidou^{60a}, M.K. Ayoub^{15a}, A.M. Azoulay^{168b}, G. Azuelos^{109,av}, A.E. Baas^{61a}, M.J. Baca²¹, H. Bachacou¹⁴⁵, K. Bachas^{67a,67b}, M. Backes¹³⁵, F. Backman^{45a,45b}, P. Bagnaia^{72a,72b}, M. Bahmani⁸⁴, H. Bahrasemani¹⁵², A.J. Bailey¹⁷⁴, V.R. Bailey¹⁷³, J.T. Baines¹⁴⁴, M. Bajic⁴⁰, C. Bakalis¹⁰, O.K. Baker¹⁸³, P.J. Bakker¹²⁰, D. Bakshi Gupta⁸, S. Balaji¹⁵⁷, E.M. Baldin^{122b,122a}, P. Balek¹⁸⁰, F. Balli¹⁴⁵, W.K. Balunas¹³⁵, J. Balz⁹⁹, E. Banas⁸⁴, A. Bandyopadhyay²⁴, S. Banerjee^{181,j}, A.A.E. Bannoura¹⁸², L. Barak¹⁶¹, W.M. Barbe³⁸, E.L. Barberio¹⁰⁴, D. Barberis^{55b,55a}, M. Barbero¹⁰¹, T. Barillari¹¹⁵, M-S. Barisits³⁶, J. Barkeloo¹³¹, T. Barklow¹⁵³, R. Barnea¹⁶⁰, S.L. Barnes^{60c}, B.M. Barnett¹⁴⁴, R.M. Barnett¹⁸, Z. Barnovska-Blenessy^{60a}, A. Baroncelli^{60a}, G. Barone²⁹, A.J. Barr¹³⁵, L. Barranco Navarro¹⁷⁴, F. Barreiro⁹⁸, J. Barreiro Guimarães da Costa^{15a}, R. Bartoldus¹⁵³, A.E. Barton⁸⁹, P. Bartos^{28a}, A. Basalae⁴⁶, A. Bassalat¹³², R.L. Bates⁵⁷, S.J. Batista¹⁶⁷, S. Batlamous^{35e}, J.R. Batley³², M. Battaglia¹⁴⁶, M. Bauge^{72a,72b}, F. Bauer¹⁴⁵, K.T. Bauer¹⁷¹, H.S. Bawa^{31,m}, J.B. Beacham¹²⁶, T. Beau¹³⁶, P.H. Beauchemin¹⁷⁰, P. Bechtel²⁴, H.C. Beck⁵³, H.P. Beck^{20,r}, K. Becker⁵², M. Becker⁹⁹, C. Becot⁴⁶, A. Beddall^{12d}, A.J. Beddall^{12a}, V.A. Bednyakov⁷⁹, M. Bedognetti¹²⁰, C.P. Bee¹⁵⁵, T.A. Beermann⁷⁶, M. Begalli^{80b}, M. Begel²⁹, A. Behera¹⁵⁵, J.K. Behr⁴⁶, F. Beisiegel²⁴, A.S. Bell⁹⁴, G. Bella¹⁶¹, L. Bellagamba^{23b}, A. Bellerive³⁴, P. Bellos⁹, K. Beloborodov^{122b,122a}, K. Belotskiy¹¹², N.L. Belyaev¹¹², O. Benary^{161,*}, D. Benchebkroun^{35a}, N. Benekos¹⁰, Y. Benhammou¹⁶¹, D.P. Benjamin⁶, M. Benoit⁵⁴, J.R. Bensinger²⁶, S. Bentvelsen¹²⁰, L. Beresford¹³⁵, M. Beretta⁵¹, D. Berge⁴⁶, E. Bergeaas Kuutmann¹⁷², N. Berger⁵, B. Bergmann¹⁴², L.J. Bergsten²⁶, J. Beringer¹⁸, S. Berlendis⁷, N.R. Bernard¹⁰², G. Bernardi¹³⁶, C. Bernius¹⁵³, F.U. Bernlochner²⁴, T. Berry⁹³, P. Berta⁹⁹, C. Bertella^{15a}, G. Bertoli^{45a,45b}, I.A. Bertram⁸⁹, G.J. Besjes⁴⁰, O. Bessidskaia Bylund¹⁸², N. Besson¹⁴⁵, A. Bethani¹⁰⁰, S. Bethke¹¹⁵, A. Betti²⁴, A.J. Bevan⁹², J. Beyer¹¹⁵, R. Bi¹³⁹, R.M. Bianchi¹³⁹, O. Biebel¹¹⁴, D. Biedermann¹⁹, R. Bielski³⁶, K. Bierwagen⁹⁹, N.V. Biesuz^{71a,71b}, M. Biglietti^{74a}, T.R.V. Billoud¹⁰⁹, M. Bindi⁵³, A. Bingul^{12d}, C. Bini^{72a,72b},

S. Biondi^{23b,23a}, M. Birman¹⁸⁰, T. Bisanz⁵³, J.P. Biswal¹⁶¹, A. Bitadze¹⁰⁰, C. Bittrich⁴⁸, D.M. Bjergaard⁴⁹, J.E. Black¹⁵³, K.M. Black²⁵, T. Blazek^{28a}, I. Bloch⁴⁶, C. Blocker²⁶, A. Blue⁵⁷, U. Blumenschein⁹², Dr. Blunier^{147a}, G.J. Bobbink¹²⁰, V.S. Bobrovnikov^{122b,122a}, S.S. Bocchetta⁹⁶, A. Bocci⁴⁹, D. Boerner⁴⁶, D. Bogavac¹¹⁴, A.G. Bogdanchikov^{122b,122a}, C. Boehm^{45a}, V. Boisvert⁹³, P. Bokan^{53,172}, T. Bold^{83a}, A.S. Boldyrev¹¹³, A.E. Bolz^{61b}, M. Bomben¹³⁶, M. Bona⁹², J.S. Bonilla¹³¹, M. Boonekamp¹⁴⁵, H.M. Borecka-Bielska⁹⁰, A. Borisov¹²³, G. Borissov⁸⁹, J. Bortfeldt³⁶, D. Bortoletto¹³⁵, V. Bortolotto^{73a,73b}, D. Boscherini^{23b}, M. Bosman¹⁴, J.D. Bossio Sola³⁰, K. Bouaouda^{35a}, J. Boudreau¹³⁹, E.V. Bouhova-Thacker⁸⁹, D. Boumediene³⁸, C. Bourdarios¹³², S.K. Boutle⁵⁷, A. Boveia¹²⁶, J. Boyd³⁶, D. Boye^{33b}, I.R. Boyko⁷⁹, A.J. Bozson⁹³, J. Bracinik²¹, N. Brahimi¹⁰¹, G. Brandt¹⁸², O. Brandt^{61a}, F. Braren⁴⁶, U. Bratzler¹⁶⁴, B. Brau¹⁰², J.E. Brau¹³¹, W.D. Breaden Madden⁵⁷, K. Brendlinger⁴⁶, L. Brenner⁴⁶, R. Brenner¹⁷², S. Bressler¹⁸⁰, B. Brickwedde⁹⁹, D.L. Briglin²¹, D. Britton⁵⁷, D. Britzger¹¹⁵, I. Brock²⁴, R. Brock¹⁰⁶, G. Brooijmans³⁹, T. Brooks⁹³, W.K. Brooks^{147b}, E. Brost¹²¹, J.H. Broughton²¹, P.A. Bruckman de Renstrom⁸⁴, D. Bruncko^{28b}, A. Bruni^{23b}, G. Bruni^{23b}, L.S. Bruni¹²⁰, S. Bruno^{73a,73b}, B.H. Brunt³², M. Bruschi^{23b}, N. Bruscino¹³⁹, P. Bryant³⁷, L. Bryngemark⁹⁶, T. Buanes¹⁷, Q. Buat³⁶, P. Buchholz¹⁵¹, A.G. Buckley⁵⁷, I.A. Budagov⁷⁹, M.K. Bugge¹³⁴, F. Bühner⁵², O. Bulekov¹¹², T.J. Burch¹²¹, S. Burdin⁹⁰, C.D. Burgard¹²⁰, A.M. Burger¹²⁹, B. Burghgrave⁸, K. Burka⁸⁴, I. Burmeister⁴⁷, J.T.P. Burr⁴⁶, V. Büscher⁹⁹, E. Buschmann⁵³, P.J. Bussey⁵⁷, J.M. Butler²⁵, C.M. Buttar⁵⁷, J.M. Butterworth⁹⁴, P. Butti³⁶, W. Buttinger³⁶, A. Buzatu¹⁵⁸, A.R. Buzykaev^{122b,122a}, G. Cabras^{23b,23a}, S. Cabrera Urbán¹⁷⁴, D. Caforio¹⁴², H. Cai¹⁷³, V.M.M. Cairo², O. Cakir^{4a}, N. Calace³⁶, P. Calafiura¹⁸, A. Calandri¹⁰¹, G. Calderini¹³⁶, P. Calfayan⁶⁵, G. Callea⁵⁷, L.P. Caloba^{80b}, S. Calvente Lopez⁹⁸, D. Calvet³⁸, S. Calvet³⁸, T.P. Calvet¹⁵⁵, M. Calvetti^{71a,71b}, R. Camacho Toro¹³⁶, S. Camarda³⁶, D. Camarero Munoz⁹⁸, P. Camarri^{73a,73b}, D. Cameron¹³⁴, R. Caminal Armadans¹⁰², C. Camincher³⁶, S. Campana³⁶, M. Campanelli⁹⁴, A. Camplani⁴⁰, A. Campoverde¹⁵¹, V. Canale^{69a,69b}, M. Cano Bret^{60c}, J. Cantero¹²⁹, T. Cao¹⁶¹, Y. Cao¹⁷³, M.D.M. Capeans Garrido³⁶, M. Capua^{41b,41a}, R. Cardarelli^{73a}, F.C. Cardillo¹⁴⁹, I. Carli¹⁴³, T. Carli³⁶, G. Carlino^{69a}, B.T. Carlson¹³⁹, L. Carminati^{68a,68b}, R.M.D. Carney^{45a,45b}, S. Caron¹¹⁹, E. Carquin^{147b}, S. Carra^{68a,68b}, J.W.S. Carter¹⁶⁷, M.P. Casado^{14,f}, A.F. Casha¹⁶⁷, D.W. Casper¹⁷¹, R. Castelijns¹²⁰, F.L. Castillo¹⁷⁴, V. Castillo Gimenez¹⁷⁴, N.F. Castro^{140a,140e}, A. Catinaccio³⁶, J.R. Catmore¹³⁴, A. Cattai³⁶, J. Caudron²⁴, V. Cavaliere²⁹, E. Cavallaro¹⁴, D. Cavalli^{68a}, M. Cavalli-Sforza¹⁴, V. Cavasinni^{71a,71b}, E. Celebi^{12b}, L. Cerda Alberich¹⁷⁴, A.S. Cerqueira^{80a}, A. Cerri¹⁵⁶, L. Cerrito^{73a,73b}, F. Cerutti¹⁸, A. Cervelli^{23b,23a}, S.A. Cetin^{12b}, A. Chafaq^{35a}, D. Chakraborty¹²¹, S.K. Chan⁵⁹, W.S. Chan¹²⁰, W.Y. Chan⁹⁰, J.D. Chapman³², B. Chargeishvili^{159b}, D.G. Charlton²¹, C.C. Chau³⁴, C.A. Chavez Barajas¹⁵⁶, S. Che¹²⁶, A. Chegwidden¹⁰⁶, S. Chekanov⁶, S.V. Chekulaev^{168a}, G.A. Chelkov^{79,au}, M.A. Chelstowska³⁶, B. Chen⁷⁸, C. Chen^{60a}, C.H. Chen⁷⁸, H. Chen²⁹, J. Chen^{60a}, J. Chen³⁹, S. Chen¹³⁷, S.J. Chen^{15c}, X. Chen^{15b,at}, Y. Chen⁸², Y.-H. Chen⁴⁶, H.C. Cheng^{63a}, H.J. Cheng^{15a,15d}, A. Cheplakov⁷⁹, E. Cheremushkina¹²³, R. Cherkouki El Moursli^{35e}, E. Cheu⁷, K. Cheung⁶⁴, T.J.A. Chevaléras¹⁴⁵, L. Chevalier¹⁴⁵, V. Chiarella⁵¹, G. Chiarelli^{71a}, G. Chiodini^{67a}, A.S. Chisholm^{36,21}, A. Chitan^{27b}, I. Chiu¹⁶³, Y.H. Chiu¹⁷⁶, M.V. Chizhov⁷⁹, K. Choi⁶⁵, A.R. Chomont¹³², S. Chouridou¹⁶², Y.S. Chow¹²⁰, M.C. Chu^{63a}, J. Chudoba¹⁴¹, A.J. Chuinard¹⁰³, J.J. Chwastowski⁸⁴, L. Chytka¹³⁰, D. Cinca⁴⁷, V. Cindro⁹¹, I.A. Cioară^{27b}, A. Ciocio¹⁸, F. Ciotto^{69a,69b}, Z.H. Citron¹⁸⁰, M. Citterio^{68a}, B.M. Ciungu¹⁶⁷, A. Clark⁵⁴, M.R. Clark³⁹, P.J. Clark⁵⁰, C. Clement^{45a,45b}, Y. Coadou¹⁰¹, M. Cobl^{66a,66c}, A. Cocco^{55b}, J. Cochran⁷⁸, H. Cohen¹⁶¹, A.E.C. Coimbra¹⁸⁰, L. Colasurdo¹¹⁹, B. Cole³⁹, A.P. Colijn¹²⁰, J. Collot⁵⁸, P. Conde Muiño^{140a,g}, E. Coniavitis⁵², S.H. Connell^{33b}, I.A. Connolly¹⁰⁰, S. Constantinescu^{27b}, F. Conventi^{69a,aw}, A.M. Cooper-Sarkar¹³⁵, F. Cormier¹⁷⁵, K.J.R. Cormier¹⁶⁷, L.D. Corpe⁹⁴, M. Corradi^{72a,72b}, E.E. Corrigan⁹⁶, F. Corriveau^{103,ad},

A. Cortes-Gonzalez³⁶, M.J. Costa¹⁷⁴, F. Costanza⁵, D. Costanzo¹⁴⁹, G. Cowan⁹³, J.W. Cowley³², J. Crane¹⁰⁰, K. Cranmer¹²⁴, S.J. Crawley⁵⁷, R.A. Creager¹³⁷, S. Crépé-Renaudin⁵⁸, F. Crescioli¹³⁶, M. Cristinziani²⁴, V. Croft¹²⁴, G. Crosetti^{41b,41a}, A. Cueto⁹⁸, T. Cuhadar Donszelmann¹⁴⁹, A.R. Cukierman¹⁵³, S. Czekierda⁸⁴, P. Czodrowski³⁶, M.J. Da Cunha Sargedas De Sousa^{60b}, J.V. Da Fonseca Pinto^{80b}, C. Da Via¹⁰⁰, W. Dabrowski^{83a}, T. Dado^{28a}, S. Dahbi^{35e}, T. Dai¹⁰⁵, C. Dallapiccola¹⁰², M. Dam⁴⁰, G. D’amen^{23b,23a}, J. Damp⁹⁹, J.R. Dandoy¹³⁷, M.F. Daneri³⁰, N.P. Dang^{181j}, N.D. Dann¹⁰⁰, M. Danninger¹⁷⁵, V. Dao³⁶, G. Darbo^{55b}, O. Dartsis⁵, A. Dattagupta¹³¹, T. Daubney⁴⁶, S. D’Auria^{68a,68b}, W. Davey²⁴, C. David⁴⁶, T. Davidek¹⁴³, D.R. Davis⁴⁹, E. Dawe¹⁰⁴, I. Dawson¹⁴⁹, K. De⁸, R. De Asmundis^{69a}, A. De Benedetti¹²⁸, M. De Beurs¹²⁰, S. De Castro^{23b,23a}, S. De Cecco^{72a,72b}, N. De Groot¹¹⁹, P. de Jong¹²⁰, H. De la Torre¹⁰⁶, A. De Maria^{71a,71b}, D. De Pedis^{72a}, A. De Salvo^{72a}, U. De Sanctis^{73a,73b}, M. De Santis^{73a,73b}, A. De Santo¹⁵⁶, K. De Vasconcelos Corga¹⁰¹, J.B. De Vivie De Regie¹³², C. Debenedetti¹⁴⁶, D.V. Dedovich⁷⁹, A.M. Deiana⁴², M. Del Gaudio^{41b,41a}, J. Del Peso⁹⁸, Y. Delabat Diaz⁴⁶, D. Delgove¹³², F. Deliot¹⁴⁵, C.M. Delitzsch⁷, M. Della Pietra^{69a,69b}, D. Della Volpe⁵⁴, A. Dell’Acqua³⁶, L. Dell’Asta²⁵, M. Delmastro⁵, C. Delporte¹³², P.A. Delsart⁵⁸, D.A. DeMarco¹⁶⁷, S. Demers¹⁸³, M. Demichev⁷⁹, S.P. Denisov¹²³, D. Denysiuk¹²⁰, L. D’Eramo¹³⁶, D. Derendarz⁸⁴, J.E. Derkaoui^{35d}, F. Derue¹³⁶, P. Dervan⁹⁰, K. Desch²⁴, C. Deterre⁴⁶, K. Dette¹⁶⁷, M.R. Devesa³⁰, P.O. Deviveiros³⁶, A. Dewhurst¹⁴⁴, S. Dhaliwal²⁶, F.A. Di Bello⁵⁴, A. Di Ciaccio^{73a,73b}, L. Di Ciaccio⁵, W.K. Di Clemente¹³⁷, C. Di Donato^{69a,69b}, A. Di Girolamo³⁶, G. Di Gregorio^{71a,71b}, B. Di Micco^{74a,74b}, R. Di Nardo¹⁰², K.F. Di Petrillo⁵⁹, R. Di Sipio¹⁶⁷, D. Di Valentino³⁴, C. Diaconu¹⁰¹, F.A. Dias⁴⁰, T. Dias Do Vale^{140a,140e}, M.A. Diaz^{147a}, J. Dickinson¹⁸, E.B. Diehl¹⁰⁵, J. Dietrich¹⁹, S. Díez Cornell⁴⁶, A. Dimitrievska¹⁸, J. Dingfelder²⁴, F. Dittus³⁶, F. Djama¹⁰¹, T. Djobava^{159b}, J.I. Djuvsland¹⁷, M.A.B. Do Vale^{80c}, M. Dobre^{27b}, D. Dodsworth²⁶, C. Doglioni⁹⁶, J. Dolejsi¹⁴³, Z. Dolezal¹⁴³, M. Donadelli^{80d}, J. Donini³⁸, A. D’onofrio⁹², M. D’Onofrio⁹⁰, J. Dopke¹⁴⁴, A. Doria^{69a}, M.T. Dova⁸⁸, A.T. Doyle⁵⁷, E. Drechsler¹⁵², E. Dreyer¹⁵², T. Dreyer⁵³, Y. Du^{60b}, Y. Duan^{60b}, F. Dubinin¹¹⁰, M. Dubovsky^{28a}, A. Dubreuil⁵⁴, E. Duchovni¹⁸⁰, G. Duckeck¹¹⁴, A. Ducourthial¹³⁶, O.A. Ducu^{109,x}, D. Duda¹¹⁵, A. Dudarev³⁶, A.C. Dudder⁹⁹, E.M. Duffield¹⁸, L. Dufflot¹³², M. Dührssen³⁶, C. Dülken¹⁸², M. Dumancic¹⁸⁰, A.E. Dumitriu^{27b}, A.K. Duncan⁵⁷, M. Dunford^{61a}, A. Duperrin¹⁰¹, H. Duran Yildiz^{4a}, M. Düren⁵⁶, A. Durglishvili^{159b}, D. Duschinger⁴⁸, B. Dutta⁴⁶, D. Duvnjak¹, G.I. Dyckes¹³⁷, M. Dyndal⁴⁶, S. Dysch¹⁰⁰, B.S. Dziedzic⁸⁴, K.M. Ecker¹¹⁵, R.C. Edgar¹⁰⁵, T. Eifert³⁶, G. Eigen¹⁷, K. Einsweiler¹⁸, T. Ekelof¹⁷², M. El Kacimi^{35c}, R. El Kosseifi¹⁰¹, V. Ellajosyula¹⁷², M. Ellert¹⁷², F. Ellinghaus¹⁸², A.A. Elliot⁹², N. Ellis³⁶, J. Elmsheuser²⁹, M. Elsing³⁶, D. Emeliyanov¹⁴⁴, A. Emerman³⁹, Y. Enari¹⁶³, J.S. Ennis¹⁷⁸, M.B. Epland⁴⁹, J. Erdmann⁴⁷, A. Ereditato²⁰, M. Escalier¹³², C. Escobar¹⁷⁴, O. Estrada Pastor¹⁷⁴, A.I. Etienvre¹⁴⁵, E. Etzion¹⁶¹, H. Evans⁶⁵, A. Ezhilov¹³⁸, M. Ezzi^{35e}, F. Fabbri⁵⁷, L. Fabbri^{23b,23a}, V. Fabiani¹¹⁹, G. Facini⁹⁴, R.M. Faisca Rodrigues Pereira^{140a}, R.M. Fakhruddinov¹²³, S. Falciano^{72a}, P.J. Falke⁵, S. Falke⁵, J. Faltova¹⁴³, Y. Fang^{15a}, Y. Fang^{15a}, G. Fanourakis⁴⁴, M. Fanti^{68a,68b}, A. Farbin⁸, A. Farilla^{74a}, E.M. Farina^{70a,70b}, T. Farooque¹⁰⁶, S. Farrell¹⁸, S.M. Farrington¹⁷⁸, P. Farthouat³⁶, F. Fassi^{35e}, P. Fassnacht³⁶, D. Fassouliotis⁹, M. Fauci Giannelli⁵⁰, W.J. Fawcett³², L. Fayard¹³², O.L. Fedin^{138,p}, W. Fedorko¹⁷⁵, M. Feickert⁴², S. Feigl¹³⁴, L. Feligioni¹⁰¹, C. Feng^{60b}, E.J. Feng³⁶, M. Feng⁴⁹, M.J. Fenton⁵⁷, A.B. Fenjuk¹²³, J. Ferrando⁴⁶, A. Ferrari¹⁷², P. Ferrari¹²⁰, R. Ferrari^{70a}, D.E. Ferreira de Lima^{61b}, A. Ferrer¹⁷⁴, D. Ferrere⁵⁴, C. Ferretti¹⁰⁵, F. Fiedler⁹⁹, A. Filipčič⁹¹, F. Filthaut¹¹⁹, K.D. Finelli²⁵, M.C.N. Fiolhais^{140a,140c,a}, L. Fiorini¹⁷⁴, C. Fischer¹⁴, W.C. Fisher¹⁰⁶, I. Fleck¹⁵¹, P. Fleischmann¹⁰⁵, R.R.M. Fletcher¹³⁷, T. Flick¹⁸², B.M. Flierl¹¹⁴, L.M. Flores¹³⁷, L.R. Flores Castillo^{63a}, F.M. Follega^{75a,75b}, N. Fomin¹⁷, G.T. Forcolin^{75a,75b}, A. Formica¹⁴⁵, F.A. Förster¹⁴, A.C. Forti¹⁰⁰, A.G. Foster²¹, D. Fournier¹³², H. Fox⁸⁹, S. Fracchia¹⁴⁹, P. Francavilla^{71a,71b}, M. Franchini^{23b,23a}, S. Franchino^{61a}, D. Francis³⁶, L. Franconi¹⁴⁶,

M. Franklin⁵⁹, M. Frate¹⁷¹, A.N. Fray⁹², B. Freund¹⁰⁹, W.S. Freund^{80b}, E.M. Freundlich⁴⁷, D.C. Frizzell¹²⁸, D. Froidevaux³⁶, J.A. Frost¹³⁵, C. Fukunaga¹⁶⁴, E. Fullana Torregrosa¹⁷⁴, E. Fumagalli^{55b,55a}, T. Fusayasu¹¹⁶, J. Fuster¹⁷⁴, A. Gabrielli^{23b,23a}, A. Gabrielli¹⁸, G.P. Gach^{83a}, S. Gadatsch⁵⁴, P. Gadow¹¹⁵, G. Gagliardi^{55b,55a}, L.G. Gagnon¹⁰⁹, C. Galea^{27b}, B. Galhardo^{140a,140c}, E.J. Gallas¹³⁵, B.J. Gallop¹⁴⁴, P. Gallus¹⁴², G. Galster⁴⁰, R. Gamboa Goni⁹², K.K. Gan¹²⁶, S. Ganguly¹⁸⁰, J. Gao^{60a}, Y. Gao⁹⁰, Y.S. Gao^{31,m}, C. García¹⁷⁴, J.E. García Navarro¹⁷⁴, J.A. García Pascual^{15a}, C. Garcia-Argos⁵², M. Garcia-Sciveres¹⁸, R.W. Gardner³⁷, N. Garelli¹⁵³, S. Gargiulo⁵², V. Garonne¹³⁴, A. Gaudiello^{55b,55a}, G. Gaudio^{70a}, I.L. Gavrilenko¹¹⁰, A. Gavriluk¹¹¹, C. Gay¹⁷⁵, G. Gaycken²⁴, E.N. Gazis¹⁰, C.N.P. Gee¹⁴⁴, J. Geisen⁵³, M. Geisen⁹⁹, M.P. Geisler^{61a}, C. Gemme^{55b}, M.H. Genest⁵⁸, C. Geng¹⁰⁵, S. Gentile^{72a,72b}, S. George⁹³, T. Geralis⁴⁴, D. Gerbaudo¹⁴, G. Gessner⁴⁷, S. Ghasemi¹⁵¹, M. Ghasemi Bostanabad¹⁷⁶, M. Ghneimat²⁴, A. Ghosh⁷⁷, B. Giacobbe^{23b}, S. Giagu^{72a,72b}, N. Giangiacomi^{23b,23a}, P. Giannetti^{71a}, A. Giannini^{69a,69b}, S.M. Gibson⁹³, M. Gignac¹⁴⁶, D. Gillberg³⁴, G. Gilles¹⁸², D.M. Gingrich^{3,av}, M.P. Giordani^{66a,66c}, F.M. Giorgi^{23b}, P.F. Giraud¹⁴⁵, G. Giudliarelli^{66a,66c}, D. Giugni^{68a}, F. Giuli¹³⁵, M. Giulini^{61b}, S. Gkaitatzis¹⁶², I. Gkialas^{9,i}, E.L. Gkoukousis¹⁴, P. Gkoutounis¹⁰, L.K. Gladilin¹¹³, C. Glasman⁹⁸, J. Glatzer¹⁴, P.C.F. Glaysher⁴⁶, A. Glazov⁴⁶, M. Goblirsch-Kolb²⁶, S. Goldfarb¹⁰⁴, T. Golling⁵⁴, D. Golubkov¹²³, A. Gomes^{140a,140b}, R. Goncalves Gama⁵³, R. Gonçalo^{140a,140b}, G. Gonella⁵², L. Gonella²¹, A. Gongadze⁷⁹, F. Gonnella²¹, J.L. Gonski⁵⁹, S. González de la Hoz¹⁷⁴, S. Gonzalez-Sevilla⁵⁴, G.R. Gonzalvo Rodriguez¹⁷⁴, L. Goossens³⁶, P.A. Gorbounov¹¹¹, H.A. Gordon²⁹, B. Gorini³⁶, E. Gorini^{67a,67b}, A. Gorišek⁹¹, A.T. Goshaw⁴⁹, C. Gössling⁴⁷, M.I. Gostkin⁷⁹, C.A. Gottardo²⁴, C.R. Goudet¹³², D. Goujdami^{35c}, A.G. Goussiou¹⁴⁸, N. Govender^{33b,b}, C. Goy⁵, E. Gozani¹⁶⁰, I. Grabowska-Bold^{83a}, P.O.J. Gradin¹⁷², E.C. Graham⁹⁰, J. Gramling¹⁷¹, E. Gramstad¹³⁴, S. Grancagnolo¹⁹, M. Grandi¹⁵⁶, V. Gratchev¹³⁸, P.M. Gravila^{27f}, F.G. Gravili^{67a,67b}, C. Gray⁵⁷, H.M. Gray¹⁸, C. Grefe²⁴, K. Gregersen⁹⁶, I.M. Gregor⁴⁶, P. Grenier¹⁵³, K. Grevtsov⁴⁶, N.A. Grieser¹²⁸, J. Griffiths⁸, A.A. Grillo¹⁴⁶, K. Grimm^{31,l}, S. Grinstein^{14,y}, J.-F. Grivaz¹³², S. Groh⁹⁹, E. Gross¹⁸⁰, J. Grosse-Knetter⁵³, Z.J. Grout⁹⁴, C. Grud¹⁰⁵, A. Grummer¹¹⁸, L. Guan¹⁰⁵, W. Guan¹⁸¹, J. Guenther³⁶, A. Guerguichon¹³², F. Guescini^{168a}, D. Guest¹⁷¹, R. Gugel⁵², B. Gui¹²⁶, T. Guillemin⁵, S. Guindon³⁶, U. Gul⁵⁷, J. Guo^{60c}, W. Guo¹⁰⁵, Y. Guo^{60a,s}, Z. Guo¹⁰¹, R. Gupta⁴⁶, S. Gurbuz^{12c}, G. Gustavino¹²⁸, P. Gutierrez¹²⁸, C. Gutsche⁹⁴, C. Guyot¹⁴⁵, M.P. Guzik^{83a}, C. Gwenlan¹³⁵, C.B. Gwilliam⁹⁰, A. Haas¹²⁴, C. Haber¹⁸, H.K. Hadavand⁸, N. Haddad^{35e}, A. Hader^{60a}, S. Hageböck³⁶, M. Hagihara¹⁶⁹, M. Haleem¹⁷⁷, J. Haley¹²⁹, G. Halladjian¹⁰⁶, G.D. Hallewell¹⁰¹, K. Hamacher¹⁸², P. Hamal¹³⁰, K. Hamano¹⁷⁶, H. Hamdaoui^{35e}, G.N. Hamity¹⁴⁹, K. Han^{60a,ak}, L. Han^{60a}, S. Han^{15a,15d}, K. Hanagaki^{81,v}, M. Hance¹⁴⁶, D.M. Handl¹¹⁴, B. Haney¹³⁷, R. Hankache¹³⁶, P. Hanke^{61a}, E. Hansen⁹⁶, J.B. Hansen⁴⁰, J.D. Hansen⁴⁰, M.C. Hansen²⁴, P.H. Hansen⁴⁰, E.C. Hanson¹⁰⁰, K. Hara¹⁶⁹, A.S. Hard¹⁸¹, T. Harenberg¹⁸², S. Harkusha¹⁰⁷, P.F. Harrison¹⁷⁸, N.M. Hartmann¹¹⁴, Y. Hasegawa¹⁵⁰, A. Hasib⁵⁰, S. Hassani¹⁴⁵, S. Haug²⁰, R. Hauser¹⁰⁶, L. Hauswald⁴⁸, L.B. Havener³⁹, M. Havranek¹⁴², C.M. Hawkes²¹, R.J. Hawkins³⁶, D. Hayden¹⁰⁶, C. Hayes¹⁵⁵, R.L. Hayes¹⁷⁵, C.P. Hays¹³⁵, J.M. Hays⁹², H.S. Hayward⁹⁰, S.J. Haywood¹⁴⁴, F. He^{60a}, M.P. Heath⁵⁰, V. Hedberg⁹⁶, L. Heelan⁸, S. Heer²⁴, K.K. Heidegger⁵², J. Heilman³⁴, S. Heim⁴⁶, T. Heim¹⁸, B. Heinemann^{46,aq}, J.J. Heinrich¹¹⁴, L. Heinrich¹²⁴, C. Heinz⁵⁶, J. Hejbal¹⁴¹, L. Helary^{61b}, A. Held¹⁷⁵, S. Hellesund¹³⁴, C.M. Helling¹⁴⁶, S. Hellman^{45a,45b}, C. Helsen³⁶, R.C.W. Henderson⁸⁹, Y. Heng¹⁸¹, S. Henkelmann¹⁷⁵, A.M. Henriques Correia³⁶, G.H. Herbert¹⁹, H. Herde²⁶, V. Herget¹⁷⁷, Y. Hernández Jiménez^{33c}, H. Herr⁹⁹, M.G. Herrmann¹¹⁴, T. Herrmann⁴⁸, G. Herten⁵², R. Hertenberger¹¹⁴, L. Hervas³⁶, T.C. Herwig¹³⁷, G.G. Hesketh⁹⁴, N.P. Hessey^{168a}, A. Higashida¹⁶³, S. Higashino⁸¹, E. Higón-Rodríguez¹⁷⁴, K. Hildebrand³⁷, E. Hill¹⁷⁶, J.C. Hill³², K.K. Hill²⁹, K.H. Hiller⁴⁶, S.J. Hillier²¹, M. Hils⁴⁸, I. Hinchliffe¹⁸, F. Hinterkeuser²⁴, M. Hirose¹³³,

D. Hirschbuehl¹⁸², B. Hiti⁹¹, O. Hladik¹⁴¹, D.R. Hlaluku^{33c}, X. Hoad⁵⁰, J. Hobbs¹⁵⁵, N. Hod¹⁸⁰, M.C. Hodgkinson¹⁴⁹, A. Hoecker³⁶, F. Hoenig¹¹⁴, D. Hohn⁵², D. Hohov¹³², T.R. Holmes³⁷, M. Holzbock¹¹⁴, L.B.A.H. Hommels³², S. Honda¹⁶⁹, T. Honda⁸¹, T.M. Hong¹³⁹, A. Hönle¹¹⁵, B.H. Hooberman¹⁷³, W.H. Hopkins⁶, Y. Horii¹¹⁷, P. Horn⁴⁸, A.J. Horton¹⁵², L.A. Horyn³⁷, J.-Y. Hostachy⁵⁸, A. Hostiuc¹⁴⁸, S. Hou¹⁵⁸, A. Hoummada^{35a}, J. Howarth¹⁰⁰, J. Hoya⁸⁸, M. Hrabovsky¹³⁰, J. Hrdinka³⁶, I. Hristova¹⁹, J. Hrivnac¹³², A. Hrynevich¹⁰⁸, T. Hryn'ova⁵, P.J. Hsu⁶⁴, S.-C. Hsu¹⁴⁸, Q. Hu²⁹, S. Hu^{60c}, Y. Huang^{15a}, Z. Hubacek¹⁴², F. Hubaut¹⁰¹, M. Huebner²⁴, F. Huegging²⁴, T.B. Huffman¹³⁵, M. Huhtinen³⁶, R.F.H. Hunter³⁴, P. Huo¹⁵⁵, A.M. Hupe³⁴, N. Huseynov^{79,af}, J. Huston¹⁰⁶, J. Huth⁵⁹, R. Hyneman¹⁰⁵, G. Iacobucci⁵⁴, G. Iakovidis²⁹, I. Ibragimov¹⁵¹, L. Iconomidou-Fayard¹³², Z. Idrissi^{35e}, P.I. Iengo³⁶, R. Ignazzi⁴⁰, O. Igonkina^{120,aa}, R. Iguchi¹⁶³, T. Iizawa⁵⁴, Y. Ikegami⁸¹, M. Ikeno⁸¹, D. Iliadis¹⁶², N. Ilic¹¹⁹, F. Iltzsche⁴⁸, G. Introzzi^{70a,70b}, M. Iodice^{74a}, K. Iordanidou³⁹, V. Ippolito^{72a,72b}, M.F. Isacson¹⁷², N. Ishijima¹³³, M. Ishino¹⁶³, M. Ishitsuka¹⁶⁵, W. Islam¹²⁹, C. Issever¹³⁵, S. Istin¹⁶⁰, F. Ito¹⁶⁹, J.M. Iturbe Ponce^{63a}, R. Iuppa^{75a,75b}, A. Ivina¹⁸⁰, H. Iwasaki⁸¹, J.M. Izen⁴³, V. Izzo^{69a}, P. Jacka¹⁴¹, P. Jackson¹, R.M. Jacobs²⁴, V. Jain², G. Jäkel¹⁸², K.B. Jakobi⁹⁹, K. Jakobs⁵², S. Jakobsen⁷⁶, T. Jakoubek¹⁴¹, D.O. Jamin¹²⁹, R. Jansky⁵⁴, J. Janssen²⁴, M. Janus⁵³, P.A. Janus^{83a}, G. Jarlskog⁹⁶, N. Javadov^{79,af}, T. Javůrek³⁶, M. Javurkova⁵², F. Jeanneau¹⁴⁵, L. Jeanty¹³¹, J. Jejelava^{159a,ag}, A. Jelinskas¹⁷⁸, P. Jenni^{52,c}, J. Jeong⁴⁶, N. Jeong⁴⁶, S. Jézéquel⁵, H. Ji¹⁸¹, J. Jia¹⁵⁵, H. Jiang⁷⁸, Y. Jiang^{60a}, Z. Jiang^{153,q}, S. Jiggins⁵², F.A. Jimenez Morales³⁸, J. Jimenez Pena¹⁷⁴, S. Jin^{15c}, A. Jinaru^{27b}, O. Jinnouchi¹⁶⁵, H. Jivan^{33c}, P. Johansson¹⁴⁹, K.A. Johns⁷, C.A. Johnson⁶⁵, K. Jon-And^{45a,45b}, R.W.L. Jones⁸⁹, S.D. Jones¹⁵⁶, S. Jones⁷, T.J. Jones⁹⁰, J. Jongmanns^{61a}, P.M. Jorge^{140a,140b}, J. Jovicevic^{168a}, X. Ju¹⁸, J.J. Jungeburth¹¹⁵, A. Juste Rozas^{14,y}, A. Kaczmarek⁸⁴, M. Kado¹³², H. Kagan¹²⁶, M. Kagan¹⁵³, T. Kaji¹⁷⁹, E. Kajomovitz¹⁶⁰, C.W. Kalderon⁹⁶, A. Kaluza⁹⁹, A. Kamenshchikov¹²³, L. Kanjir⁹¹, Y. Kano¹⁶³, V.A. Kantserov¹¹², J. Kanzaki⁸¹, L.S. Kaplan¹⁸¹, D. Kar^{33c}, M.J. Kareem^{168b}, E. Karentzos¹⁰, S.N. Karpov⁷⁹, Z.M. Karpova⁷⁹, V. Kartvelishvili⁸⁹, A.N. Karyukhin¹²³, L. Kashif¹⁸¹, R.D. Kass¹²⁶, A. Kastanas^{45a,45b}, Y. Kataoka¹⁶³, C. Kato^{60d,60c}, J. Katzy⁴⁶, K. Kawade⁸², K. Kawagoe⁸⁷, T. Kawaguchi¹¹⁷, T. Kawamoto¹⁶³, G. Kawamura⁵³, E.F. Kay¹⁷⁶, V.F. Kazanin^{122b,122a}, R. Keeler¹⁷⁶, R. Kehoe⁴², J.S. Keller³⁴, E. Kellermann⁹⁶, J.J. Kempster²¹, J. Kendrick²¹, O. Kepka¹⁴¹, S. Kersten¹⁸², B.P. Kerševan⁹¹, S. Ketabchi Haghighat¹⁶⁷, R.A. Keyes¹⁰³, M. Khader¹⁷³, F. Khalil-Zada¹³, A. Khanov¹²⁹, A.G. Kharlamov^{122b,122a}, T. Kharlamova^{122b,122a}, E.E. Khoda¹⁷⁵, A. Khodinov¹⁶⁶, T.J. Khoo⁵⁴, E. Khramov⁷⁹, J. Khubua^{159b}, S. Kido⁸², M. Kiehn⁵⁴, C.R. Kilby⁹³, Y.K. Kim³⁷, N. Kimura^{66a,66c}, O.M. Kind¹⁹, B.T. King^{90,*}, D. Kirchmeier⁴⁸, J. Kirk¹⁴⁴, A.E. Kiryunin¹¹⁵, T. Kishimoto¹⁶³, V. Kitali⁴⁶, O. Kivernyk⁵, E. Kladiva^{28b,*}, T. Klapdor-Kleingrothaus⁵², M.H. Klein¹⁰⁵, M. Klein⁹⁰, U. Klein⁹⁰, K. Kleinknecht⁹⁹, P. Klimek¹²¹, A. Klimentov²⁹, T. Klingl²⁴, T. Klioutchnikova³⁶, F.F. Klitzner¹¹⁴, P. Kluit¹²⁰, S. Kluth¹¹⁵, E. Kneringer⁷⁶, E.B.F.G. Knoops¹⁰¹, A. Knue⁵², D. Kobayashi⁸⁷, T. Kobayashi¹⁶³, M. Kobel⁴⁸, M. Kocian¹⁵³, P. Kodys¹⁴³, P.T. Koenig²⁴, T. Koffas³⁴, N.M. Köhler¹¹⁵, T. Koi¹⁵³, M. Kolb^{61b}, I. Koletsou⁵, T. Kondo⁸¹, N. Kondrashova^{60c}, K. Köneke⁵², A.C. König¹¹⁹, T. Kono¹²⁵, R. Konoplich^{124,an}, V. Konstantinides⁹⁴, N. Konstantinidis⁹⁴, B. Konya⁹⁶, R. Kopeliansky⁶⁵, S. Koperny^{83a}, K. Korcyl⁸⁴, K. Kordas¹⁶², G. Koren¹⁶¹, A. Korn⁹⁴, I. Korolkov¹⁴, E.V. Korolkova¹⁴⁹, N. Korotkova¹¹³, O. Kortner¹¹⁵, S. Kortner¹¹⁵, T. Kosek¹⁴³, V.V. Kostyukhin²⁴, A. Kotwal⁴⁹, A. Koulouris¹⁰, A. Kourkoumeli-Charalampidi^{70a,70b}, C. Kourkoumelis⁹, E. Kourlitis¹⁴⁹, V. Kouskoura²⁹, A.B. Kowalewska⁸⁴, R. Kowalewski¹⁷⁶, C. Kozakai¹⁶³, W. Kozanecki¹⁴⁵, A.S. Kozhin¹²³, V.A. Kramarenko¹¹³, G. Kramberger⁹¹, D. Krasnopevtsev^{60a}, M.W. Krasny¹³⁶, A. Krasznahorkay³⁶, D. Krauss¹¹⁵, J.A. Kremer^{83a}, J. Kretschmar⁹⁰, P. Krieger¹⁶⁷, K. Krizka¹⁸, K. Kroeninger⁴⁷, H. Kroha¹¹⁵, J. Kroll¹⁴¹, J. Kroll¹³⁷, J. Krstic¹⁶, U. Kruchonak⁷⁹, H. Krüger²⁴, N. Krumnack⁷⁸, M.C. Kruse⁴⁹, T. Kubota¹⁰⁴,

S. Kuday^{4b}, J.T. Kuechler⁴⁶, S. Kuehn³⁶, A. Kugel^{61a}, T. Kuhl⁴⁶, V. Kukhtin⁷⁹, R. Kukla¹⁰¹, Y. Kulchitsky^{107,aj}, S. Kuleshov^{147b}, Y.P. Kulinich¹⁷³, M. Kuna⁵⁸, T. Kunigo⁸⁵, A. Kupco¹⁴¹, T. Kupfer⁴⁷, O. Kuprash⁵², H. Kurashige⁸², L.L. Kurchaninov^{168a}, Y.A. Kurochkin¹⁰⁷, A. Kurova¹¹², M.G. Kurth^{15a,15d}, E.S. Kuwertz³⁶, M. Kuze¹⁶⁵, J. Kvita¹³⁰, T. Kwan¹⁰³, A. La Rosa¹¹⁵, J.L. La Rosa Navarro^{80d}, L. La Rotonda^{41b,41a}, F. La Ruffa^{41b,41a}, C. Lacasta¹⁷⁴, F. Lacava^{72a,72b}, D.P.J. Lack¹⁰⁰, H. Lacker¹⁹, D. Lacour¹³⁶, E. Ladygin⁷⁹, R. Lafaye⁵, B. Laforge¹³⁶, T. Lagouri^{33c}, S. Lai⁵³, S. Lammers⁶⁵, W. Lampl⁷, E. Lançon²⁹, U. Landgraf⁵², M.P.J. Landon⁹², M.C. Lanfermann⁵⁴, V.S. Lang⁴⁶, J.C. Lange⁵³, R.J. Langenberg³⁶, A.J. Lankford¹⁷¹, F. Lanni²⁹, K. Lantzsch²⁴, A. Lanza^{70a}, A. Lapertosa^{55b,55a}, S. Laplace¹³⁶, J.F. Laporte¹⁴⁵, T. Lari^{68a}, F. Lasagni Manghi^{23b,23a}, M. Lassnig³⁶, T.S. Lau^{63a}, A. Laudrain¹³², A. Laurier³⁴, M. Lavorgna^{69a,69b}, M. Lazzaroni^{68a,68b}, B. Le¹⁰⁴, O. Le Dortz¹³⁶, E. Le Guirriec¹⁰¹, M. LeBlanc⁷, T. LeCompte⁶, F. Ledroit-Guillon⁵⁸, C.A. Lee²⁹, G.R. Lee^{147a}, L. Lee⁵⁹, S.C. Lee¹⁵⁸, S.J. Lee³⁴, B. Lefebvre¹⁰³, M. Lefebvre¹⁷⁶, F. Legger¹¹⁴, C. Leggett¹⁸, K. Lehmann¹⁵², N. Lehmann¹⁸², G. Lehmann Miotto³⁶, W.A. Leight⁴⁶, A. Leisos^{162,w}, M.A.L. Leite^{80d}, R. Leitner¹⁴³, D. Lellouch^{180,*}, K.J.C. Leney⁴², T. Lenz²⁴, B. Lenzi³⁶, R. Leone⁷, S. Leone^{71a}, C. Leonidopoulos⁵⁰, A. Leopold¹³⁶, G. Lerner¹⁵⁶, C. Leroy¹⁰⁹, R. Les¹⁶⁷, C.G. Lester³², M. Levchenko¹³⁸, J. Levêque⁵, D. Levin¹⁰⁵, L.J. Levinson¹⁸⁰, B. Li^{15b}, B. Li¹⁰⁵, C.-Q. Li^{60a,am}, H. Li^{60a}, H. Li^{60b}, K. Li¹⁵³, L. Li^{60c}, M. Li^{15a}, Q. Li^{15a,15d}, Q.Y. Li^{60a}, S. Li^{60d,60c}, X. Li^{60c}, Y. Li⁴⁶, Z. Liang^{15a}, B. Liberti^{73a}, A. Liblong¹⁶⁷, K. Lie^{63c}, S. Liem¹²⁰, C.Y. Lin³², K. Lin¹⁰⁶, T.H. Lin⁹⁹, R.A. Linck⁶⁵, J.H. Lindon²¹, A.L. Lioni⁵⁴, E. Lipeles¹³⁷, A. Lipniacka¹⁷, M. Lisovyi^{61b}, T.M. Liss^{173,as}, A. Lister¹⁷⁵, A.M. Litke¹⁴⁶, J.D. Little⁸, B. Liu⁷⁸, B.L. Liu⁶, H.B. Liu²⁹, H. Liu¹⁰⁵, J.B. Liu^{60a}, J.K.K. Liu¹³⁵, K. Liu¹³⁶, M. Liu^{60a}, P. Liu¹⁸, Y. Liu^{15a,15d}, Y.L. Liu^{60a}, Y.W. Liu^{60a}, M. Livan^{70a,70b}, A. Lleres⁵⁸, J. Llorente Merino^{15a}, S.L. Lloyd⁹², C.Y. Lo^{63b}, F. Lo Sterzo⁴², E.M. Lobodzinska⁴⁶, P. Loch⁷, T. Lohse¹⁹, K. Lohwasser¹⁴⁹, M. Lokajicek¹⁴¹, J.D. Long¹⁷³, R.E. Long⁸⁹, L. Longo³⁶, K.A. Looper¹²⁶, J.A. Lopez^{147b}, I. Lopez Paz¹⁰⁰, A. Lopez Solis¹⁴⁹, J. Lorenz¹¹⁴, N. Lorenzo Martinez⁵, M. Losada²², P.J. Lösel¹¹⁴, A. Lösle⁵², X. Lou⁴⁶, X. Lou^{15a}, A. Lounis¹³², J. Love⁶, P.A. Love⁸⁹, J.J. Lozano Bahilo¹⁷⁴, H. Lu^{63a}, M. Lu^{60a}, Y.J. Lu⁶⁴, H.J. Lubatti¹⁴⁸, C. Luci^{72a,72b}, A. Lucotte⁵⁸, C. Luedtke⁵², F. Luehring⁶⁵, I. Luise¹³⁶, L. Luminari^{72a}, B. Lund-Jensen¹⁵⁴, M.S. Lutz¹⁰², D. Lynn²⁹, R. Lysak¹⁴¹, E. Lytken⁹⁶, F. Lyu^{15a}, V. Lyubushkin⁷⁹, T. Lyubushkina⁷⁹, H. Ma²⁹, L.L. Ma^{60b}, Y. Ma^{60b}, G. Maccarrone⁵¹, A. Macchiolo¹¹⁵, C.M. Macdonald¹⁴⁹, J. Machado Miguens^{137,140b}, D. Madaffari¹⁷⁴, R. Madar³⁸, W.F. Mader⁴⁸, N. Madysa⁴⁸, J. Maeda⁸², K. Maekawa¹⁶³, S. Maeland¹⁷, T. Maeno²⁹, M. Maerker⁴⁸, A.S. Maevskiy¹¹³, V. Magerl⁵², N. Magini⁷⁸, D.J. Mahon³⁹, C. Maidantchik^{80b}, T. Maier¹¹⁴, A. Maio^{140a,140b,140d}, O. Majersky^{28a}, S. Majewski¹³¹, Y. Makida⁸¹, N. Makovec¹³², B. Malaescu¹³⁶, Pa. Malecki⁸⁴, V.P. Maleev¹³⁸, F. Malek⁵⁸, U. Mallik⁷⁷, D. Malon⁶, C. Malone³², S. Maltezos¹⁰, S. Malyukov³⁶, J. Mamuzic¹⁷⁴, G. Mancini⁵¹, I. Mandić⁹¹, L. Manhaes de Andrade Filho^{80a}, I.M. Maniatis¹⁶², J. Manjarres Ramos⁴⁸, K.H. Mankinen⁹⁶, A. Mann¹¹⁴, A. Manousos⁷⁶, B. Mansoulie¹⁴⁵, I. Manthos¹⁶², S. Manzoni¹²⁰, A. Marantis¹⁶², G. Marceca³⁰, L. Marchese¹³⁵, G. Marchiori¹³⁶, M. Marcisovsky¹⁴¹, C. Marcon⁹⁶, C.A. Marin Tobon³⁶, M. Marjanovic³⁸, F. Marroquim^{80b}, Z. Marshall¹⁸, M.U.F. Martensson¹⁷², S. Marti-Garcia¹⁷⁴, C.B. Martin¹²⁶, T.A. Martin¹⁷⁸, V.J. Martin⁵⁰, B. Martin dit Latour¹⁷, M. Martinez^{14,y}, V.I. Martinez Outschoorn¹⁰², S. Martin-Haugh¹⁴⁴, V.S. Martoiu^{27b}, A.C. Martyniuk⁹⁴, A. Marzin³⁶, L. Masetti⁹⁹, T. Mashimo¹⁶³, R. Mashinistov¹¹⁰, J. Masik¹⁰⁰, A.L. Maslennikov^{122b,122a}, L.H. Mason¹⁰⁴, L. Massa^{73a,73b}, P. Massarotti^{69a,69b}, P. Mastrandrea^{71a,71b}, A. Mastroberardino^{41b,41a}, T. Masubuchi¹⁶³, A. Matic¹¹⁴, P. Mättig²⁴, J. Maurer^{27b}, B. Maček⁹¹, S.J. Maxfield⁹⁰, D.A. Maximov^{122b,122a}, R. Mazini¹⁵⁸, I. Maznas¹⁶², S.M. Mazza¹⁴⁶, S.P. Mc Kee¹⁰⁵, T.G. McCarthy¹¹⁵, L.I. McClymont⁹⁴, W.P. McCormack¹⁸, E.F. McDonald¹⁰⁴, J.A. Mcfayden³⁶, G. Mchedlidze⁵³, M.A. McKay⁴², K.D. McLean¹⁷⁶,

S.J. McMahon¹⁴⁴, P.C. McNamara¹⁰⁴, C.J. McNicol¹⁷⁸, R.A. McPherson^{176,ad}, J.E. Mdhluli^{33c}, Z.A. Meadows¹⁰², S. Meehan¹⁴⁸, T. Megy⁵², S. Mehlhase¹¹⁴, A. Mehta⁹⁰, T. Meideck⁵⁸, B. Meirose⁴³, D. Melini¹⁷⁴, B.R. Mellado Garcia^{33c}, J.D. Mellenthin⁵³, M. Melo^{28a}, F. Meloni⁴⁶, A. Melzer²⁴, S.B. Menary¹⁰⁰, E.D. Mendes Gouveia^{140a,140e}, L. Meng³⁶, X.T. Meng¹⁰⁵, S. Menke¹¹⁵, E. Meoni^{41b,41a}, S. Mergelmeyer¹⁹, S.A.M. Merkt¹³⁹, C. Merlassino²⁰, P. Mermod⁵⁴, L. Merola^{69a,69b}, C. Meroni^{68a}, J.K.R. Meshreki¹⁵¹, A. Messina^{72a,72b}, J. Metcalfe⁶, A.S. Mete¹⁷¹, C. Meyer⁶⁵, J. Meyer¹⁶⁰, J.-P. Meyer¹⁴⁵, H. Meyer Zu Theenhausen^{61a}, F. Miano¹⁵⁶, R.P. Middleton¹⁴⁴, L. Mijović⁵⁰, G. Mikenberg¹⁸⁰, M. Mikestikova¹⁴¹, M. Mikuz⁹¹, M. Milesi¹⁰⁴, A. Milic¹⁶⁷, D.A. Millar⁹², D.W. Miller³⁷, A. Milov¹⁸⁰, D.A. Milstead^{45a,45b}, R.A. Mina^{153,q}, A.A. Minaenko¹²³, M. Miñano Moya¹⁷⁴, I.A. Minashvili^{159b}, A.I. Mincer¹²⁴, B. Mindur^{83a}, M. Mineev⁷⁹, Y. Minegishi¹⁶³, Y. Ming¹⁸¹, L.M. Mir¹⁴, A. Mirto^{67a,67b}, K.P. Mistry¹³⁷, T. Mitani¹⁷⁹, J. Mitrevski¹¹⁴, V.A. Mitsou¹⁷⁴, M. Mittal^{160c}, A. Miucci²⁰, P.S. Miyagawa¹⁴⁹, A. Mizukami⁸¹, J.U. Mjörnmark⁹⁶, T. Mkrtchyan¹⁸⁴, M. Mlynarikova¹⁴³, T. Moa^{45a,45b}, K. Mochizuki¹⁰⁹, P. Mogg⁵², S. Mohapatra³⁹, R. Moles-Valls²⁴, M.C. Mondragon¹⁰⁶, K. Mönig⁴⁶, J. Monk⁴⁰, E. Monnier¹⁰¹, A. Montalbano¹⁵², J. Montejo Berlingen³⁶, M. Montella⁹⁴, F. Monticelli⁸⁸, S. Monzani^{68a}, N. Morange¹³², D. Moreno²², M. Moreno Llácer³⁶, P. Morettini^{55b}, M. Morgenstern¹²⁰, S. Morgenstern⁴⁸, D. Mori¹⁵², M. Morii⁵⁹, M. Morinaga¹⁷⁹, V. Morisbak¹³⁴, A.K. Morley³⁶, G. Mornacchi³⁶, A.P. Morris⁹⁴, L. Morvaj¹⁵⁵, P. Moschovakos¹⁰, M. Mosidze^{159b}, H.J. Moss¹⁴⁹, J. Moss^{31,n}, K. Motohashi¹⁶⁵, E. Mountricha³⁶, E.J.W. Moyse¹⁰², S. Muanza¹⁰¹, F. Mueller¹¹⁵, J. Mueller¹³⁹, R.S.P. Mueller¹¹⁴, D. Muenstermann⁸⁹, G.A. Mullier⁹⁶, F.J. Munoz Sanchez¹⁰⁰, P. Murin^{28b}, W.J. Murray^{178,144}, A. Murrone^{68a,68b}, M. Muškinja⁹¹, C. Mwewa^{33a}, A.G. Myagkov^{123,ao}, J. Myers¹³¹, M. Myska¹⁴², B.P. Nachman¹⁸, O. Nackenhorst⁴⁷, K. Nagai¹³⁵, K. Nagano⁸¹, Y. Nagasaka⁶², M. Nagel⁵², E. Nagy¹⁰¹, A.M. Nairz³⁶, Y. Nakahama¹¹⁷, K. Nakamura⁸¹, T. Nakamura¹⁶³, I. Nakano¹²⁷, H. Nanjo¹³³, F. Napolitano^{61a}, R.F. Naranjo Garcia⁴⁶, R. Narayan¹¹, D.I. Narrias Villar^{61a}, I. Naryshkin¹³⁸, T. Naumann⁴⁶, G. Navarro²², H.A. Neal^{105,*}, P.Y. Nechaeva¹¹⁰, F. Nechansky⁴⁶, T.J. Neep¹⁴⁵, A. Negri^{70a,70b}, M. Negrini^{23b}, S. Nektarijevic¹¹⁹, C. Nellist⁵³, M.E. Nelson¹³⁵, S. Nemecek¹⁴¹, P. Nemethy¹²⁴, M. Nessi^{36,e}, M.S. Neubauer¹⁷³, M. Neumann¹⁸², P.R. Newman²¹, T.Y. Ng^{63c}, Y.S. Ng¹⁹, Y.W.Y. Ng¹⁷¹, H.D.N. Nguyen¹⁰¹, T. Nguyen Manh¹⁰⁹, E. Nibigira³⁸, R.B. Nickerson¹³⁵, R. Nicolaidou¹⁴⁵, D.S. Nielsen⁴⁰, J. Nielsen¹⁴⁶, N. Nikiforou¹¹, V. Nikolaenko^{123,ao}, I. Nikolic-Audit¹³⁶, K. Nikolopoulos²¹, P. Nilsson²⁹, H.R. Nindhito⁵⁴, Y. Ninomiya⁸¹, A. Nisati^{72a}, N. Nishu^{60c}, R. Nisius¹¹⁵, I. Nitsche⁴⁷, T. Nitta¹⁷⁹, T. Nobe¹⁶³, Y. Noguchi⁸⁵, M. Nomachi¹³³, I. Nomidis¹³⁶, M.A. Nomura²⁹, M. Nordberg³⁶, N. Norjoharuddeen¹³⁵, T. Novak⁹¹, O. Novgorodova⁴⁸, R. Novotny¹⁴², L. Nozka¹³⁰, K. Ntekas¹⁷¹, E. Nurse⁹⁴, F. Nuti¹⁰⁴, F.G. Oakham^{34,av}, H. Oberlack¹¹⁵, J. Ocariz¹³⁶, A. Ochi⁸², I. Ochoa³⁹, J.P. Ochoa-Ricoux^{147a}, K. O'Connor²⁶, S. Oda⁸⁷, S. Odaka⁸¹, S. Oerdek⁵³, A. Ogrodnik^{83a}, A. Oh¹⁰⁰, S.H. Oh⁴⁹, C.C. Ohm¹⁵⁴, H. Oide^{55b,55a}, M.L. Ojeda¹⁶⁷, H. Okawa¹⁶⁹, Y. Okazaki⁸⁵, Y. Okumura¹⁶³, T. Okuyama⁸¹, A. Olariu^{27b}, L.F. Oleiro Seabra^{140a}, S.A. Olivares Pino^{147a}, D. Oliveira Damazio²⁹, J.L. Oliver¹, M.J.R. Olsson³⁷, A. Olszewski⁸⁴, J. Olszowska⁸⁴, D.C. O'Neil¹⁵², A. Onofre^{140a,140e}, K. Onogi¹¹⁷, P.U.E. Onyisi¹¹, H. Oppen¹³⁴, M.J. Oreglia³⁷, G.E. Orellana⁸⁸, Y. Oren¹⁶¹, D. Orestano^{74a,74b}, N. Orlando¹⁴, R.S. Orr¹⁶⁷, B. Osculati^{55b,55a,*}, V. O'Shea⁵⁷, R. Ospanov^{60a}, G. Otero y Garzon³⁰, H. Otono⁸⁷, M. Ouchrif^{35d}, F. Ould-Saada¹³⁴, A. Ouraou¹⁴⁵, Q. Ouyang^{15a}, M. Owen⁵⁷, R.E. Owen²¹, V.E. Ozcan^{12c}, N. Ozturk⁸, J. Pacalt¹³⁰, H.A. Pacey³², K. Pachal⁴⁹, A. Pacheco Pages¹⁴, C. Padilla Aranda¹⁴, S. Pagan Griso¹⁸, M. Paganini¹⁸³, G. Palacino⁶⁵, S. Palazzo⁵⁰, S. Palestini³⁶, M. Palka^{83b}, D. Pallin³⁸, I. Panagoulas¹⁰, C.E. Pandini³⁶, J.G. Panduro Vazquez⁹³, P. Pani⁴⁶, G. Panizzo^{66a,66c}, L. Paolozzi⁵⁴, K. Papageorgiou^{9,i}, A. Paramonov⁶, D. Paredes Hernandez^{63b}, S.R. Paredes Saenz¹³⁵, B. Parida¹⁶⁶, T.H. Park¹⁶⁷, A.J. Parker⁸⁹, M.A. Parker³², F. Parodi^{55b,55a}, E.W.P. Parrish¹²¹, J.A. Parsons³⁹, U. Parzefall⁵²,

L. Pascual Dominguez¹³⁶, V.R. Pascuzzi¹⁶⁷, J.M.P. Pasner¹⁴⁶, E. Pasqualucci^{72a}, S. Passaggio^{55b}, F. Pastore⁹³, P. Pasuwan^{45a,45b}, S. Pataria⁹⁹, J.R. Pater¹⁰⁰, A. Pathak^{181,j}, T. Pauly³⁶, B. Pearson¹¹⁵, M. Pedersen¹³⁴, L. Pedraza Diaz¹¹⁹, R. Pedro^{140a,140b}, S.V. Peleganchuk^{122b,122a}, O. Penc¹⁴¹, C. Peng^{15a}, H. Peng^{60a}, B.S. Peralva^{80a}, M.M. Perego¹³², A.P. Pereira Peixoto^{140a,140e}, D.V. Perepelitsa²⁹, F. Peri¹⁹, L. Perini^{68a,68b}, H. Pernegger³⁶, S. Perrella^{69a,69b}, V.D. Peshekhonov^{79,*}, K. Peters⁴⁶, R.F.Y. Peters¹⁰⁰, B.A. Petersen³⁶, T.C. Petersen⁴⁰, E. Petit⁵⁸, A. Petridis¹, C. Petridou¹⁶², P. Petroff¹³², M. Petrov¹³⁵, F. Petrucci^{74a,74b}, M. Pettee¹⁸³, N.E. Pettersson¹⁰², K. Petukhova¹⁴³, A. Peyaud¹⁴⁵, R. Pezoa^{147b}, T. Pham¹⁰⁴, F.H. Phillips¹⁰⁶, P.W. Phillips¹⁴⁴, M.W. Phipps¹⁷³, G. Piacquadio¹⁵⁵, E. Pianori¹⁸, A. Picazio¹⁰², R.H. Pickles¹⁰⁰, R. Piegaia³⁰, J.E. Pilcher³⁷, A.D. Pilkington¹⁰⁰, M. Pinamonti^{73a,73b}, J.L. Pinfold³, M. Pitt¹⁸⁰, L. Pizzimento^{73a,73b}, M.-A. Pleier²⁹, V. Pleskot¹⁴³, E. Plotnikova⁷⁹, D. Pluth⁷⁸, P. Podberezko^{122b,122a}, R. Poettgen⁹⁶, R. Poggi⁵⁴, L. Poggioli¹³², I. Pogrebnyak¹⁰⁶, D. Pohl²⁴, I. Pokharel⁵³, G. Polesello^{70a}, A. Poley¹⁸, A. Policicchio^{72a,72b}, R. Polifka³⁶, A. Polini^{23b}, C.S. Pollard⁴⁶, V. Polychronakos²⁹, D. Ponomarenko¹¹², L. Pontecorvo³⁶, G.A. Popeneciu^{27d}, D.M. Portillo Quintero¹³⁶, S. Pospisil¹⁴², K. Potamianos⁴⁶, I.N. Potrap⁷⁹, C.J. Potter³², H. Potti¹¹, T. Poulsen⁹⁶, J. Poveda³⁶, T.D. Powell¹⁴⁹, M.E. Pozo Astigarraga³⁶, P. Pralavorio¹⁰¹, S. Prell⁷⁸, D. Price¹⁰⁰, M. Primavera^{67a}, S. Prince¹⁰³, M.L. Proffitt¹⁴⁸, N. Proklova¹¹², K. Prokofiev^{63c}, F. Prokoshin^{147b}, S. Protopopescu²⁹, J. Proudfoot⁶, M. Przybycien^{83a}, A. Puri¹⁷³, P. Puzo¹³², J. Qian¹⁰⁵, Y. Qin¹⁰⁰, A. Quad⁵³, M. Queitsch-Maitland⁴⁶, A. Qureshi¹, P. Rados¹⁰⁴, F. Ragusa^{68a,68b}, G. Rahal⁹⁷, J.A. Raine⁵⁴, S. Rajagopalan²⁹, A. Ramirez Morales⁹², K. Ran^{15a,15d}, T. Rashid¹³², S. Raspopov⁵, M.G. Ratti^{68a,68b}, D.M. Rauch⁴⁶, F. Rauscher¹¹⁴, S. Rave⁹⁹, B. Ravina¹⁴⁹, I. Ravinovitch¹⁸⁰, J.H. Rawling¹⁰⁰, M. Raymond³⁶, A.L. Read¹³⁴, N.P. Readioff⁵⁸, M. Reale^{67a,67b}, D.M. Rebuzzi^{70a,70b}, A. Redelbach¹⁷⁷, G. Redlinger²⁹, R.G. Reed^{33c}, K. Reeves⁴³, L. Rehnisch¹⁹, J. Reichert¹³⁷, D. Reikher¹⁶¹, A. Reiss⁹⁹, A. Rej¹⁵¹, C. Rembser³⁶, H. Ren^{15a}, M. Rescigno^{72a}, S. Resconi^{68a}, E.D. Resseguie¹³⁷, S. Rettie¹⁷⁵, E. Reynolds²¹, O.L. Rezanova^{122b,122a}, P. Reznicek¹⁴³, E. Ricci^{75a,75b}, R. Richter¹¹⁵, S. Richter⁴⁶, E. Richter-Was^{83b}, O. Ricken²⁴, M. Ridel¹³⁶, P. Rieck¹¹⁵, C.J. Riegel¹⁸², O. Rifki⁴⁶, M. Rijssenbeek¹⁵⁵, A. Rimoldi^{70a,70b}, M. Rimoldi²⁰, L. Rinaldi^{23b}, G. Ripellino¹⁵⁴, B. Ristic⁸⁹, E. Ritsch³⁶, I. Riu¹⁴, J.C. Rivera Vergara^{147a}, F. Rizatdinova¹²⁹, E. Rizvi⁹², C. Rizzi¹⁴, R.T. Roberts¹⁰⁰, S.H. Robertson^{103,ad}, D. Robinson³², J.E.M. Robinson⁴⁶, A. Robson⁵⁷, E. Rocco⁹⁹, C. Roda^{71a,71b}, Y. Rodina¹⁰¹, S. Rodriguez Bosca¹⁷⁴, A. Rodriguez Perez¹⁴, D. Rodriguez Rodriguez¹⁷⁴, A.M. Rodríguez Vera^{168b}, S. Roe³⁶, O. Röhne¹³⁴, R. Röhrig¹¹⁵, C.P.A. Roland⁶⁵, J. Roloff⁵⁹, A. Romaniouk¹¹², M. Romano^{23b,23a}, N. Rompotis⁹⁰, M. Ronzani¹²⁴, L. Roos¹³⁶, S. Rosati^{72a}, K. Rosbach⁵², N.-A. Rosien⁵³, B.J. Rosser¹³⁷, E. Rossi⁴⁶, E. Rossi^{74a,74b}, E. Rossi^{69a,69b}, L.P. Rossi^{55b}, L. Rossini^{68a,68b}, J.H.N. Rosten³², R. Rosten¹⁴, M. Rotaru^{27b}, J. Rothberg¹⁴⁸, D. Rousseau¹³², D. Roy^{33c}, A. Rozanov¹⁰¹, Y. Rozen¹⁶⁰, X. Ruan^{33c}, F. Rubbo¹⁵³, F. Rühr⁵², A. Ruiz-Martinez¹⁷⁴, Z. Rurikova⁵², N.A. Rusakovitch⁷⁹, H.L. Russell¹⁰³, L. Rustige^{38,47}, J.P. Rutherford⁷, E.M. Rüttinger^{46,k}, Y.F. Ryabov¹³⁸, M. Rybar³⁹, G. Rybkin¹³², S. Ryu⁶, A. Ryzhov¹²³, G.F. Rzehorz⁵³, P. Sabatini⁵³, G. Sabato¹²⁰, S. Sacerdoti¹³², H.F.-W. Sadrozinski¹⁴⁶, R. Sadykov⁷⁹, F. Safai Tehrani^{72a}, P. Saha¹²¹, M. Sahinsoy^{61a}, A. Sahu¹⁸², M. Saimpert⁴⁶, M. Saito¹⁶³, T. Saito¹⁶³, H. Sakamoto¹⁶³, A. Sakharov^{124,an}, D. Salamani⁵⁴, G. Salamanna^{74a,74b}, J.E. Salazar Loyola^{147b}, P.H. Sales De Bruin¹⁷², D. Salihagic^{115,*}, A. Salmikov¹⁵³, J. Salt¹⁷⁴, D. Salvatore^{41b,41a}, F. Salvatore¹⁵⁶, A. Salvucci^{63a,63b,63c}, A. Salzburger³⁶, J. Samarati³⁶, D. Sammel⁵², D. Sampsonidis¹⁶², D. Sampsonidou¹⁶², J. Sánchez¹⁷⁴, A. Sanchez Pineda^{66a,66c}, H. Sandaker¹³⁴, C.O. Sander⁴⁶, M. Sandhoff¹⁸², C. Sandoval²², D.P.C. Sankey¹⁴⁴, M. Sannino^{55b,55a}, Y. Sano¹¹⁷, A. Sansoni⁵¹, C. Santoni³⁸, H. Santos^{140a,140b}, S.N. Santpur¹⁸, A. Santra¹⁷⁴, A. Sapronov⁷⁹, J.G. Saraiva^{140a,140d}, O. Sasaki⁸¹, K. Sato¹⁶⁹, E. Sauvan⁵, P. Savard^{167,av}, N. Savic¹¹⁵, R. Sawada¹⁶³, C. Sawyer¹⁴⁴, L. Sawyer^{95,al}, C. Sbarra^{23b}, A. Sbrizzi^{23a},

T. Scanlon⁹⁴, J. Schaarschmidt¹⁴⁸, P. Schacht¹¹⁵, B.M. Schachtner¹¹⁴, D. Schaefer³⁷, L. Schaefer¹³⁷, J. Schaeffer⁹⁹, S. Schaepe³⁶, U. Schäfer⁹⁹, A.C. Schaffer¹³², D. Schaile¹¹⁴, R.D. Schamberger¹⁵⁵, N. Scharmberg¹⁰⁰, V.A. Schegelsky¹³⁸, D. Scheirich¹⁴³, F. Schenck¹⁹, M. Schernau¹⁷¹, C. Schiavi^{55b,55a}, S. Schier¹⁴⁶, L.K. Schildgen²⁴, Z.M. Schillaci²⁶, E.J. Schioppa³⁶, M. Schioppa^{41b,41a}, K.E. Schleicher⁵², S. Schlenker³⁶, K.R. Schmidt-Sommerfeld¹¹⁵, K. Schmieden³⁶, C. Schmitt⁹⁹, S. Schmitt⁴⁶, S. Schmitz⁹⁹, J.C. Schmoeckel⁴⁶, U. Schnoor⁵², L. Schoeffel¹⁴⁵, A. Schoening^{61b}, E. Schopf¹³⁵, M. Schott⁹⁹, J.F.P. Schouwenberg¹¹⁹, J. Schovancova³⁶, S. Schramm⁵⁴, A. Schulte⁹⁹, H-C. Schultz-Coulon^{61a}, M. Schumacher⁵², B.A. Schumm¹⁴⁶, Ph. Schune¹⁴⁵, A. Schwartzman¹⁵³, T.A. Schwarz¹⁰⁵, Ph. Schwemling¹⁴⁵, R. Schwienhorst¹⁰⁶, A. Sciandra²⁴, G. Sciolla²⁶, M. Scornajenghi^{41b,41a}, F. Scuri^{71a}, F. Scutti¹⁰⁴, L.M. Scyboz¹¹⁵, C.D. Sebastiani^{72a,72b}, P. Seema¹⁹, S.C. Seidel¹¹⁸, A. Seiden¹⁴⁶, T. Seiss³⁷, J.M. Seixas^{80b}, G. Sekhniaidze^{69a}, K. Sekhon¹⁰⁵, S.J. Sekula⁴², N. Semprini-Cesari^{23b,23a}, S. Sen⁴⁹, S. Senkin³⁸, C. Serfon⁷⁶, L. Serin¹³², L. Serkin^{66a,66b}, M. Sessa^{60a}, H. Severini¹²⁸, F. Sforza¹⁷⁰, A. Sfyrila⁵⁴, E. Shabalina⁵³, J.D. Shahinian¹⁴⁶, N.W. Shaikh^{45a,45b}, D. Shaked Renous¹⁸⁰, L.Y. Shan^{15a}, R. Shang¹⁷³, J.T. Shank²⁵, M. Shapiro¹⁸, A.S. Sharma¹, A. Sharma¹³⁵, P.B. Shatalov¹¹¹, K. Shaw¹⁵⁶, S.M. Shaw¹⁰⁰, A. Shcherbakova¹³⁸, Y. Shen¹²⁸, N. Sherafati³⁴, A.D. Sherman²⁵, P. Sherwood⁹⁴, L. Shi^{158,ar}, S. Shimizu⁸¹, C.O. Shimmin¹⁸³, Y. Shimogama¹⁷⁹, M. Shimojima¹¹⁶, I.P.J. Shipsey¹³⁵, S. Shirabe⁸⁷, M. Shiyakova^{79,ab}, J. Shlomi¹⁸⁰, A. Shmeleva¹¹⁰, M.J. Shochet³⁷, S. Shojaii¹⁰⁴, D.R. Shope¹²⁸, S. Shrestha¹²⁶, E. Shulga¹¹², P. Sicho¹⁴¹, A.M. Sickles¹⁷³, P.E. Sidebo¹⁵⁴, E. Sideras Haddad^{33c}, O. Sidiropoulou³⁶, A. Sidoti^{23b,23a}, F. Siegert⁴⁸, Dj. Sijacki¹⁶, J. Silva^{140a}, M. Silva Jr.¹⁸¹, M.V. Silva Oliveira^{80a}, S.B. Silverstein^{45a}, S. Simion¹³², E. Simioni⁹⁹, M. Simon⁹⁹, R. Simoniello⁹⁹, P. Sinervo¹⁶⁷, N.B. Sinev¹³¹, M. Sioli^{23b,23a}, I. Siral¹⁰⁵, S.Yu. Sivoklov¹¹³, J. Sjölin^{45a,45b}, E. Skorda⁹⁶, P. Skubic¹²⁸, M. Slawinska⁸⁴, K. Sliwa¹⁷⁰, R. Slovak¹⁴³, V. Smakhtin¹⁸⁰, B.H. Smart⁵, J. Smiesko^{28a}, N. Smirnov¹¹², S.Yu. Smirnov¹¹², Y. Smirnov¹¹², L.N. Smirnova^{113,t}, O. Smirnova⁹⁶, J.W. Smith⁵³, M. Smizanska⁸⁹, K. Smolek¹⁴², A. Smykiewicz⁸⁴, A.A. Snesarev¹¹⁰, I.M. Snyder¹³¹, S. Snyder²⁹, R. Sobie^{176,ad}, A.M. Soffa¹⁷¹, A. Soffer¹⁶¹, A. Sogaard⁵⁰, F. Sohns⁵³, G. Sokhrannyi⁹¹, C.A. Solans Sanchez³⁶, E.Yu. Soldatov¹¹², U. Soldevila¹⁷⁴, A.A. Solodkov¹²³, A. Soloshenko⁷⁹, O.V. Solovyanov¹²³, V. Solovyev¹³⁸, P. Sommer¹⁴⁹, H. Son¹⁷⁰, W. Song¹⁴⁴, W.Y. Song^{168b}, A. Sopczak¹⁴², F. Sopkova^{28b}, C.L. Sotiropoulou^{71a,71b}, S. Sottocornola^{70a,70b}, R. Soualah^{66a,66c,h}, A.M. Soukharev^{122b,122a}, D. South⁴⁶, S. Spagnolo^{67a,67b}, M. Spalla¹¹⁵, M. Spangenberg¹⁷⁸, F. Spano⁹³, D. Sperlich¹⁹, T.M. Spieker^{61a}, R. Spighi^{23b}, G. Spigo³⁶, L.A. Spiller¹⁰⁴, D.P. Spiteri⁵⁷, M. Spousta¹⁴³, A. Stabile^{68a,68b}, B.L. Stamas¹²¹, R. Stamen^{61a}, M. Stamenkovic¹²⁰, S. Stamm¹⁹, E. Stanecka⁸⁴, R.W. Stanek⁶, B. Stanislaus¹³⁵, M.M. Stanitzki⁴⁶, B. Stapf¹²⁰, E.A. Starchenko¹²³, G.H. Stark¹⁴⁶, J. Stark⁵⁸, S.H. Stark⁴⁰, P. Staroba¹⁴¹, P. Starovoitov^{61a}, S. Stärz¹⁰³, R. Staszewski⁸⁴, G. Stavropoulos⁴⁴, M. Stegler⁴⁶, P. Steinberg²⁹, B. Stelzer¹⁵², H.J. Stelzer³⁶, O. Stelzer-Chilton^{168a}, H. Stenzel⁵⁶, T.J. Stevenson¹⁵⁶, G.A. Stewart³⁶, M.C. Stockton³⁶, G. Stoicea^{27b}, M. Stolarski^{140a}, P. Stolte⁵³, S. Stonjek¹¹⁵, A. Straessner⁴⁸, J. Strandberg¹⁵⁴, S. Strandberg^{45a,45b}, M. Strauss¹²⁸, P. Strizenec^{28b}, R. Ströhmer¹⁷⁷, D.M. Strom¹³¹, R. Stroynowski⁴², A. Strubig⁵⁰, S.A. Stucci²⁹, B. Stugu¹⁷, J. Stupak¹²⁸, N.A. Styles⁴⁶, D. Su¹⁵³, S. Suchek^{61a}, Y. Sugaya¹³³, V.V. Sulin¹¹⁰, M.J. Sullivan⁹⁰, D.M.S. Sultan⁵⁴, S. Sultansoy^{4c}, T. Sumida⁸⁵, S. Sun¹⁰⁵, X. Sun³, K. Suruliz¹⁵⁶, C.J.E. Suster¹⁵⁷, M.R. Sutton¹⁵⁶, S. Suzuki⁸¹, M. Svatos¹⁴¹, M. Swiatlowski³⁷, S.P. Swift², A. Sydorenko⁹⁹, I. Sykora^{28a}, M. Sykora¹⁴³, T. Sykora¹⁴³, D. Ta⁹⁹, K. Tackmann^{46,z}, J. Taenzer¹⁶¹, A. Taffard¹⁷¹, R. Tafirout^{168a}, E. Tahirovic⁹², H. Takai²⁹, R. Takashima⁸⁶, K. Takeda⁸², T. Takeshita¹⁵⁰, Y. Takubo⁸¹, M. Talby¹⁰¹, A.A. Talyshchev^{122b,122a}, J. Tanaka¹⁶³, M. Tanaka¹⁶⁵, R. Tanaka¹³², B.B. Tannenwald¹²⁶, S. Tapia Araya¹⁷³, S. Tapprogge⁹⁹, A. Tarek Abouelfadl Mohamed¹³⁶, S. Tarem¹⁶⁰, G. Tarna^{27b,d}, G.F. Tartarelli^{68a}, P. Tas¹⁴³, M. Tasevsky¹⁴¹, T. Tashiro⁸⁵,

E. Tassi^{41b,41a}, A. Tavares Delgado^{140a,140b}, Y. Tayalati^{35e}, A.J. Taylor⁵⁰, G.N. Taylor¹⁰⁴, P.T.E. Taylor¹⁰⁴, W. Taylor^{168b}, A.S. Tee⁸⁹, R. Teixeira De Lima¹⁵³, P. Teixeira-Dias⁹³, H. Ten Kate³⁶, J.J. Teoh¹²⁰, S. Terada⁸¹, K. Terashi¹⁶³, J. Terron⁹⁸, S. Terzo¹⁴, M. Testa⁵¹, R.J. Teuscher^{167,ad}, S.J. Thais¹⁸³, T. Theveneaux-Pelzer⁴⁶, F. Thiele⁴⁰, D.W. Thomas⁹³, J.P. Thomas²¹, A.S. Thompson⁵⁷, P.D. Thompson²¹, L.A. Thomsen¹⁸³, E. Thomson¹³⁷, Y. Tian³⁹, R.E. Ticse Torres⁵³, V.O. Tikhomirov^{110,ap}, Yu.A. Tikhonov^{122b,122a}, S. Timoshenko¹¹², P. Tipton¹⁸³, S. Tisserant¹⁰¹, K. Todome¹⁶⁵, S. Todorova-Nova⁵, S. Todt⁴⁸, J. Tojo⁸⁷, S. Tokár^{28a}, K. Tokushuku⁸¹, E. Tolley¹²⁶, K.G. Tomiwa^{33c}, M. Tomoto¹¹⁷, L. Tompkins^{153,q}, K. Toms¹¹⁸, B. Tong⁵⁹, P. Tornambe⁵², E. Torrence¹³¹, H. Torres⁴⁸, E. Torró Pastor¹⁴⁸, C. Tosciri¹³⁵, J. Toth^{101,ac}, D.R. Tovey¹⁴⁹, C.J. Treado¹²⁴, T. Trefzger¹⁷⁷, F. Tresoldi¹⁵⁶, A. Tricoli²⁹, I.M. Trigger^{168a}, S. Trincaz-Duvold¹³⁶, W. Trischuk¹⁶⁷, B. Trocme⁵⁸, A. Trofymov¹³², C. Troncon^{68a}, M. Trovatelli¹⁷⁶, F. Trovato¹⁵⁶, L. Truong^{33b}, M. Trzebinski⁸⁴, A. Trzupek⁸⁴, F. Tsai⁴⁶, J.C.-L. Tseng¹³⁵, P.V. Tsiarshka^{107,aj}, A. Tsirigotis¹⁶², N. Tsirintanis⁹, V. Tsiskaridze¹⁵⁵, E.G. Tskhadadze^{159a}, M. Tsopoulou¹⁶², I.I. Tsukerman¹¹¹, V. Tsulaia¹⁸, S. Tsuno⁸¹, D. Tsybychev¹⁵⁵, Y. Tu^{63b}, A. Tudorache^{27b}, V. Tudorache^{27b}, T.T. Tulbure^{27a}, A.N. Tuna⁵⁹, S. Turchikhin⁷⁹, D. Turgeman¹⁸⁰, I. Turk Cakir^{4b,u}, R.J. Turner²¹, R.T. Turra^{68a}, P.M. Tuts³⁹, S. Tzamarias¹⁶², E. Tzovara⁹⁹, G. Ucchielli⁴⁷, I. Ueda⁸¹, M. Ughetto^{45a,45b}, F. Ukegawa¹⁶⁹, G. Unal³⁶, A. Undrus²⁹, G. Unel¹⁷¹, F.C. Ungaro¹⁰⁴, Y. Unno⁸¹, K. Uno¹⁶³, J. Urban^{28b}, P. Urquijo¹⁰⁴, G. Usai⁸, J. Usui⁸¹, L. Vacavant¹⁰¹, V. Vacek¹⁴², B. Vachon¹⁰³, K.O.H. Vadla¹³⁴, A. Vaidya⁹⁴, C. Valderanis¹¹⁴, E. Valdes Santurio^{45a,45b}, M. Valente⁵⁴, S. Valentinetti^{23b,23a}, A. Valero¹⁷⁴, L. Valéry⁴⁶, R.A. Vallance²¹, A. Vallier⁵, J.A. Valls Ferrer¹⁷⁴, T.R. Van Daalen¹⁴, P. Van Gemmeren⁶, I. Van Vulpen¹²⁰, M. Vanadia^{73a,73b}, W. Vandelli³⁶, A. Vaniachine¹⁶⁶, R. Vari^{72a}, E.W. Varnes⁷, C. Varni^{55b,55a}, T. Varol⁴², D. Varouchas¹³², K.E. Varvell¹⁵⁷, G.A. Vasquez^{147b}, J.G. Vasquez¹⁸³, F. Vazeille³⁸, D. Vazquez Furelos¹⁴, T. Vazquez Schroeder³⁶, J. Veatch⁵³, V. Vecchio^{74a,74b}, L.M. Veloce¹⁶⁷, F. Veloso^{140a,140c}, S. Veneziano^{72a}, A. Ventura^{67a,67b}, N. Venturi³⁶, A. Verbytskyi¹¹⁵, V. Vercesi^{70a}, M. Verducci^{74a,74b}, C.M. Vergel Infante⁷⁸, C. Vergis²⁴, W. Verkerke¹²⁰, A.T. Vermeulen¹²⁰, J.C. Vermeulen¹²⁰, M.C. Vetterli^{152,av}, N. Viaux Maira^{147b}, M. Vicente Barreto Pinto⁵⁴, I. Vichou^{173,*}, T. Vickey¹⁴⁹, O.E. Vickey Boeriu¹⁴⁹, G.H.A. Viehhauser¹³⁵, L. Viganì¹³⁵, M. Villa^{23b,23a}, M. Villaplana Perez^{68a,68b}, E. Vilucchi⁵¹, M.G. Vincker³⁴, V.B. Vinogradov⁷⁹, A. Vishwakarma⁴⁶, C. Vittori^{23b,23a}, I. Vivarelli¹⁵⁶, M. Vogel¹⁸², P. Vokac¹⁴², G. Volpi¹⁴, S.E. von Buddenbrock^{33c}, E. Von Toerne²⁴, V. Vorobel¹⁴³, K. Vorobev¹¹², M. Vos¹⁷⁴, J.H. Vosseveld⁹⁰, N. Vranjes¹⁶, M. Vranjes Milosavljevic¹⁶, V. Vrba¹⁴², M. Vreeswijk¹²⁰, T. Šfiligoj⁹¹, R. Vuillermet³⁶, I. Vukotic³⁷, T. Ženiš^{28a}, L. Živković¹⁶, P. Wagner²⁴, W. Wagner¹⁸², J. Wagner-Kuhr¹¹⁴, H. Wahlberg⁸⁸, S. Wahrmund⁴⁸, K. Wakamiya⁸², V.M. Walbrecht¹¹⁵, J. Walder⁸⁹, R. Walker¹¹⁴, S.D. Walker⁹³, W. Walkowiak¹⁵¹, V. Wallangen^{45a,45b}, A.M. Wang⁵⁹, C. Wang^{60b}, F. Wang¹⁸¹, H. Wang¹⁸, H. Wang³, J. Wang¹⁵⁷, J. Wang^{61b}, P. Wang⁴², Q. Wang¹²⁸, R.-J. Wang¹³⁶, R. Wang^{60a}, R. Wang⁶, S.M. Wang¹⁵⁸, W.T. Wang^{60a}, W. Wang^{15c,ae}, W.X. Wang^{60a,ae}, Y. Wang^{60a,am}, Z. Wang^{60c}, C. Wanotayaroj⁴⁶, A. Warburton¹⁰³, C.P. Ward³², D.R. Wardrope⁹⁴, A. Washbrook⁵⁰, A.T. Watson²¹, M.F. Watson²¹, G. Watts¹⁴⁸, B.M. Waugh⁹⁴, A.F. Webb¹¹, S. Webb⁹⁹, C. Weber¹⁸³, M.S. Weber²⁰, S.A. Weber³⁴, S.M. Weber^{61a}, A.R. Weidberg¹³⁵, J. Weingarten⁴⁷, M. Weirich⁹⁹, C. Weiser⁵², P.S. Wells³⁶, T. Wenaus²⁹, T. Wengler³⁶, S. Wenig³⁶, N. Wermes²⁴, M.D. Werner⁷⁸, P. Werner³⁶, M. Wessels^{61a}, T.D. Weston²⁰, K. Whalen¹³¹, N.L. Whallon¹⁴⁸, A.M. Wharton⁸⁹, A.S. White¹⁰⁵, A. White⁸, M.J. White¹, R. White^{147b}, D. Whiteson¹⁷¹, B.W. Whitmore⁸⁹, F.J. Wickens¹⁴⁴, W. Wiedenmann¹⁸¹, M. Wielers¹⁴⁴, C. Wiglesworth⁴⁰, L.A.M. Wiik-Fuchs⁵², F. Wilk¹⁰⁰, H.G. Wilkens³⁶, L.J. Wilkins⁹³, H.H. Williams¹³⁷, S. Williams³², C. Willis¹⁰⁶, S. Willocq¹⁰², J.A. Wilson²¹, I. Wingerter-Seez⁵, E. Winkels¹⁵⁶, F. Winklmeier¹³¹, O.J. Winston¹⁵⁶, B.T. Winter⁵², M. Wittgen¹⁵³, M. Wobisch⁹⁵, A. Wolf⁹⁹, T.M.H. Wolf¹²⁰,

R. Wolff¹⁰¹, J. Wollrath⁵², M.W. Wolter⁸⁴, H. Wolters^{140a,140c}, V.W.S. Wong¹⁷⁵, N.L. Woods¹⁴⁶, S.D. Worm²¹, B.K. Wosiek⁸⁴, K.W. Woźniak⁸⁴, K. Wraight⁵⁷, S.L. Wu¹⁸¹, X. Wu⁵⁴, Y. Wu^{60a}, T.R. Wyatt¹⁰⁰, B.M. Wynne⁵⁰, S. Xella⁴⁰, Z. Xi¹⁰⁵, L. Xia¹⁷⁸, D. Xu^{15a}, H. Xu^{60a,d}, L. Xu²⁹, T. Xu¹⁴⁵, W. Xu¹⁰⁵, Z. Xu¹⁵³, B. Yabsley¹⁵⁷, S. Yacoob^{33a}, K. Yajima¹³³, D.P. Yallup⁹⁴, D. Yamaguchi¹⁶⁵, Y. Yamaguchi¹⁶⁵, A. Yamamoto⁸¹, T. Yamanaka¹⁶³, F. Yamane⁸², M. Yamatani¹⁶³, T. Yamazaki¹⁶³, Y. Yamazaki⁸², Z. Yan²⁵, H.J. Yang^{60c,60d}, H.T. Yang¹⁸, S. Yang⁷⁷, Y. Yang¹⁶³, Z. Yang¹⁷, W.-M. Yao¹⁸, Y.C. Yap⁴⁶, Y. Yasu⁸¹, E. Yatsenko^{60c,60d}, J. Ye⁴², S. Ye²⁹, I. Yeletsikh⁷⁹, E. Yigitbasi²⁵, E. Yildirim⁹⁹, K. Yorita¹⁷⁹, K. Yoshihara¹³⁷, C.J.S. Young³⁶, C. Young¹⁵³, J. Yu⁷⁸, X. Yue^{61a}, S.P.Y. Yuen²⁴, B. Zabinski⁸⁴, G. Zacharis¹⁰, E. Zaffaroni⁵⁴, R. Zaidan¹⁴, A.M. Zaitsev^{123,ao}, T. Zakareishvili^{159b}, N. Zakharchuk³⁴, S. Zambito⁵⁹, D. Zanzi³⁶, D.R. Zaripovas⁵⁷, S.V. Zeißner⁴⁷, C. Zeitnitz¹⁸², G. Zemaityte¹³⁵, J.C. Zeng¹⁷³, O. Zenin¹²³, D. Zerwas¹³², M. Zgubić¹³⁵, D.F. Zhang^{15b}, F. Zhang¹⁸¹, G. Zhang^{60a}, G. Zhang^{15b}, H. Zhang^{15c}, J. Zhang⁶, L. Zhang^{15c}, L. Zhang^{60a}, M. Zhang¹⁷³, R. Zhang^{60a}, R. Zhang²⁴, X. Zhang^{60b}, Y. Zhang^{15a,15d}, Z. Zhang^{63a}, Z. Zhang¹³², P. Zhao⁴⁹, Y. Zhao^{60b}, Z. Zhao^{60a}, A. Zhemchugov⁷⁹, Z. Zheng¹⁰⁵, D. Zhong¹⁷³, B. Zhou¹⁰⁵, C. Zhou¹⁸¹, M.S. Zhou^{15a,15d}, M. Zhou¹⁵⁵, N. Zhou^{60c}, Y. Zhou⁷, C.G. Zhu^{60b}, H.L. Zhu^{60a}, H. Zhu^{15a}, J. Zhu¹⁰⁵, Y. Zhu^{60a}, X. Zhuang^{15a}, K. Zhukov¹¹⁰, V. Zhulanov^{122b,122a}, D. Zieminska⁶⁵, N.I. Zimine⁷⁹, S. Zimmermann⁵², Z. Zinonos¹¹⁵, M. Ziolkowski¹⁵¹, G. Zoernig¹⁸¹, A. Zoccoli^{23b,23a}, K. Zoch⁵³, T.G. Zorbas¹⁴⁹, R. Zou³⁷, L. Zwalinski³⁶.

¹ Department of Physics, University of Adelaide, Adelaide; Australia.

² Physics Department, SUNY Albany, Albany NY; United States of America.

³ Department of Physics, University of Alberta, Edmonton AB; Canada.

⁴ ^(a) Department of Physics, Ankara University, Ankara; ^(b) Istanbul Aydin University, Istanbul; ^(c) Division of Physics, TOBB University of Economics and Technology, Ankara; Turkey.

⁵ LAPP, Université Grenoble Alpes, Université Savoie Mont Blanc, CNRS/IN2P3, Annecy; France.

⁶ High Energy Physics Division, Argonne National Laboratory, Argonne IL; United States of America.

⁷ Department of Physics, University of Arizona, Tucson AZ; United States of America.

⁸ Department of Physics, University of Texas at Arlington, Arlington TX; United States of America.

⁹ Physics Department, National and Kapodistrian University of Athens, Athens; Greece.

¹⁰ Physics Department, National Technical University of Athens, Zografou; Greece.

¹¹ Department of Physics, University of Texas at Austin, Austin TX; United States of America.

¹² ^(a) Bahcesehir University, Faculty of Engineering and Natural Sciences, Istanbul; ^(b) Istanbul Bilgi University, Faculty of Engineering and Natural Sciences, Istanbul; ^(c) Department of Physics, Bogazici University, Istanbul; ^(d) Department of Physics Engineering, Gaziantep University, Gaziantep; Turkey.

¹³ Institute of Physics, Azerbaijan Academy of Sciences, Baku; Azerbaijan.

¹⁴ Institut de Física d'Altes Energies (IFAE), Barcelona Institute of Science and Technology, Barcelona; Spain.

¹⁵ ^(a) Institute of High Energy Physics, Chinese Academy of Sciences, Beijing; ^(b) Physics Department, Tsinghua University, Beijing; ^(c) Department of Physics, Nanjing University, Nanjing; ^(d) University of Chinese Academy of Science (UCAS), Beijing; China.

¹⁶ Institute of Physics, University of Belgrade, Belgrade; Serbia.

¹⁷ Department for Physics and Technology, University of Bergen, Bergen; Norway.

¹⁸ Physics Division, Lawrence Berkeley National Laboratory and University of California, Berkeley CA; United States of America.

¹⁹ Institut für Physik, Humboldt Universität zu Berlin, Berlin; Germany.

²⁰ Albert Einstein Center for Fundamental Physics and Laboratory for High Energy Physics, University of Bern, Bern; Switzerland.

²¹ School of Physics and Astronomy, University of Birmingham, Birmingham; United Kingdom.

²² Facultad de Ciencias y Centro de Investigaciones, Universidad Antonio Nariño, Bogota; Colombia.

- ²³ ^(a) INFN Bologna and Università di Bologna, Dipartimento di Fisica; ^(b) INFN Sezione di Bologna; Italy.
- ²⁴ Physikalisches Institut, Universität Bonn, Bonn; Germany.
- ²⁵ Department of Physics, Boston University, Boston MA; United States of America.
- ²⁶ Department of Physics, Brandeis University, Waltham MA; United States of America.
- ²⁷ ^(a) Transilvania University of Brasov, Brasov; ^(b) Horia Hulubei National Institute of Physics and Nuclear Engineering, Bucharest; ^(c) Department of Physics, Alexandru Ioan Cuza University of Iasi, Iasi; ^(d) National Institute for Research and Development of Isotopic and Molecular Technologies, Physics Department, Cluj-Napoca; ^(e) University Politehnica Bucharest, Bucharest; ^(f) West University in Timisoara, Timisoara; Romania.
- ²⁸ ^(a) Faculty of Mathematics, Physics and Informatics, Comenius University, Bratislava; ^(b) Department of Subnuclear Physics, Institute of Experimental Physics of the Slovak Academy of Sciences, Kosice; Slovak Republic.
- ²⁹ Physics Department, Brookhaven National Laboratory, Upton NY; United States of America.
- ³⁰ Departamento de Física, Universidad de Buenos Aires, Buenos Aires; Argentina.
- ³¹ California State University, CA; United States of America.
- ³² Cavendish Laboratory, University of Cambridge, Cambridge; United Kingdom.
- ³³ ^(a) Department of Physics, University of Cape Town, Cape Town; ^(b) Department of Mechanical Engineering Science, University of Johannesburg, Johannesburg; ^(c) School of Physics, University of the Witwatersrand, Johannesburg; South Africa.
- ³⁴ Department of Physics, Carleton University, Ottawa ON; Canada.
- ³⁵ ^(a) Faculté des Sciences Ain Chock, Réseau Universitaire de Physique des Hautes Energies — Université Hassan II, Casablanca; ^(b) Faculté des Sciences, Université Ibn-Tofail, Kénitra; ^(c) Faculté des Sciences Semlalia, Université Cadi Ayyad, LPHEA-Marrakech; ^(d) Faculté des Sciences, Université Mohamed Premier and LPTPM, Oujda; ^(e) Faculté des sciences, Université Mohammed V, Rabat; Morocco.
- ³⁶ CERN, Geneva; Switzerland.
- ³⁷ Enrico Fermi Institute, University of Chicago, Chicago IL; United States of America.
- ³⁸ LPC, Université Clermont Auvergne, CNRS/IN2P3, Clermont-Ferrand; France.
- ³⁹ Nevis Laboratory, Columbia University, Irvington NY; United States of America.
- ⁴⁰ Niels Bohr Institute, University of Copenhagen, Copenhagen; Denmark.
- ⁴¹ ^(a) Dipartimento di Fisica, Università della Calabria, Rende; ^(b) INFN Gruppo Collegato di Cosenza, Laboratori Nazionali di Frascati; Italy.
- ⁴² Physics Department, Southern Methodist University, Dallas TX; United States of America.
- ⁴³ Physics Department, University of Texas at Dallas, Richardson TX; United States of America.
- ⁴⁴ National Centre for Scientific Research “Demokritos”, Agia Paraskevi; Greece.
- ⁴⁵ ^(a) Department of Physics, Stockholm University; ^(b) Oskar Klein Centre, Stockholm; Sweden.
- ⁴⁶ Deutsches Elektronen-Synchrotron DESY, Hamburg and Zeuthen; Germany.
- ⁴⁷ Lehrstuhl für Experimentelle Physik IV, Technische Universität Dortmund, Dortmund; Germany.
- ⁴⁸ Institut für Kern- und Teilchenphysik, Technische Universität Dresden, Dresden; Germany.
- ⁴⁹ Department of Physics, Duke University, Durham NC; United States of America.
- ⁵⁰ SUPA — School of Physics and Astronomy, University of Edinburgh, Edinburgh; United Kingdom.
- ⁵¹ INFN e Laboratori Nazionali di Frascati, Frascati; Italy.
- ⁵² Physikalisches Institut, Albert-Ludwigs-Universität Freiburg, Freiburg; Germany.
- ⁵³ II. Physikalisches Institut, Georg-August-Universität Göttingen, Göttingen; Germany.
- ⁵⁴ Département de Physique Nucléaire et Corpusculaire, Université de Genève, Genève; Switzerland.
- ⁵⁵ ^(a) Dipartimento di Fisica, Università di Genova, Genova; ^(b) INFN Sezione di Genova; Italy.
- ⁵⁶ II. Physikalisches Institut, Justus-Liebig-Universität Giessen, Giessen; Germany.
- ⁵⁷ SUPA — School of Physics and Astronomy, University of Glasgow, Glasgow; United Kingdom.
- ⁵⁸ LPSC, Université Grenoble Alpes, CNRS/IN2P3, Grenoble INP, Grenoble; France.
- ⁵⁹ Laboratory for Particle Physics and Cosmology, Harvard University, Cambridge MA; United States of America.

- ⁶⁰ ^(a) *Department of Modern Physics and State Key Laboratory of Particle Detection and Electronics, University of Science and Technology of China, Hefei;* ^(b) *Institute of Frontier and Interdisciplinary Science and Key Laboratory of Particle Physics and Particle Irradiation (MOE), Shandong University, Qingdao;* ^(c) *School of Physics and Astronomy, Shanghai Jiao Tong University, KLPPAC-MoE, SKLPPC, Shanghai;* ^(d) *Tsung-Dao Lee Institute, Shanghai; China.*
- ⁶¹ ^(a) *Kirchhoff-Institut für Physik, Ruprecht-Karls-Universität Heidelberg, Heidelberg;* ^(b) *Physikalisches Institut, Ruprecht-Karls-Universität Heidelberg, Heidelberg; Germany.*
- ⁶² *Faculty of Applied Information Science, Hiroshima Institute of Technology, Hiroshima; Japan.*
- ⁶³ ^(a) *Department of Physics, Chinese University of Hong Kong, Shatin, N.T., Hong Kong;* ^(b) *Department of Physics, University of Hong Kong, Hong Kong;* ^(c) *Department of Physics and Institute for Advanced Study, Hong Kong University of Science and Technology, Clear Water Bay, Kowloon, Hong Kong; China.*
- ⁶⁴ *Department of Physics, National Tsing Hua University, Hsinchu; Taiwan.*
- ⁶⁵ *Department of Physics, Indiana University, Bloomington IN; United States of America.*
- ⁶⁶ ^(a) *INFN Gruppo Collegato di Udine, Sezione di Trieste, Udine;* ^(b) *ICTP, Trieste;* ^(c) *Dipartimento Politecnico di Ingegneria e Architettura, Università di Udine, Udine; Italy.*
- ⁶⁷ ^(a) *INFN Sezione di Lecce;* ^(b) *Dipartimento di Matematica e Fisica, Università del Salento, Lecce; Italy.*
- ⁶⁸ ^(a) *INFN Sezione di Milano;* ^(b) *Dipartimento di Fisica, Università di Milano, Milano; Italy.*
- ⁶⁹ ^(a) *INFN Sezione di Napoli;* ^(b) *Dipartimento di Fisica, Università di Napoli, Napoli; Italy.*
- ⁷⁰ ^(a) *INFN Sezione di Pavia;* ^(b) *Dipartimento di Fisica, Università di Pavia, Pavia; Italy.*
- ⁷¹ ^(a) *INFN Sezione di Pisa;* ^(b) *Dipartimento di Fisica E. Fermi, Università di Pisa, Pisa; Italy.*
- ⁷² ^(a) *INFN Sezione di Roma;* ^(b) *Dipartimento di Fisica, Sapienza Università di Roma, Roma; Italy.*
- ⁷³ ^(a) *INFN Sezione di Roma Tor Vergata;* ^(b) *Dipartimento di Fisica, Università di Roma Tor Vergata, Roma; Italy.*
- ⁷⁴ ^(a) *INFN Sezione di Roma Tre;* ^(b) *Dipartimento di Matematica e Fisica, Università Roma Tre, Roma; Italy.*
- ⁷⁵ ^(a) *INFN-TIFPA;* ^(b) *Università degli Studi di Trento, Trento; Italy.*
- ⁷⁶ *Institut für Astro- und Teilchenphysik, Leopold-Franzens-Universität, Innsbruck; Austria.*
- ⁷⁷ *University of Iowa, Iowa City IA; United States of America.*
- ⁷⁸ *Department of Physics and Astronomy, Iowa State University, Ames IA; United States of America.*
- ⁷⁹ *Joint Institute for Nuclear Research, Dubna; Russia.*
- ⁸⁰ ^(a) *Departamento de Engenharia Elétrica, Universidade Federal de Juiz de Fora (UFJF), Juiz de Fora;* ^(b) *Universidade Federal do Rio De Janeiro COPPE/EE/IF, Rio de Janeiro;* ^(c) *Universidade Federal de São João del Rei (UFSJ), São João del Rei;* ^(d) *Instituto de Física, Universidade de São Paulo, São Paulo; Brazil.*
- ⁸¹ *KEK, High Energy Accelerator Research Organization, Tsukuba; Japan.*
- ⁸² *Graduate School of Science, Kobe University, Kobe; Japan.*
- ⁸³ ^(a) *AGH University of Science and Technology, Faculty of Physics and Applied Computer Science, Krakow;* ^(b) *Marian Smoluchowski Institute of Physics, Jagiellonian University, Krakow; Poland.*
- ⁸⁴ *Institute of Nuclear Physics Polish Academy of Sciences, Krakow; Poland.*
- ⁸⁵ *Faculty of Science, Kyoto University, Kyoto; Japan.*
- ⁸⁶ *Kyoto University of Education, Kyoto; Japan.*
- ⁸⁷ *Research Center for Advanced Particle Physics and Department of Physics, Kyushu University, Fukuoka; Japan.*
- ⁸⁸ *Instituto de Física La Plata, Universidad Nacional de La Plata and CONICET, La Plata; Argentina.*
- ⁸⁹ *Physics Department, Lancaster University, Lancaster; United Kingdom.*
- ⁹⁰ *Oliver Lodge Laboratory, University of Liverpool, Liverpool; United Kingdom.*
- ⁹¹ *Department of Experimental Particle Physics, Jožef Stefan Institute and Department of Physics, University of Ljubljana, Ljubljana; Slovenia.*
- ⁹² *School of Physics and Astronomy, Queen Mary University of London, London; United Kingdom.*
- ⁹³ *Department of Physics, Royal Holloway University of London, Egham; United Kingdom.*
- ⁹⁴ *Department of Physics and Astronomy, University College London, London; United Kingdom.*

- ⁹⁵ *Louisiana Tech University, Ruston LA; United States of America.*
- ⁹⁶ *Fysiska institutionen, Lunds universitet, Lund; Sweden.*
- ⁹⁷ *Centre de Calcul de l'Institut National de Physique Nucléaire et de Physique des Particules (IN2P3), Villeurbanne; France.*
- ⁹⁸ *Departamento de Física Teórica C-15 and CIAFF, Universidad Autónoma de Madrid, Madrid; Spain.*
- ⁹⁹ *Institut für Physik, Universität Mainz, Mainz; Germany.*
- ¹⁰⁰ *School of Physics and Astronomy, University of Manchester, Manchester; United Kingdom.*
- ¹⁰¹ *CPPM, Aix-Marseille Université, CNRS/IN2P3, Marseille; France.*
- ¹⁰² *Department of Physics, University of Massachusetts, Amherst MA; United States of America.*
- ¹⁰³ *Department of Physics, McGill University, Montreal QC; Canada.*
- ¹⁰⁴ *School of Physics, University of Melbourne, Victoria; Australia.*
- ¹⁰⁵ *Department of Physics, University of Michigan, Ann Arbor MI; United States of America.*
- ¹⁰⁶ *Department of Physics and Astronomy, Michigan State University, East Lansing MI; United States of America.*
- ¹⁰⁷ *B.I. Stepanov Institute of Physics, National Academy of Sciences of Belarus, Minsk; Belarus.*
- ¹⁰⁸ *Research Institute for Nuclear Problems of Byelorussian State University, Minsk; Belarus.*
- ¹⁰⁹ *Group of Particle Physics, University of Montreal, Montreal QC; Canada.*
- ¹¹⁰ *P.N. Lebedev Physical Institute of the Russian Academy of Sciences, Moscow; Russia.*
- ¹¹¹ *Institute for Theoretical and Experimental Physics of the National Research Centre Kurchatov Institute, Moscow; Russia.*
- ¹¹² *National Research Nuclear University MEPhI, Moscow; Russia.*
- ¹¹³ *D. V. Skobel'syn Institute of Nuclear Physics, M.V. Lomonosov Moscow State University, Moscow; Russia.*
- ¹¹⁴ *Fakultät für Physik, Ludwig-Maximilians-Universität München, München; Germany.*
- ¹¹⁵ *Max-Planck-Institut für Physik (Werner-Heisenberg-Institut), München; Germany.*
- ¹¹⁶ *Nagasaki Institute of Applied Science, Nagasaki; Japan.*
- ¹¹⁷ *Graduate School of Science and Kobayashi-Maskawa Institute, Nagoya University, Nagoya; Japan.*
- ¹¹⁸ *Department of Physics and Astronomy, University of New Mexico, Albuquerque NM; United States of America.*
- ¹¹⁹ *Institute for Mathematics, Astrophysics and Particle Physics, Radboud University Nijmegen/Nikhef, Nijmegen; Netherlands.*
- ¹²⁰ *Nikhef National Institute for Subatomic Physics and University of Amsterdam, Amsterdam; Netherlands.*
- ¹²¹ *Department of Physics, Northern Illinois University, DeKalb IL; United States of America.*
- ¹²² *^(a) Budker Institute of Nuclear Physics and NSU, SB RAS, Novosibirsk; ^(b) Novosibirsk State University Novosibirsk; Russia.*
- ¹²³ *Institute for High Energy Physics of the National Research Centre Kurchatov Institute, Protvino; Russia.*
- ¹²⁴ *Department of Physics, New York University, New York NY; United States of America.*
- ¹²⁵ *Ochanomizu University, Otsuka, Bunkyo-ku, Tokyo; Japan.*
- ¹²⁶ *Ohio State University, Columbus OH; United States of America.*
- ¹²⁷ *Faculty of Science, Okayama University, Okayama; Japan.*
- ¹²⁸ *Homer L. Dodge Department of Physics and Astronomy, University of Oklahoma, Norman OK; United States of America.*
- ¹²⁹ *Department of Physics, Oklahoma State University, Stillwater OK; United States of America.*
- ¹³⁰ *Palacký University, RCPTM, Joint Laboratory of Optics, Olomouc; Czech Republic.*
- ¹³¹ *Center for High Energy Physics, University of Oregon, Eugene OR; United States of America.*
- ¹³² *LAL, Université Paris-Sud, CNRS/IN2P3, Université Paris-Saclay, Orsay; France.*
- ¹³³ *Graduate School of Science, Osaka University, Osaka; Japan.*
- ¹³⁴ *Department of Physics, University of Oslo, Oslo; Norway.*
- ¹³⁵ *Department of Physics, Oxford University, Oxford; United Kingdom.*
- ¹³⁶ *LPNHE, Sorbonne Université, Paris Diderot Sorbonne Paris Cité, CNRS/IN2P3, Paris; France.*

- ¹³⁷ *Department of Physics, University of Pennsylvania, Philadelphia PA; United States of America.*
- ¹³⁸ *Konstantinov Nuclear Physics Institute of National Research Centre “Kurchatov Institute”, PNPI, St. Petersburg; Russia.*
- ¹³⁹ *Department of Physics and Astronomy, University of Pittsburgh, Pittsburgh PA; United States of America.*
- ¹⁴⁰ ^(a) *Laboratório de Instrumentação e Física Experimental de Partículas — LIP;* ^(b) *Departamento de Física, Faculdade de Ciências, Universidade de Lisboa, Lisboa;* ^(c) *Departamento de Física, Universidade de Coimbra, Coimbra;* ^(d) *Centro de Física Nuclear da Universidade de Lisboa, Lisboa;* ^(e) *Departamento de Física, Universidade do Minho, Braga;* ^(f) *Universidad de Granada, Granada (Spain);* ^(g) *Dep Física and CEFITEC of Faculdade de Ciências e Tecnologia, Universidade Nova de Lisboa, Caparica; Portugal.*
- ¹⁴¹ *Institute of Physics of the Czech Academy of Sciences, Prague; Czech Republic.*
- ¹⁴² *Czech Technical University in Prague, Prague; Czech Republic.*
- ¹⁴³ *Charles University, Faculty of Mathematics and Physics, Prague; Czech Republic.*
- ¹⁴⁴ *Particle Physics Department, Rutherford Appleton Laboratory, Didcot; United Kingdom.*
- ¹⁴⁵ *IRFU, CEA, Université Paris-Saclay, Gif-sur-Yvette; France.*
- ¹⁴⁶ *Santa Cruz Institute for Particle Physics, University of California Santa Cruz, Santa Cruz CA; United States of America.*
- ¹⁴⁷ ^(a) *Departamento de Física, Pontificia Universidad Católica de Chile, Santiago;* ^(b) *Departamento de Física, Universidad Técnica Federico Santa María, Valparaíso; Chile.*
- ¹⁴⁸ *Department of Physics, University of Washington, Seattle WA; United States of America.*
- ¹⁴⁹ *Department of Physics and Astronomy, University of Sheffield, Sheffield; United Kingdom.*
- ¹⁵⁰ *Department of Physics, Shinshu University, Nagano; Japan.*
- ¹⁵¹ *Department Physik, Universität Siegen, Siegen; Germany.*
- ¹⁵² *Department of Physics, Simon Fraser University, Burnaby BC; Canada.*
- ¹⁵³ *SLAC National Accelerator Laboratory, Stanford CA; United States of America.*
- ¹⁵⁴ *Physics Department, Royal Institute of Technology, Stockholm; Sweden.*
- ¹⁵⁵ *Departments of Physics and Astronomy, Stony Brook University, Stony Brook NY; United States of America.*
- ¹⁵⁶ *Department of Physics and Astronomy, University of Sussex, Brighton; United Kingdom.*
- ¹⁵⁷ *School of Physics, University of Sydney, Sydney; Australia.*
- ¹⁵⁸ *Institute of Physics, Academia Sinica, Taipei; Taiwan.*
- ¹⁵⁹ ^(a) *E. Andronikashvili Institute of Physics, Iv. Javakhishvili Tbilisi State University, Tbilisi;* ^(b) *High Energy Physics Institute, Tbilisi State University, Tbilisi; Georgia.*
- ¹⁶⁰ *Department of Physics, Technion, Israel Institute of Technology, Haifa; Israel.*
- ¹⁶¹ *Raymond and Beverly Sackler School of Physics and Astronomy, Tel Aviv University, Tel Aviv; Israel.*
- ¹⁶² *Department of Physics, Aristotle University of Thessaloniki, Thessaloniki; Greece.*
- ¹⁶³ *International Center for Elementary Particle Physics and Department of Physics, University of Tokyo, Tokyo; Japan.*
- ¹⁶⁴ *Graduate School of Science and Technology, Tokyo Metropolitan University, Tokyo; Japan.*
- ¹⁶⁵ *Department of Physics, Tokyo Institute of Technology, Tokyo; Japan.*
- ¹⁶⁶ *Tomsk State University, Tomsk; Russia.*
- ¹⁶⁷ *Department of Physics, University of Toronto, Toronto ON; Canada.*
- ¹⁶⁸ ^(a) *TRIUMF, Vancouver BC;* ^(b) *Department of Physics and Astronomy, York University, Toronto ON; Canada.*
- ¹⁶⁹ *Division of Physics and Tomonaga Center for the History of the Universe, Faculty of Pure and Applied Sciences, University of Tsukuba, Tsukuba; Japan.*
- ¹⁷⁰ *Department of Physics and Astronomy, Tufts University, Medford MA; United States of America.*
- ¹⁷¹ *Department of Physics and Astronomy, University of California Irvine, Irvine CA; United States of America.*
- ¹⁷² *Department of Physics and Astronomy, University of Uppsala, Uppsala; Sweden.*

- ¹⁷³ *Department of Physics, University of Illinois, Urbana IL; United States of America.*
- ¹⁷⁴ *Instituto de Física Corpuscular (IFIC), Centro Mixto Universidad de Valencia — CSIC, Valencia; Spain.*
- ¹⁷⁵ *Department of Physics, University of British Columbia, Vancouver BC; Canada.*
- ¹⁷⁶ *Department of Physics and Astronomy, University of Victoria, Victoria BC; Canada.*
- ¹⁷⁷ *Fakultät für Physik und Astronomie, Julius-Maximilians-Universität Würzburg, Würzburg; Germany.*
- ¹⁷⁸ *Department of Physics, University of Warwick, Coventry; United Kingdom.*
- ¹⁷⁹ *Waseda University, Tokyo; Japan.*
- ¹⁸⁰ *Department of Particle Physics, Weizmann Institute of Science, Rehovot; Israel.*
- ¹⁸¹ *Department of Physics, University of Wisconsin, Madison WI; United States of America.*
- ¹⁸² *Fakultät für Mathematik und Naturwissenschaften, Fachgruppe Physik, Bergische Universität Wuppertal, Wuppertal; Germany.*
- ¹⁸³ *Department of Physics, Yale University, New Haven CT; United States of America.*
- ¹⁸⁴ *Yerevan Physics Institute, Yerevan; Armenia.*
- ^a *Also at Borough of Manhattan Community College, City University of New York, New York NY; United States of America.*
- ^b *Also at Centre for High Performance Computing, CSIR Campus, Rosebank, Cape Town; South Africa.*
- ^c *Also at CERN, Geneva; Switzerland.*
- ^d *Also at CPPM, Aix-Marseille Université, CNRS/IN2P3, Marseille; France.*
- ^e *Also at Département de Physique Nucléaire et Corpusculaire, Université de Genève, Genève; Switzerland.*
- ^f *Also at Departament de Física de la Universitat Autònoma de Barcelona, Barcelona; Spain.*
- ^g *Also at Departamento de Física, Instituto Superior Técnico, Universidade de Lisboa, Lisboa; Portugal.*
- ^h *Also at Department of Applied Physics and Astronomy, University of Sharjah, Sharjah; United Arab Emirates.*
- ⁱ *Also at Department of Financial and Management Engineering, University of the Aegean, Chios; Greece.*
- ^j *Also at Department of Physics and Astronomy, University of Louisville, Louisville, KY; United States of America.*
- ^k *Also at Department of Physics and Astronomy, University of Sheffield, Sheffield; United Kingdom.*
- ^l *Also at Department of Physics, California State University, East Bay; United States of America.*
- ^m *Also at Department of Physics, California State University, Fresno; United States of America.*
- ⁿ *Also at Department of Physics, California State University, Sacramento; United States of America.*
- ^o *Also at Department of Physics, King's College London, London; United Kingdom.*
- ^p *Also at Department of Physics, St. Petersburg State Polytechnical University, St. Petersburg; Russia.*
- ^q *Also at Department of Physics, Stanford University, Stanford CA; United States of America.*
- ^r *Also at Department of Physics, University of Fribourg, Fribourg; Switzerland.*
- ^s *Also at Department of Physics, University of Michigan, Ann Arbor MI; United States of America.*
- ^t *Also at Faculty of Physics, M.V. Lomonosov Moscow State University, Moscow; Russia.*
- ^u *Also at Giresun University, Faculty of Engineering, Giresun; Turkey.*
- ^v *Also at Graduate School of Science, Osaka University, Osaka; Japan.*
- ^w *Also at Hellenic Open University, Patras; Greece.*
- ^x *Also at Horia Hulubei National Institute of Physics and Nuclear Engineering, Bucharest; Romania.*
- ^y *Also at Institutio Catalana de Recerca i Estudis Avancats, ICREA, Barcelona; Spain.*
- ^z *Also at Institut für Experimentalphysik, Universität Hamburg, Hamburg; Germany.*
- ^{aa} *Also at Institute for Mathematics, Astrophysics and Particle Physics, Radboud University Nijmegen/Nikhef, Nijmegen; Netherlands.*
- ^{ab} *Also at Institute for Nuclear Research and Nuclear Energy (INRNE) of the Bulgarian Academy of Sciences, Sofia; Bulgaria.*

- ^{ac} Also at Institute for Particle and Nuclear Physics, Wigner Research Centre for Physics, Budapest; Hungary.
- ^{ad} Also at Institute of Particle Physics (IPP); Canada.
- ^{ae} Also at Institute of Physics, Academia Sinica, Taipei; Taiwan.
- ^{af} Also at Institute of Physics, Azerbaijan Academy of Sciences, Baku; Azerbaijan.
- ^{ag} Also at Institute of Theoretical Physics, Ilia State University, Tbilisi; Georgia.
- ^{ah} Also at Instituto de Fisica Teorica, IFT-UAM/CSIC, Madrid; Spain.
- ^{ai} Also at Istanbul University, Dept. of Physics, Istanbul; Turkey.
- ^{aj} Also at Joint Institute for Nuclear Research, Dubna; Russia.
- ^{ak} Also at LAL, Université Paris-Sud, CNRS/IN2P3, Université Paris-Saclay, Orsay; France.
- ^{al} Also at Louisiana Tech University, Ruston LA; United States of America.
- ^{am} Also at LPNHE, Sorbonne Université, Paris Diderot Sorbonne Paris Cité, CNRS/IN2P3, Paris; France.
- ^{an} Also at Manhattan College, New York NY; United States of America.
- ^{ao} Also at Moscow Institute of Physics and Technology State University, Dolgoprudny; Russia.
- ^{ap} Also at National Research Nuclear University MEPhI, Moscow; Russia.
- ^{aq} Also at Physikalisches Institut, Albert-Ludwigs-Universität Freiburg, Freiburg; Germany.
- ^{ar} Also at School of Physics, Sun Yat-sen University, Guangzhou; China.
- ^{as} Also at The City College of New York, New York NY; United States of America.
- ^{at} Also at The Collaborative Innovation Center of Quantum Matter (CICQM), Beijing; China.
- ^{au} Also at Tomsk State University, Tomsk, and Moscow Institute of Physics and Technology State University, Dolgoprudny; Russia.
- ^{av} Also at TRIUMF, Vancouver BC; Canada.
- ^{aw} Also at Università di Napoli Parthenope, Napoli; Italy.
- * Deceased